UNIVERSITY OF BELGRADE

FACULTY OF BIOLOGY

Aleksandra Vukojičić

COMPLEMENT AND MICROGLIA MEDIATE SENSORY-MOTOR SYNAPTIC LOSS IN NORMAL DEVELOPMENT AND IN SPINAL MUSCULAR ATROPHY

Doctoral dissertation

Belgrade, 2020.

УНИВЕРЗИТЕТ У БЕОГРАДУ

БИОЛОШКИ ФАКУЛТЕТ

Александра Вукојичић

КОМПЛЕМЕНТ И МИКРОГЛИЈА КАО ПОСРЕДНИЦИ ГУБИТКА СЕНЗОРНО-МОТОРНИХ СИНАПСИ ТОКОМ НОРМАЛНОГ РАЗВИЋА И У СПИНАЛНОЈ МИШИЋНОЈ АТРОФИЈИ

Докторска дисертација

Београд, 2020.

MENTORS:

dr George Z. Mentis, associate professor, Columbia University, Center for Motor Neuron Biology and Disease, New York, USA.

dr Biljana Božić Nedeljković, professor, University of Belgrade – Faculty of Biology

COMMITTEE MEMBERS:

dr George Z. Mentis, associate professor, Columbia University, Center for Motor Neuron Biology and Disease, New York, USA.

dr Biljana Božić Nedeljković, professor, University of Belgrade – Faculty of Biology

academician Vladimir Kostić, professor, University of Belgrade – Faculty of Medicine, president of Serbian Academy of Sciences and Arts

dr Serge Przedborski, professor, Columbia University, Center for Motor Neuron Biology and Disease, New York, USA.

dr Pavle Andjus, professor, University of Belgrade – Faculty of Biology

Defense date: _____

ACKNOWLEDGMENTS

Complement and microglia mediate sensory-motor synaptic loss in normal development and in spinal muscular atrophy

Abstract

Movement is an essential behavior that is controlled by motor circuits. Within spinal motor circuits, motor neurons bridge the central and peripheral nervous systems by conveying central commands to the skeletal muscles. The precise assembly and refinement of spinal motor circuits is required for normal motor behavior. It is known for several brain regions that during development a larger than needed number of synapses are produced and subsequently eliminated. However, the mechanisms responsible for spinal motor circuit refinement and synapse maintenance are poorly understood. Similarly, the molecular mechanisms by which gene mutations cause dysfunction and elimination of synapses in neurodegenerative diseases that occur during the development are unknown.

Complement proteins have emerged as critical mediators of synaptic refinement and circuit plasticity. Therefore, this study aimed to address whether complement proteins are involved in the synaptic refinement of spinal sensory-motor circuitry. Additionally, to address whether similar mechanisms are responsible for elimination of synapses in neurodegeneration, spinal muscular atrophy (SMA) was utilized as a model disease. SMA is a neurodegenerative disease that occurs during early development. It is caused by reduced levels of the ubiquitously expressed SMN protein. The hallmarks of SMA are loss of motor neurons, muscle atrophy and abnormal postural reflexes. It has been previously shown that decreased number of select synapses and sensory-motor circuit dysfunction precede motor neuron loss. The mechanisms leading to this selective synapse loss on SMN deficient motor neurons remained unknown. This study investigated whether complement-dependent mechanisms are involved in synapse elimination in SMA.

Results of this study demonstrated that the complement protein C1q – initiating protein of classical pathway, is required for the refinement of spinal sensory-motor circuits during the normal development. Synaptic density analysis revealed significantly higher number of proprioceptive synapses in C1q-/- mice. Functional assays showed a larger response in spinal reflexes in C1q-/- mice compared to WT mice, demonstrating that these synapses are functional. Strikingly, results of this study demonstrate that specific muscle-identified motor pools in C1q-/- mice receive inappropriate proprioceptive synapses at the end of the first postnatal week – the period during which behavioral studies revealed impaired righting times. Collectively, findings of this study

demonstrate an important and novel role for complement proteins in early postnatal development of spinal sensory-motor circuits.

Importantly, results of this study also demonstrate in a mouse model of spinal muscular atrophy that synaptic dysfunction and elimination is mediated by complement proteins and microglia-dependent mechanisms. C1q was found to tag vulnerable SMA synapses, leading to activation of the classical complement pathway, deposition of C3 protein and microglia-mediated elimination. Beside the phagocytic role in synapse elimination, microglia were found to be the main source of C1q in developing spinal cord. *In vivo* neutralization of C1q rescued synapses destined to be eliminated alleviating the severe SMA mouse phenotype. In addition, functional assays employing the *ex vivo* spinal cord preparation demonstrated that synapses rescued from elimination are functional, providing further evidence that SMA is a disease of motor circuits. Similarly, pharmacological depletion of microglia rescued the number of synapses, conferring behavioral benefit in SMA mice. These findings suggest that aberrant activation of classical complement pathway and microglial phagocytic activity mediate synaptic loss in a mouse model of SMA and identify blockade of C1q as a novel therapeutic target.

Collectively, results of this study identify a critical role for the classical complement pathway in the refinement of developing spinal sensory-motor circuits, while its aberrant activation contributes to the pathology of neurodegenerative motor neuron disease spinal muscular atrophy.

Key words: C1q, complement, motor neuron, proprioceptive synapse, sensory-motor circuit, spinal muscular atrophy, microglia, SMN

Scientific field: Biology

Scientific subfield: Immunology, Neurobiology (Neuroimmunology)

Комплемент и микроглија као посредници губитка сензорно-моторних синапси током нормалног развића и у спиналној мишићној атрофији

Сажетак

Кретање је есенцијално понашање које је контролисано од стране моторних неуронских мрежа. У оквиру кичмених моторних мрежа, моторни нурони служе као мост између централног и периферног нервног система преносећи централне команде скелетним мишићима. Прецизно успостављање и преуређивање кичмених моторних мрежа је неопходно за нормално моторичко понашање. Познато је да се током развића појединих деловима мозга формира више него што је потребно синапси које касније бивају елиминисане. Међутим, механизми који су одговорни за преуређивање кичмених моторних мрежа и за одржавање синапси недовољно су испитани. Слично, молекуларни механизми одговорни за генским мутацијама изазвану дисфункцију и елиминацију синапси у неуродегенеративним болестима које се јављају током развића тренутно су непознати.

Протеини система комплемента су се показали као критични медијатори финог синаптичког подешавања и пластичности неуронских мрежа. Стога је ова студија имала за циљ да испита да ли су протеини комплемент система умешани у синаптичко преуређивање кичмене сензорно-моторне неуронске мреже. Додатно, не би ли се испитало да ли су слични механизми одговорни за елиминацију синапси током неуродегенерације, спинална мишићна атрофија (CMA) је коришћена као модел неуродегенартивне болести. CMA је неуродегенеративна болест која се јавља рано током развића. Изазивана је смањењем нивоа убиквитно експримираног SMN (енг. survival motor neuron) протеина. Карактеристике CMA су губитак моторних неурона, атрофија мишића и абнормални постурални рефлекси. Претходно је показано да снижени бројеви одређених синапси и дисфункција сензорно-моторне неуронске мреже предходе губитку моторних неурона. Механизми који доводе до овог селективног губитка синапси на моторним неуронима којима недостаје SMN тренутно су непознати. У овој студији је испитано да ли су комплемент-зависни мезанизми умешани у елиминацију синапси у CMA.

Резултати ове студије показују да је комплемент протеин C1q – иницијални протеин класичног пута, неопходан за преуређивање кичмених сензорно-моторних мрежа током

нормалног развића. Анализе синаптичке густине откриле су знатно већи број проприоцептивних синапси код C1q-/- мишева. Функционални тестови су показали већи одговор кичмених рефлекса код C1q-/- мишева у поређењу са WT (енг. Wild Type) мишевима, доказујући да су ове синапсе функционалне. Изненађујуће, резултати ове студије показују да специфичнни мишићем-идентификовани моторни неурони C1q-/- мишева примају неадекватне проприоцептивне синапсе на крају прве постнаталне недеље – период током ког су студије понашања откриле поремећај у времену потребном да се мишеви усправе. Свеукупно, резултати ове студије показали су важну и нову улогу протеина система комплемента у раном постнаталном развићу кичмених сензорно-моторних мрежа.

Оно што је битно, резултати ове студије додатно су још показали, у мишјем моделу спиналне мишићне атрофије, да је дисфункција и елиминација синапси посредована протеинима система комплемента и микроглија-зависним механизмима. Откривено је да C1q означава рањиве CMA синасе, што води активацији класичног пута комплемента, таложењу C3 протеина и микроглија-посредованој елиминацији. Поред фагоцитне улоге у елиминацији синапси, откривено је још да је микроглија и главни извор C1q протеина током развића кичмене мождине. *In vivo* неутрализација C1q протеина спасила је синапсе предвиђене за елиминацију ублажавајући тешки фенотип CMA код мишева. Поред тога, функционални тестови користећи *ex vivo* препарате кичмене мождине показали су да су синапсе спашене од елиминације функционалне, пружајући додатне доказе да је CMA болест моторних мрежа. Слично томе, фармаколошко уклањање микроглије утицало је на очување броја синапси, доприносећи побољшању понашања CMA мишева. Ова открића сугеришу да неадекватна активација класичног пута комплемента и фагоцитна активност микроглије посредују у губитку синапси у мишјем моделу CMA и идентификују блокаду C1q као нову терапијску мету.

Свеукупно, резултати ове студије идентификују критичну улогу класичног пута система комплемента у преуређивању кичмених сензорно-моторних неуронских мрежа у развоју, док његова неадекватна активација доприноси патологији неуродегенеративне болести моторних неурона, спиналној мишићној атрофији.

Кључне речи: C1q, комплемент, моторни неурон, проприоцептивна синапса, сензорно-моторна мрежа, спинална мишићна атрофија, микроглија, SMN

Научна област: Биологија

Ужа научна област: Имунологија, Неуробиологија (Неуроимунологија)

List of abbreviations

AAV – adeno-associated virus

Ab – antibody

aCSF – artificial cerebrospinal fluid

AD - Alzheimer's disease

ALS – amyotrophic lateral sclerosis

ASO – antisense oligonucleotide

BBB – blood-brain barrier

BDNF – brain-derived neurotrophic factor

BTX – a-bungarotoxin

CD45 – cluster of Differentiation 45

CD68 – cluster of Differentiation 68

ChAT – Choline Acetyltransferase

CLR – collagen-like region

CMAP – compound muscle action potentials

CNS – central nervous system

CR3 – complement receptor 3

CRP - C reactive protein

CSF1R – colony stimulating factor 1 receptor

CTb – cholera toxin β-subunit

Ctr Ab – control antibody

DAPI – 4',6-diamidino-2-phenylindole

Dext – fluorescein dextran

DNA – deoxyribonucleic acid

DRG – dorsal root ganglion

EDL – lat. *extensor digitorum longus*

EPSP – excitatory postsynaptic potential

FDA – Food and Drug Administration

FISH – fluorescent in situ hybridization

FTD – Frontotemporal dementia

GABA - gamma-aminobutyric acid

GAD65 – glutamic acid decarboxylase 65-kilodalton isoform

GAD67 – glutamic acid decarboxylase 67-kilodalton isoform

Gastro – lat. *Gastrocnemius*

HD – Huntington's disease

HMC - hypaxial motor column

IACUC – Columbia animal care and use committee

IAP – integrin-associated protein

Iba1 – ionized calcium-binding adapter molecule 1

IgG – Immunoglobulin G

IL – interleukin

IN – inter neuron

IP – intraperitoneal

KO – knockout

LGN – lateral geniculate nucleus

LMC - lateral motor column

MAC - membrane attack complex

MBL – mannose binding lectin

MMC - medial motor column

MN – motor neuron

mRNA - messenger ribonucleic acid

NF – neurofilament

NMJ – neuromuscular junction

P0 – postnatal day 0

P11 – postnatal day 11

P2 – postnatal day 2

P4 – postnatal day 4

P7 – postnatal day 7

PBS – phosphate buffer saline

PCR – polymerase chain reaction

PD – Parkinson's disease

PFA – paraformaldehyde

PGC - preganglionic motor column

PMC - phrenic motor column

Pv – Parvalbumin

QL – lat. *quadratus lumborum*

RNA - ribonucleic acid

RT-qPCR – quantitative reverse transcription polymerase chain reaction

SEM – standard error of the mean

SMA – spinal muscular atrophy

SMA – Spinal muscular atrophy

SMN - survival motor neuron

SN – sensory neuron

snRNP – spliceosomal small nuclear ribonucleoprotein

TA – lat. *tibialis anterior*

TMEM119 – transmembrane protein 119

TNF – tumor necrosis factor

VGAT – vesicular GABAergic transporter

VGluT1 – vesicular glutamate transporter 1

WT – wild type

TABLE OF CONTENTS

1. INTRODUCTION

1.1.   The spinal sensory–motor reflex circuit

The development of coordinated locomotor behavior in vertebrates depends on the precise establishment of selective contacts between the discrete neuronal populations in the spinal cord and the peripheral nervous system. The precise assembly of the circuits needed for movement requires generation of many different cell types to facilitate the complex connections between the motor neurons (MN), sensory neurons (SN), interneurons (IN), and the muscle (Dasen, 2009; Grillner and Jessell, 2009). The specification of distinct neuronal subtypes in the spinal cord is largely mediated through inductive signals and transcription factors networks which are operating within the progenitor and postmitotic cells (Dasen, 2009; Jessell, 2000). The mechanisms that specify the identity of neural cells transcription factor expression patterns appear to specify the precise cellular programs that control axonal guidance as well as synaptic specificities of neurons (Dasen, 2009; Goulding and Pfaff, 2005). Spinal circuits have to be adequately fined tuned in order to recruit in a specific order the different muscle groups and smoothly execute motor commands. The critical step in the spinal circuits formation is the precise navigation of motor axons toward their specific muscle targets. All subsequent connections to motor neurons including descending inputs originating from higher brain centers, sensory neurons and local interneurons, are confined by the motor neuron axons' peripheral connections (Dasen, 2009). All these synaptic inputs have to be properly formed and maintained in order to have precise fine output from spinal motor circuits resulting in recruitment of specific muscles and generation of movement.

Pioneering studies which characterized the spinal sensory–motor reflex circuit were performed by Eccles and colleagues back in the 1950s (Eccles et al., 1957) . They demonstrated that stretch of a peripheral muscle is carried through proprioceptive sensory neuron afferents onto specific spinal motor neurons. This information is then relayed back to the muscle – via the spinal cord - from which it originated, thus driving reflex contraction (Figure 1) (Eccles et al., 1957; Mears and Frank, 1997; Plant et al., 2018; Windhorst, 2007). The stretch reflex can be thought as the primary building unit of controlled movements in vertebrates, including humans. The circuitry of stretch reflex includes three distinct cell types: muscle fibers in the periphery, alpha motor neurons in the spinal cord whose axons project to the muscle, and proprioceptive sensory neurons in dorsal root ganglion, whose afferents project into the spinal cord through dorsal roots and originate in skeletal muscle (Figure 1). Muscle spindles are specialized sensory endings which are embedded in the muscle. Upon muscle stretch they increase their length which leads to the increase in firing

frequency of primary proprioceptive sensory afferents. Proprioceptive neurons synapse directly onto alpha motor neurons and on other spinal interneurons. They release glutamate which activates ionotropic glutamate receptors present on soma and dendrites of motor neurons. This evokes excitatory postsynaptic potentials (EPSPs) and depolarizes motor neurons membrane to reach the voltage threshold needed to generate an action potential. Action potentials are propagated along axons of motor neurons in order to reach their peripheral targets which results in the muscle fibers activation, causing the contraction of muscle fibers they innervate. Hence, muscle contraction is counteracting the initial muscle stretch (Fletcher and Mentis, 2017).

The sensory–motor circuit is devoted to proprioceptive control - stabilization and the sense of the limb in space. From the behavioral point of view, sensory-motor circuit has been well characterized. Experimental disruptions of the circuit result in characteristic functional and behavioral abnormalities. Perturbations to proprioceptive sensory afferents projecting onto motor neurons causes serious disorganization of locomotor function (Arber et al., 2000; Plant et al., 2018). Coordinated stepping movements, which are needed for locomotor behaviors, are significantly impaired if missing proprioceptive feedback (Akay et al., 2014; Plant et al., 2018; Takeoka et al., 2014).
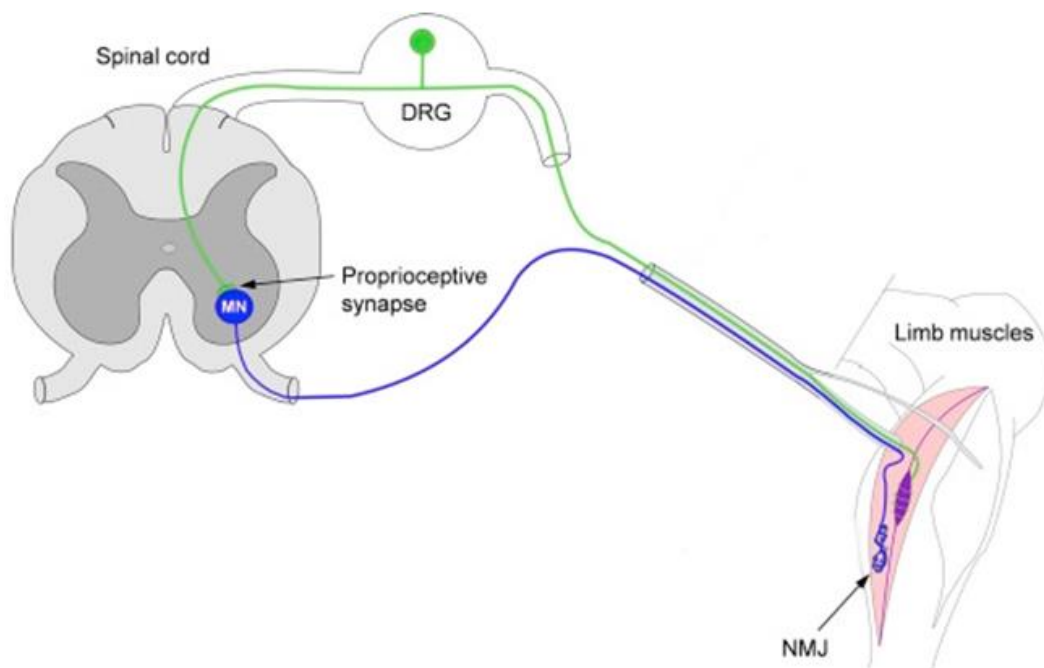
Figure 1. The stretch reflex in mammals. (A) A schematic illustration of the spinal sensory-motor circuit. Motor neurons (shown in blue) are located within the ventral spinal cord. They project their axons to the skeletal muscle and synapse at the NMJ. Muscle spindles (shown in purple) are specialized sensory organs which are embedded within the muscle and get activated by muscle stretch. While the cell bodies of proprioceptive sensory neurons (shown in green) are located within

the dorsal root ganglia (DRG), their axons originate from the muscle spindle. The proximal part of proprioceptive axons makes entry to the spinal cord via the dorsal root. In the spinal cord they make direct – monosynaptic excitatory contacts with motor neurons. Adapted from (Fletcher and Mentis, 2017).

1.1.1. Motor neurons

Motor neurons are the sole mediators through which brain triggers contractions of skeletal muscles in order to control all body movements, from walking to those critical for survival such as breathing and swallowing (Kanning et al., 2010). Spinal motor neurons are unique as they are one of a few neuronal cell types whose axons span outside of CNS. Also unique to spinal motor neurons is the output of their activity – contraction of a muscle. Consequently, it does not surprise that they are probably the best molecularly and functionally characterized neuronal cell type in vertebrates (Price and Briscoe, 2004). The specification of motor neuron identity can be seen as a three-stage process (Jessell, 2000). The generic motor neuron specification of identity happens first, leading to generation of appropriately positioned motor neurons in the spinal cord. During the second stage, the somata of functionally associated motor neuron groups, which are destined to have common projection targets, will settle in columns longitudinally oriented in spinal cord with axons projecting toward the target regions. Finally, during the third stage, cell bodies of motor neurons innervating same muscle form clusters known as motor pools, and in which are specialized synaptic contacts formed between premotor neurons and motor neurons. All these steps require extracellular signals which regulate cell-autonomous intrinsic determinants of motor neuron identity, and together shape and define the development of motor neurons (Jessell, 2000; Price and Briscoe, 2004).

Spinal motor neurons are divided into columns which are topographically segregated and innervate distinct peripheral domains (Figure 2) (Dasen and Jessell, 2009). The hypaxial motor column (HMC) and the medial motor column (MMC) are evolutionarily the oldest motor subclasses, innervating body wall and axial musculature, respectively (Fetcho, 1987; Gutman et al., 1993). Preganglionic motor column (PGC) and the lateral motor column (LMC) are evolutionary younger. They appeared with the development of paired appendages (Jung and Dasen, 2015). The LMC motor neurons which innervate limb muscles, are formed at limb levels of spinal cord (Romanes, 1951). Rostral and thoracic lumbar levels of spinal cord are home to PGC motor neurons which innervate sympathetic ganglia (Prasad and Hollyday, 1991). Formation of the phrenic motor column (PMC) is reserved to cervical levels of the spinal cord. PMC motor neurons innervate the diaphragm, and are found only in mammals (Allan and Greer, 1997; Jung and Dasen, 2015). Lastly,

located in the most caudal aspects of the spinal cord are sacral motor neurons which innervate pelvic floor muscles (Figure 2) (Dasen and Jessell, 2009; Hancock and Peveto, 1979; Mendelsohn, 2016).
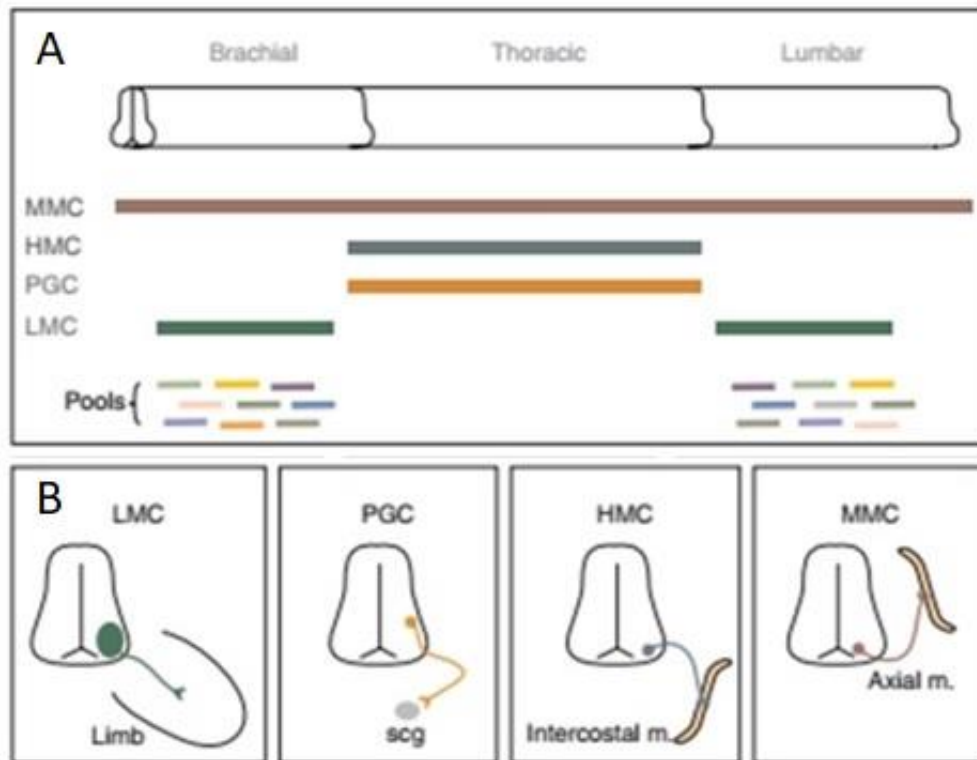
Figure 2. Motor neuron divisional, columnar and pool organization. (A) Motor pools and motor columns are specifically positioned along the rostro-caudal axis. The somata of motor neurons that send axons to limbs are located within the lateral motor column (LMC) at lumbar and brachial spinal cord levels. Preganglionic column (PGC) motor neurons and hypaxial motor column (HMC) motor neurons are located at thoracic levels. Medial motor column (MMC) motor neurons are located at all rostro-caudal spinal cord levels. Within the LMC motor pools are generated at specific rostro-caudal positions. (B) Projection patterns of columnar motor neuron subtypes. LMC motor neurons send their axons to the limb. PGC motor neurons project to the sympathetic chain ganglia (scg), HMC motor neurons send their axons to intercostal muscles and body wall muscles (m), MMC neurons project to the axial muscle. Adapted from (Dasen and Jessell, 2009).

Within a column, the collection of motor neurons innervating a single skeletal muscle represent a motor pool. The overall organization of motor pools within the spinal cord is topological: more rostral pools innervate more proximally positioned muscles in a limb, whereas medial and lateral motor neurons innervate ventral and dorsal limb muscles, respectively (Figure 3) (Kanning et al., 2010; Landmesser, 1978; Romanes, 1951; Vanderhorst and Holstege, 1997).
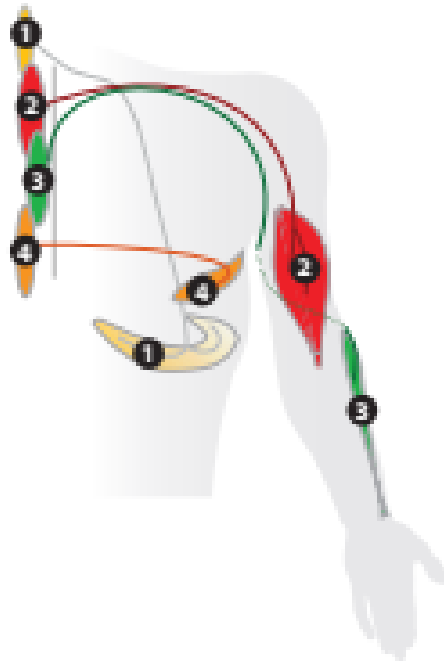
Figure 3. Example of topological organization of motor pools. Within the limb innervating pools (2: biceps – shown in red and 3: brachioradialis – shown in green), those that innervate more proximal muscles are located more rostrally in spinal cord. Thoracic motor neurons (4) innervate intercostal muscles (4) whereas phrenic motor neurons (1) located in the cervical spinal cord innervate the diaphragm (1), which is due to the more rostral position of the diaphragm precursors during development. Adapted from (Kanning et al., 2010).

Motor neurons of an adult are classified based on functionally distinct characteristics into diverse classes and subtypes. According to the muscle fiber type that each class innervates motor neurons can be divided into alpha (α), beta (β), and gamma (γ) motor neurons. Alpha motor neurons (α-MNs) drive muscle contraction and innervate extrafusal skeletal muscle fibers. Gamma motor neurons also known as fusimotor neurons (γ-MNs) selectively innervate intrafusal muscle fibers of the muscle spindle (Kanning et al., 2010). Phylogenetically, they are the most developed neurons in mammals, whereas lower vertebrates regulate sensitivity of their muscle spindles through β-skeleto-fusimotor system alone (Shneider et al., 2009). Gamma and alpha motor neurons differ in their central and peripheral patterns of connectivity as well as in their morphology (Friese et al., 2009). While α-MNs predominate within motor pools γ-MNs compose approximately a third of all motor neurons in a given pool. Alpha motor neurons are responsible for generation of force to move the skeleton by contracting extrafusal muscle fibers. Gamma motor neurons, on the other hand, innervate intrafusal fibers that modulate muscle spindles sensitivity to stretch (Friese et al., 2009; Kanning et al., 2010; Kuffler et al., 1951). Alpha and gamma motor neurons are also profoundly

different with respect to their connectivity profile and morphology, reflecting upon their different functions and targets. (Friese et al., 2009; Kanning et al., 2010). Gamma motor neurons are significantly smaller than α-MNs with the average diameter of their cell body being half the length of the smallest alpha motor neurons. Gamma motor neurons also have smaller axon caliber which results in slower conduction velocities (Burke et al., 1977; Kanning et al., 2010; Shneider et al., 2009). The dendritic trees of alpha and gamma motor neurons are similar in length, but those of gamma motor neurons have overall simpler dendritic arborization with significantly less branching (Kanning et al., 2010; Westbury, 1982). Alpha and gamma motor neurons also differ in their connectivity patterns within the spinal cord. While most of α-MNs receive direct Ia input from proprioceptive sensory neurons, all γ-MNs lack monosynaptic connections from Ia proprioceptive sensory afferents (Eccles et al., 1960; Eccles et al., 1957; Friese et al., 2009; Kanning et al., 2010). Hence, alpha and gamma motor neurons have generally distinct presynaptic inputs and postsynaptic targets. The third class of motor neurons called β-motor neurons represents less well-defined population of spinal motor neurons and innervate both extra- and intrafusal fibers (Kanning et al., 2010).

1.1.2. Sensory neurons

A precise control of motor behaviors is achieved by integration of motor and sensory systems in the central nervous system (CNS) (Imai and Yoshida, 2018). Motor output coordination depends on sensory feedback which informs CNS about muscle status and external stimuli in real time. Sensory neurons (SNs) have their cell bodies within dorsal root ganglion (DRG) but their projections extend to the peripheral targets and relay to CNS neurons (Catela et al., 2015). Similar to motor neurons, the specific functions and identities of sensory neurons are encoded within their unique molecular profiles (Catela et al., 2015; Zheng et al., 2019). Nonetheless, sensory neurons and motor neurons differ largely in their organization. While motor neurons are organized into discrete motor pool and columnar subtypes, sensory neurons are scattered throughout the DRG. Thus, an individual DRG accommodates sensory neurons with unique profiles and differing peripheral targets (Abraira and Ginty, 2013; Catela et al., 2015; Dasen, 2009).

1.1.2.1. Proprioceptive sensory neurons

Motor neuron activity, which delivers directions to muscles in all motor behaviors, is in part coordinated, by proprioceptive sensory neurons. They transmit information from the periphery

about muscle position as well as the contraction status to the motor neurons, acting as a feedback loop to generate correct motor responses. Proprioceptive sensory neurons are subdivided into large and medium diameter neurons. Large diameter proprioceptive neurons are groups Ia and Ib, whereas medium diameter proprioceptive neurons represent group II (Brown, 1981; Imai and Yoshida, 2018). Both group Ia and group II proprioceptive neurons synapse in the periphery at muscle spindles - structures enclosed in skeletal muscles, transmitting the information about changes in muscle stretch or length (Figure 4) (Brown, 1981; Catela et al., 2015; Hoheisel U, 1989; SA., 1992). Group Ib proprioceptive neurons project their axons peripherally to Golgi tendon organs which are embedded within the muscle, and centrally to the intermediate spinal cord, in which they form indirect connections with motor neurons via spinal interneurons. In the ventral spinal cord, group II proprioceptive neurons project sparsely (Brown and Fyffe, 1979; Catela et al., 2015).
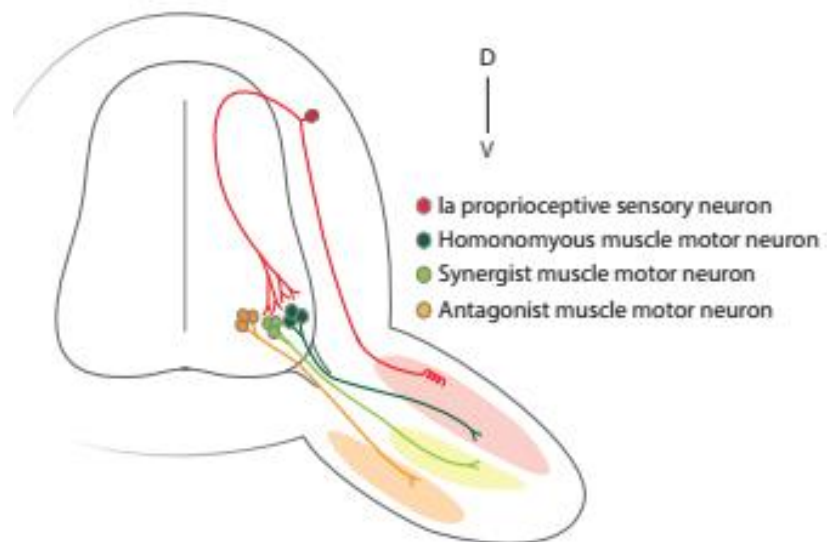
Figure 4. Sensorimotor circuits. Simplified illustration of the monosynaptic reflex circuit in which proprioceptive sensory neurons (shown in red) send information to the spinal cord from a specific muscle. Proprioceptive neurons synapse directly onto motor neurons that innervate same muscle peripherally. Proprioceptive neurons also make secondary connections with motor neurons that innervate muscle synergists but not with the motor neurons that innervate antagonistic muscles. Adapted from (Catela et al., 2015).

In mice, proprioceptive afferents reach muscles and the spinal cord around embryonic day 10.5 (E10.5) (Imai and Yoshida, 2018; Ozaki and Snider, 1997). Axons enter the spinal cord through dorsal root around E12.5, forming monosynaptic contacts with motor neurons by E17 (Imai

and Yoshida, 2018; Mears and Frank, 1997; Ozaki and Snider, 1997; Seebach and Ziskind-Conhaim, 1994). Group Ia projections synapse directly onto alpha motor neurons innervating the same – or homonymous - muscle which their Ia afferents contact in the periphery (Brown, 1981; Burke et al., 1977; Catela et al., 2015; Eccles et al., 1957; Mears and Frank, 1997). This Ia proprioceptive sensory neurons – alpha motor neurons – muscle feedback loop represents the basis of the monosynaptic spinal reflex arc as well as the foundation of the homeostatic muscle activity maintenance (Catela et al., 2015; Windhorst, 2007). Group Ia proprioceptive neurons also synapse onto motor neurons innervating synergistic muscles – but importantly not antagonistic muscles. Beside the connections with motor neurons group Ia proprioceptive neurons also synapse onto inhibitory interneurons which are involved in control of the antagonistic muscle activity (Figure 4) (Brown, 1981; Catela et al., 2015; Mendelsohn et al., 2015).However, early during development motor neurons do receive proprioceptive inputs originating from antagonistic muscles (Seebach and Ziskind-Conhaim, 1994), that are eliminated at postnatal ages(Poliak et al., 2016) . The molecular mechanisms behind this refinement of sensory-motor circuitry are currently unknown.

Due to the fact that Ia proprioceptive afferents form specific direct monosynaptic connections with precise motor neuron pools (Eccles et al., 1957) these circuits became elegant model systems for studying the molecular mechanisms responsible for the synaptic specificity(Imai and Yoshida, 2018). Monosynaptic connections are formed by E17 and it was believed that their establishment is independent of neuronal activity (Imai and Yoshida, 2018; Mears and Frank, 1997). Results from a recent study however, demonstrate that monosynaptic heteronymous sensory-motor connections for the related muscle pair, ankle flexor muscle - tibialis anterior (TA), and toe extensor muscle – extensor digitorum longus (EDL), are coordinated via sensory neuron activity-dependent process (Mendelsohn et al., 2015).In early postnatal mouse, TA proprioceptive sensory neurons make weak heteronymous monosynaptic connections with the EDL motor neurons but strong homonymous monosynaptic homonymous connections with the TA motor neurons. When proprioceptive sensory neuron activity is blocked, the density and the number of heteronymous connections is enhanced without any effect on homonymous connections (Mendelsohn et al., 2015). This study suggests that sensory inputs coordinate establishment of heteronymous, but not homonymous connections in an activity-dependent manner.

The monosynaptic sensory-motor circuits simplicity makes them an ideal model system for studying molecular mechanisms involved in the neuronal circuits formation and maintenance and for studying mechanisms of synapse elimination and circuitry perturbations that occur in neurodegenerative diseases (Imai and Yoshida, 2018). Disintegration of neuronal networks through synaptic elimination lead to compromised neuronal output and underlies neurodegenerative

diseases such as frontotemporal dementia (FTD), Alzheimer's disease (AD) and spinal muscular atrophy (SMA)(Lui et al., 2016; Tisdale and Pellizzoni, 2015; Verret et al., 2012; Vukojicic et al., 2019). However, unlike FTD and Alzheimer's disease, SMA occurs during early development both in animal models and humans (Montes et al., 2009; Tisdale and Pellizzoni, 2015)suggesting that affected neuronal networks are immature and therefore could be more vulnerable to synaptic perturbations (Vukojicic et al., 2019).

1.2.   Spinal Muscular Atrophy

Spinal muscular atrophy (SMA) is a group of inherited neuromuscular disorders, which are genetically heterogeneous and characterized by the spinal motor neurons defect, which leads to progressive weakness and atrophy of skeletal muscles, which is associated with the loss of spinal motor neurons (Oskoui et al., 2017; Sumner and Fischbeck, 2007). The first clinical description of SMA was published in 1891 and the wide clinical spectrum of the disease, with detailed descriptions across severities, was recognized over the next century. In 1990, mapping of the gene locus to chromosome 5q13.2 in both acute and chronic forms confirmed that indeed this clinical spectrum represents the same disease (Gilliam et al., 1990; Melki et al., 1990). Shortly after, in 1995 the survival motor neuron (SMN) gene was identified on chromosome 5q (Lefebvre et al., 1995). Homozygous mutations or deletions of the *survival motor neuron 1* (**SMN1**) causing SMN protein deficiency, are associated with the most prevalent form of proximal SMA. Although SMA patients have mutations in ubiquitous *SMN1* gene, they retain copies of almost identical hypomorphic gene named *SMN2* (Lefebvre et al., 1995; Tisdale and Pellizzoni, 2015). While human have both *SMN1* and *SMN2* gene, non-human primates and the rest of the animals lack SMN2, and have only one *SMN* gene (Rochette et al., 2001). From the time SMA was first described until today, there has been a progressive growth in understanding of the disease mechanisms. Creation of SMA animal models in the early 2000s was critical in studying the mechanisms involved in the disease (Oskoui et al., 2017).

1.2.1.   The SMN Gene

The *SMN* gene region is located on chromosome 5q13 and has a 500 kb inverted duplication element. The duplicated region consists of at least four genes as well as the repetitive elements, making it prone to deletions and rearrangements. The *SMN1* gene is located within the telomeric copy and in SMA patients this gene interrupted or deleted. The *SMN2* gene, which shares more than

99% of nucleotide identity with *SMN1* and differs only in five nucleotides is located within the centromeric copy (Figure 5) (Oskoui et al., 2017; Sumner and Fischbeck, 2007). While *SMN1* gene yields full-length transcripts, *SMN2* gene mostly produces transcripts that lack exon 7. This happens due to the C-to-T transition in exon 7 of *SMN2* gene which causes creation of an exon-splicing suppressor sequence (Kashima et al., 2007; Lorson and Androphy, 2000). This doesn't change an amino acid sequence, but it does affect alternative splicing of the *SMN2* gene, which results in exon 7 exclusion from majority of SMN2 transcripts. The outcome is the production of truncated and unstable full length SMN protein. Approximately 90–95% of SMN2 transcripts will produce truncated protein and only 5–10% functional full-length protein (Kashima et al., 2007; Lefebvre et al., 1995; Oskoui et al., 2017). All healthy individuals who happen to have one *SMN1* copy and lack *SMN2* copies, will have 50% of full-length functional SMN protein which will be sufficient for a normal life. However, the majority of SMA patients have 2-3 *SMN2* copies in Type I, Type II, and in some Type III patients and no *SMN1* gene. These patients are predicted to have 20–30% of full-length SMN protein at a maximum rate of 10% per *SMN2* gene (Oskoui et al., 2017; Sumner and Fischbeck, 2007). SMA Type III patients carrying four copies of *SMN2* gene have around 40% of SMN protein, which is still below the 50% that healthy carriers produce. Additionally, asymptomatic individuals have been described lacking *SMN1*gene and carrying five copies of SMN2 gene. They would be predicted to produce 50% of functional SMN protein (Mailman et al., 2002; Oskoui et al., 2017). Within the general population carrying two copies of *SMN1*, there is a variability in the number of *SMN2* copy numbers. Approximately 15% of these individuals have no *SMN2* copies, 33% carries only one *SMN2* copy, and 50% carries two *SMN2* copies (Mailman et al., 2002). Complete depletion of SMN - absence of *SMN1* and *SMN2* genes - is incompatible with life (Deguise et al., 2017; Schrank et al., 1997b). Thus, all SMA patients carry at least one *SMN2* gene copy. Among SMA patients a rough correlation exists between *SMN2* copy numbers and clinical severity (Lefebvre et al., 1997). The levels of SMN protein range from 22% to 23% in type I SMA fetal spinal cords (Lefebvre et al., 1997). Reduction of SMN protein levels was found to be even greater in postmortem spinal cords from Type I SMA patients who carried two copies of *SMN2* (Coovert et al., 1997). In SMA patients who have affected both copies of *SMN1*, low level of SMN protein is present, depending on the quality and copy number of their *SMN2* genes (Oskoui et al., 2017; Sumner and Fischbeck, 2007).
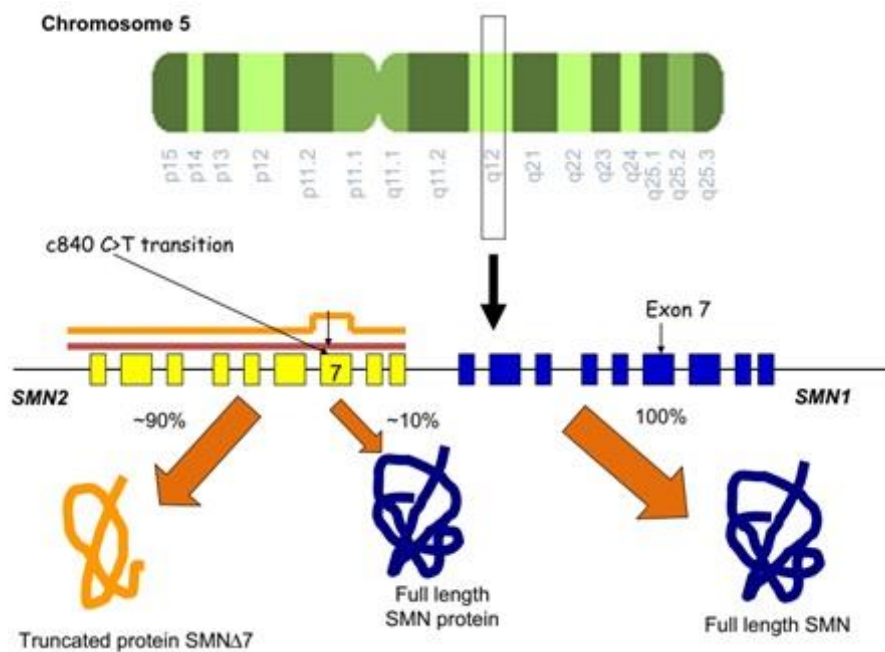
Figure 5. Schematic illustration of human *SMN1* and *SMN2* genes. *SMN1* and *SMN2* genes are located on chromosome 5. SMA patients have mutations or deletions in both copies of *SMN1*. A transition C-to-T at the 840 position of *SMN2* gene results in exon 7 skipping during splicing. A result is production of truncated, nonfunctional SMN protein. Only small portion ~ 5–10% of full-length mRNA is produced from *SMN2* gene, and results in full-length functional SMN protein. Adapted from (Darras, 2015).

The majority of SMA patients (95-98%) with the most common form – 5q SMA have a homozygous deletion that involves exon 7 of *SMN1* gene. The remaining patients have a heterozygous point mutation and a deletion. *De novo* mutations do occur at about 2% which is a relatively high rate, and happens because *SMN* gene region is unstable, and contains beside the inverted repeat of *SMN1* gene and *SMN2*, other repetitive elements - low copy number repeats, which make it more susceptible to rearrangements (Oskoui et al., 2017; Wirth et al., 1997).

The most common subtype of SMA is Type I and occurs with the prevalence of 4.1 cases per 100 000 live births (Mostacciuolo et al., 1992). The SMA Type I is the most severe form of the disease and occurs with the highest incidence compared to other subtypes. Approximately80–96% of children with SMA Type I have one or two *SMN2* gene copies and around 4–20% carry three copies. About 82% of children with SMA Type II carry three copies of *SMN2* gene, and around 96–100% of SMA Type III patients have three or four *SMN2* copies (Figure 6) (Arkblad et al., 2009; Feldkotter et al., 2002; Oskoui et al., 2017). Although copy number of *SMN2* gene is known as the main phenotype modifier it does not predict phenotype accurately. There is a growing

evidence of other factors that contribute to SMA severity. These potential modifiers of SMA include epigenetic modifiers, various proteins which interact with SMN or promote motor neuron survival and splicing or transcriptional factors influencing *SMN2* expression (Maretina et al., 2018).
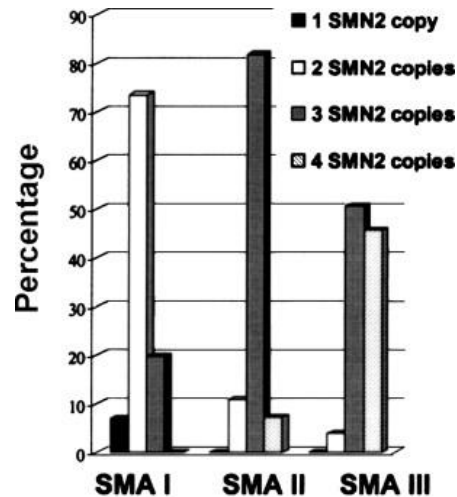
Figure 6. Diagram of the frequency of SMA patients with type I, type II, and type III SMA in comparison to *SMN2* copy number. In 80% of SMA Type I patients, one or two *SMN2* copies are present. 82% of SMA Type II patients have three *SMN2* copies, and 96% of SMA Type III patients carries three or four copies of *SMN2*. Adapted from (Feldkotter et al., 2002).

1.2.2. The SMN protein

The full-length SMN protein consist of 294 amino acids and weighs 38 kDa (also known as FL-SMN). SMN is ubiquitously expressed – found in all cells, and is located in cytoplasm and in the nucleus. In the nucleus, SMN localizes to structures called Gemini of coiled bodies, or simply "gems"(Liu and Dreyfuss, 1996). The SMA severity was found to correlate with the number of gems found in patient fibroblasts (Coovert et al., 1997). The SMN protein and several Gemin proteins form a large macromolecular complex – SMN complex - that facilitates assembly of the spliceosomal small nuclear ribonucleoproteins (snRNPs). The snRNPs are crucial components of the spliceosome complex, with an essential role in pre-mRNA splicing (Pellizzoni et al., 2002). Additionally, SMN protein may have critical roles in axonal mRNAs transport in motor neurons and in assisting arginine methylation of certain splicing-related proteins. SMN protein may be also involved in different processes neuromuscular junction and in muscle. However, it is currently unclear whether SMN deficiency caused splicing defect or disruption of axonal SMN function, or

yet unknown SMN function, or simply combination of all is behind the SMA pathogenesis (Arnold and Burghes, 2013; Oskoui et al., 2017). It has been shown in mice and other organisms, that complete absence of SMN protein is embryonic lethal (Monani et al., 2000). However, why are motor neurons specifically vulnerable in case of partial SMN deficiency is currently unclear. Function of SMN protein and its role in pathogenesis of SMA remains to be better understood (Burghes and Beattie, 2009; Oskoui et al., 2017).

1.2.3. Clinical characteristics of SMA in human

SMA patients have proximal muscle weakness that is usually symmetric and affects lower limbs more than patient's upper limbs. While disease involves intercostal muscle, diaphragm is relatively spared (Arnold and Burghes, 2013; Oskoui et al., 2017; Sumner and Fischbeck, 2007). The muscle weakness and the atrophy in SMA is attributed to motor neuron loss and dysfunction. The neuromuscular junction function and development is impaired across SMA subtypes (Goulet et al., 2013; Wadman et al., 2012).The skeletal muscle pathology observed in children affected with SMA is a reflection of motor neuron disorder with a neurogenic type atrophy and a Type I fiber hypertrophy (Oskoui et al., 2017). The severity of SMA is variable with heterogeneous clinical features across subtypes.

1.2.3.1. Type I Spinal Muscular Atrophy

Type I SMA (Werdnig–Hoffmann disease), is the most severe and the most common form of the disease. Affected infants, experience in the first 6 months of life (Zerres and Rudnik-Schoneborn, 1995) proximal weakness, which affects their legs more than arms., movement deficiencies and reduced muscle tone. These infants usually show generalized hypotonia demonstrated by "frog-leg posture" when lying horizontally and facing up, tongue fasciculations, areflexia and they slip through on a vertical suspension (Figure 7a and 7b). These babies have a weak cry, difficulty sucking and swallowing, and they do not reach developmental milestone of rolling over independently or being able to stay seated independently ("nonsitters") or sit up unassisted. Their thorax is bell-shaped, with evidence of diaphragmatic breathing and intercostal muscle weakness (Arnold and Burghes, 2013; Oskoui et al., 2017).

Figure 7. SMA Type I clinical manifestations (A) Dangling lower limbs and lack of hip flexion is notable with vertical suspension. Upper limbs tend to slip through examiner's hands. Head lag due to the lack of neck flexion. (B) When infant is supine, "frog-leg" positioning of the legs is notable with the absence of traction response. (C) Head lag with examiner's attempts to pull infant into the sitting position. Adapted from (Oskoui et al., 2017).

In the SMA Type I patients often other organ dysfunction and involvement is recognized, which points to the fact that SMN protein is ubiquitously expressed (Heier et al., 2010). In infants affected by severe forms as well as in mouse models, hypovascularity or vascular depletion are dominant characteristic. A resulting consequence of these vascular defects is functional hypoxia of spinal motor neurons (Somers et al., 2016). SMA patients have normal cognition and even higher than average intelligence has been reported (von Gontard et al., 2002). Further classification of SMA Type I disease is made based on the onset of symptoms. Infants in which symptoms are noted prenatally or during the first week of life are classified as SMA Type IA. Most of them carry only one copy of *SMN2* gene and they die in less than one month, usually soon after birth. Infants in which symptoms develop between first week of life and three months of age are classified as SMA Type IB, and those who develop symptoms sometime between three and six months of age usually have two *SMN2* copies and are classified as SMA Type IC. Most infants affected with SMA Type I, without intervention do not survive beyond the age of two years. However, with management of pulmonary complications and appropriate respiration support, gastrointestinal and nutritional support, orthopedic care and rehabilitative interventions survival has been prolonged beyond the second year (Arnold and Burghes, 2013; Oskoui et al., 2007). Until recently there was not a single medication approved for treatment of SMA patients. The first ever approved medication for treatment of SMA was Nusinersen, (commercial name Spinraza) by Biogen (Garber, 2016). Nusinersen is an antisense oligonucleotide (ASO) designed to target intron 7 on the SMN2 hnRNA

(Castro and Iannaccone, 2014; Corey, 2017; Shahryari et al., 2019) and modulate alternative splicing by increasing exon 7 inclusion in the processed final RNA, resulting in increased levels of functional full length SMN protein in the central nervous system (Corey, 2017; Shahryari et al., 2019; Zanetta et al., 2014). Nusinersen was approved in December 2016 by US Food and Drug Administration (FDA) when it also became the first antisense drug acting to restore an exon inclusion during pre-mRNA splicing(Ottesen, 2017). It involves intrathecal administration (Chiriboga, 2017). Another gene therapy drug, developed by AveXis (Novartis) under brand name Zolgensma (Onasemnogene Abeparvovec, AVXS-10), was recently FDA approved (May 2019) for SMA patients younger than two years of age. Zolgensma is a single dose, AAV9-based (adeno-associated virus) gene therapy administered intravenously. Zolgensma is a recombinant non-replicating AAV9 containing a copy of functional human *SMN1* gene which is under the control of cytomegalovirus enhancer/chicken-β-actin-hybrid promoter in order to express *SMN1* selectively in SMA patients motor neurons (Malone et al., 2019; Mendell et al., 2017; Shahryari et al., 2019; Waldrop and Kolb, 2019). Although there has been a great improvement in recent years with a development of these gene therapies for SMA, none of the treatments can cover all the aspects of the disease pathology and neither of them are considered a cure for the disease. Thus, a combinatorial therapeutic strategy might be the most effective for treating this devastating disease.

1.2.3.2. Type II Spinal Muscular Atrophy

Children affected with SMA Type II, which is known as Dubowitz disease or intermediate SMA usually present first symptoms between six and eighteen months of age. Type II patients achieve the ability to sit without support and stay seated independently, although in some cases this ability may be lost over time. Children with SMA Type II are never able to stand or walk unaided ("sitters") and majority has three *SMN2* copies (Arnold and Burghes, 2013; Arnold et al., 2015; Oskoui et al., 2017). Affected children have predominantly proximal muscle weakness involving their lower limbs more than the upper limbs, areflexia and, hypotonia. Face and muscles of the eye are usually unaffected (Butchbach, 2016). Additionally, these children may develop respiratory difficulties and hypoventilation while asleep. Survival of SMA type II patients is into adulthood, though it can be shorter especially in children with respiratory difficulties. (Arnold and Burghes, 2013; Oskoui et al., 2017). Previously reported survival rates of 98.5% at 5 years and 68.5% at 25 years have increased past their 25th birthday with respiratory and nutritional support (Zerres et al., 1997) and even greater increase may be seen in future with the recent approved gene therapies.

1.2.3.3.   Type III Spinal Muscular Atrophy

Children affected with SMA Type III, also known as Kugelberg–Welander disease achieve independent mobility ("walkers"), though proximal weakness may cause falls and difficulty climbing stairs. Additionally, some patients may lose the ability to stand and walk over time and rely on wheelchair to move around. Symptoms appear after eighteen months of age. Type III SMA patients have proximal muscles affecting their lower limbs more than upper limbs. Clinical diagnosis can be more challenging as tendon reflexes are usually preserved at the time of examination. Most patients develop scoliosis, foot deformities and respiratory muscle weakness. Most patients carry three or four *SMN2* copies (Arnold et al., 2015). Type III SMA accounts for approximately 30% of overall SMA cases. Life expectancy of SMA Type III patients does not significantly differ from the normal population (Oskoui et al., 2017; Zerres and Davies, 1999; Zerres et al., 1997).

1.2.3.4.   Type IV Spinal Muscular Atrophy

SMA Type IV is a late-onset SMA, with symptoms usually present after 21 years of age with the mean age of onset in the mid-thirties. This mildest form is the least prevalent subtype and accounts for less than 5% of all SMA cases (Arnold et al., 2015). Patients with SMA type IV have proximal limb girdle weakness but they achieve motor milestones and they maintain mobility throughout their life and carry four or eight copies of *SMN2* gene (Butchbach, 2016). Life expectancy for Type IV SMA patients is normal.

1.2.4. Animal models

In the past two decades, significant progress has been made in understanding the molecular basis of the SMA clinical spectrum which allowed creation of SMA animal models. Beside mouse models, which are perhaps the most widely used, SMA has been also studied in *Caenorhabditis elegans*, *Drosophila*, and Zebrafish models which due to the simplicity of model organisms allow for easy molecular and genetic manipulation (Edens et al., 2015). Mice, unlike humans, have only one *SMN* gene which is equivalent to human *SMN1* (DiDonato et al., 1997; Viollet et al., 1997). As in all species, homozygous knockout of *Smn1* is embryonically lethal (Schrank et al., 1997a). Introduction of one or two copies of human *SMN2* rescues the embryo, resulting in mice with a severe SMA-like phenotype. These mice die around postnatal day 5 (Hsieh-Li et al., 2000; Monani

et al., 2000). In contrast, introduction of eight to sixteen copies of human *SMN2* gene in the *Smn* knockout mouse rescues the phenotype with no difference in life span than wild-type mice(Le et al., 2005; Monani et al., 2000). The Δ7 SMA mice have in addition to two copies of human *SMN2*, and an SMN transgene that lacks exon 7 (SMNΔ7). This addition of SMNΔ7 prolongs lifespan of mice to around 13.3 days after birth. The Δ7 SMA mouse model is among most widely used SMA models to date (Hsieh-Li et al., 2000; Le et al., 2005; Monani et al., 2000). This animal model was used for all the studies presented here. SMAΔ7 mice experience selective spinal motor neuron death, muscle atrophy, and closely recapitulate clinical characteristics seen in human Type I patients (figure 8).
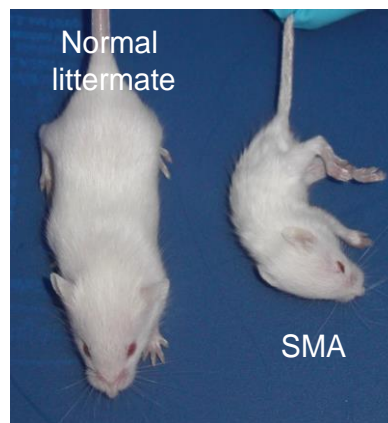
Figure 8. Late stage SMAΔ7 mouse *vs* WT littermate. Wild type (WT) mouse at postnatal day 11 (P11) on the left side of the image. SMA littermate on the right side of the image with evident severe muscle atrophy and loss of posture. Photo courtesy of Dr Charlotte Sumner.

Although hallmarks of SMA are death of motor neurons and muscle atrophy, one of the earliest manifestations of disease in SMAΔ7 mouse model is sensory-motor dysfunction (Mentis et al., 2011). Circuit dysfunction which is a consequence of SMN deficiency that causes disease could be an initiating and/or propagating drive of impaired motor behavior. Neurodegeneration is usually attributed to dysfunction of a specific neuronal cell type which is vulnerable to disease mechanisms (Rademakers et al., 2012). In SMA, although SMN is ubiquitously expressed, spinal motor neurons are somehow selectively susceptible to SMN deficiency. SMA was thought to be motor neuron - autonomous disease, in which neurodegeneration is due to the motor neuron death and dysfunction *per se*. However, it is possible that dysfunction of neurons that are primary targets in the disease process may affect their synaptic partners and further aggravate the disease (Palop and Mucke, 2010). Animal models have a key role in addressing these and similar questions in order to decipher the disease mechanisms and in testing the therapeutic effect of potential drugs.

1.2.5. Motor Neuron Death

Majority of the autopsy studies on postnatal spinal cords from SMA patients have described motor neuron loss as severe (Korinthenberg et al., 1997; Simic et al., 2000). Although SMN level is reduced in all tissues, the hallmark of the SMA is selective loss of motor neurons in spinal cord in humans as well as in mouse models of the disease (Burghes and Beattie, 2009; Simon et al., 2017; Tisdale and Pellizzoni, 2015). Furthermore, even within individual motor neuron pools there is marked differential vulnerability (Simon et al., 2017). It has been demonstrated that, spinal alpha MNs (which innervate proximal muscles) are preferentially affected and also degenerate early compared to alpha MNs that innervate distal muscles which are relatively spared (Mentis et al., 2011). Moreover, motor neurons in SMA show segment-specific, differential vulnerabilities noted along the rostro-caudal axis. Motor neurons from lumbar level L1, that innervate proximal and axial muscles are affected more profoundly and earlier in the disease process than motor neurons in the L5 region, that innervate distal hindlimb muscles (Mentis et al., 2011; Tisdale and Pellizzoni, 2015). Furthermore, medial motor column motor neurons which innervate axial muscles are affected more than the lateral motor column motor neurons that innervate distal muscles. This is consistent with observations in SMA patients (Mentis et al., 2011). Additionally, in a severe model of SMA gamma MNs were observed to be spared (Powis and Gillingwater, 2016). Interestingly, ubiquitous SMN deficiency induces selective death of specific vulnerable motor neuron pools while sparing resistant ones that share similar functional properties and developmental programs (Simon et al., 2017).In addition, other spinal neurons are also spared in SMA (Powis and Gillingwater, 2016). In recent study a convergent pathway involving p53 has been proposed as a key mediator of SMN deficiency-induced motor neuron death. Phosphorylation of p53 serine 18 was identified as a death-specific marker which is selectively found in vulnerable SMA motor neurons but not in resistant ones or in spinal interneurons even though nuclear accumulation of p53 are present late in the disease process in SMA mice (Simon et al., 2017).

1.2.6. Sensory-Motor circuitry impairment

Apart from spinal motor neurons death, SMA is characterized by additional pathologies occurring centrally, at synapses contacting motor neurons soma and dendrites as well as distally - at the neuromuscular junction (Figure 9). The NMJ defects involve reduced vesicle content, presynaptic neurofilament accumulation, impaired synaptic transmission, and defects in motor endplate development and in acetylcholine receptor clustering at postsynaptic membrane (Kariya et

al., 2008; Lee et al., 2011; Ling et al., 2010a; Murray et al., 2008; Tisdale and Pellizzoni, 2015). Functional and morphological impairments of the NMJ correlate with decreased myofiber size delayed NMJ development and with muscle denervation, which is all notably pronounced in vulnerable SMA muscles (Kariya et al., 2008; Kong et al., 2009; Ling et al., 2010a; Murray et al., 2008; Tisdale and Pellizzoni, 2015).

Beside appropriate connectivity needed between muscles on periphery and motor neurons in spinal cord, proper wiring between motor neurons and other neurons is crucial for normal motor behavior. Perturbations of neuronal circuits are being recognized as critical determinants of neurodegenerative disorders (Fletcher and Mentis, 2017; Tisdale and Pellizzoni, 2015). It has been shown that motor neurons in SMA have reduced glutamatergic synaptic inputs from local spinal interneurons and from proprioceptive sensory neurons (Figure 9) (Ling et al., 2010a; Mentis et al., 2011). Moreover, sensory-motor neurotransmission was showed to be severely impaired and associated with dysfunction of proprioceptive sensory synapses in SMA mice (Mentis et al., 2011). However, molecular mechanisms reponsible for dysfunction of proprioceptive synapses and for their reduced numbers are not well understood. Addtionally, it has been demonstrated that SMA motor neurons have altered firing properties along with increased intrinsic excitability (Mentis et al., 2011). This functional changes might be a homeostatic response to reduction in excitatory drive originating from premotor neurons (Mentis et al., 2011; Tisdale and Pellizzoni, 2015).
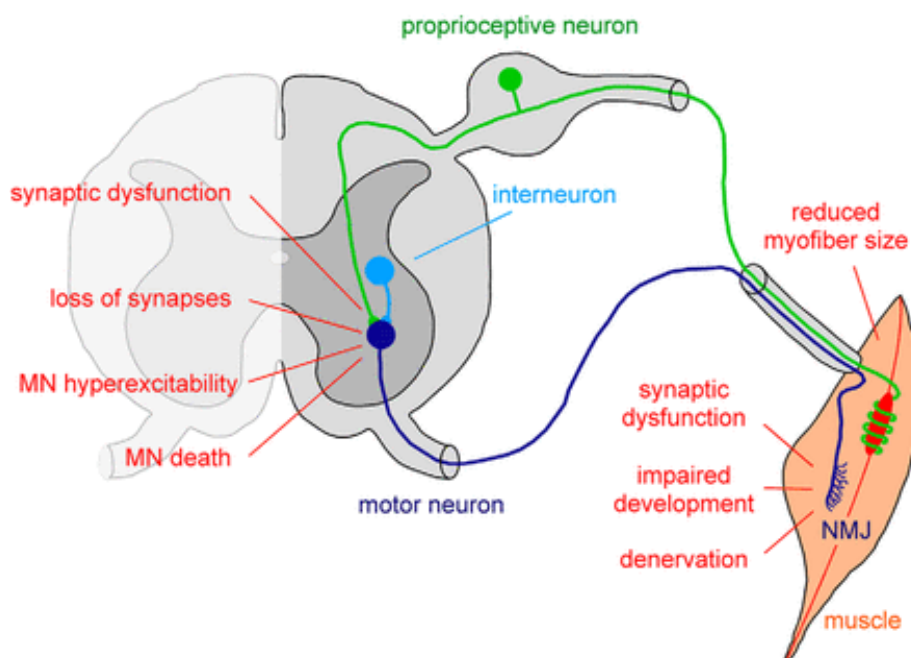
Figure 9. Schematic illustration of the key functional and morphological abnormalities of the motor system in SMA mouse models. Spinal motor neurons are shown in dark blue,

proprioceptive neurons in green and local interneurons in light blue. The specific deficits of the circuitry centrally and at the periphery are indicated. Adapted from (Tisdale and Pellizzoni, 2015).

Taken together, these findings suggest that SMN deficiency induced synaptic abnormalities in the sensory-motor system are at least partially responsible for the severe motor dysfunction seen in SMA. In support of this, is the observation that functional and structural sensory-motor circuitry impairment precede motor neuron death. To better understand disease process and design treaments it was important to identify the importance of cell-autonomous and non-cell autonomous mechanisms contributions to the disease pathology (Fletcher and Mentis, 2017; Tisdale and Pellizzoni, 2015). Previous studies have demonstrated in SMA mice that pan-neuronal SMN expression rescues disease phenotype. However, SMN specific restoration in muscles did not improve the severe phenotype (Gavrilina et al., 2008). Furthermore when SMN is selectively depleted from motor neuron progenitors, motor neurons will die and as a consequence will be a mild SMA phenotype (Park et al., 2010). Additionally, motor-neuron-specific resotration of SMN has been demonstrated to improve motor neuron loss. However, it has little effect on SMA mice survival (Gogliotti et al., 2012; Martinez et al., 2012; Tisdale and Pellizzoni, 2015). Taken together, results of these studies indicated that neuronal dysfunction plays a critical role in SMA pathology and that SMA is a disease defined by dysfunction of different motor system components and not solely motor neurons (Tisdale and Pellizzoni, 2015). In order to decipher mecanisms involved in SMA pathogenesis it is important to unravel the role(s) of different motor system components in the disease process. Although motor neuron death is a cell autonomous event, a recent study has demonstrated that SMN deficiency induces defects in other neuronal types that also contribute to pathology of motor system in SMA (Fletcher et al., 2017) suggesting that SMA is a disease defined by dysfunction of different motor system components and not solely motor neurons (Fletcher et al., 2017; Tisdale and Pellizzoni, 2015).

1.2.7. Sensory-motor circuitry pathology in SMA is due to proprioceptive – autonomous mechanisms

To determine the cellular origin of sensory-motor circuit dysfunction in SMA, Fletcher and colleagues used genetic manipulations to selectively restore SMN in the following neurons: i) solely in motor neurons, ii) solely in proprioceptive neurons, or iii) both neuronal classes in SMA mice (Fletcher et al., 2017). Parvalbumin::Cre (Pv^{Cre}) mice were crossed with the conditional inversion SMA mice to restore SMN protein in proprioceptive neurons (SMA+Pv^{Cre}). During the first ten postnatal days parvalbumin is expressed in proprioceptive neurons exclusively (Mendelsohn et al.,

2015) and has the similar level of expression in WT and SMA mice (Fletcher et al., 2017). Although parvalbumin expression is observed at P5 in the cerebellum (Fletcher et al., 2017), the righting behaviors are not dependent on cerebellar activity, until the second postnatal week (Altman, 1997; Fletcher et al., 2017). In the study by Fletcher et al (2017), the authors restored SMN in motor neurons by crossing the conditional inversion SMA mice with mice that express Cre under the ChAT (Choline Acetyltransferase) promoter (SMA+ChAT^{Cre}) (Fletcher et al., 2017).

To define the effect of SMN loss on motor neuron dysfunction, the authors performed intracellular recordings from vulnerable spinal motor neurons using whole cell patch clamp following dorsal root stimulation (Fletcher et al., 2017). The EPSP amplitude was measured in L2 motor neurons in WT, SMA, SMA+Pv^{Cre} and SMA+ChAT^{Cre} following the proprioceptive fiber stimulation. No significant change was observed in the motor neuron resting membrane potential for any of the experimental groups. Importantly, the reduction of EPSP amplitude observed in SMA motor neurons was restored in SMA+Pv^{Cre} but not in SMA+ChAT^{Cre} motor neurons (Fletcher et al., 2017) (Figure 10, A-B) suggesting that motor neuron dysfunction is a non-cell autonomous consequence of SMN deficiency from proprioceptive neurons.
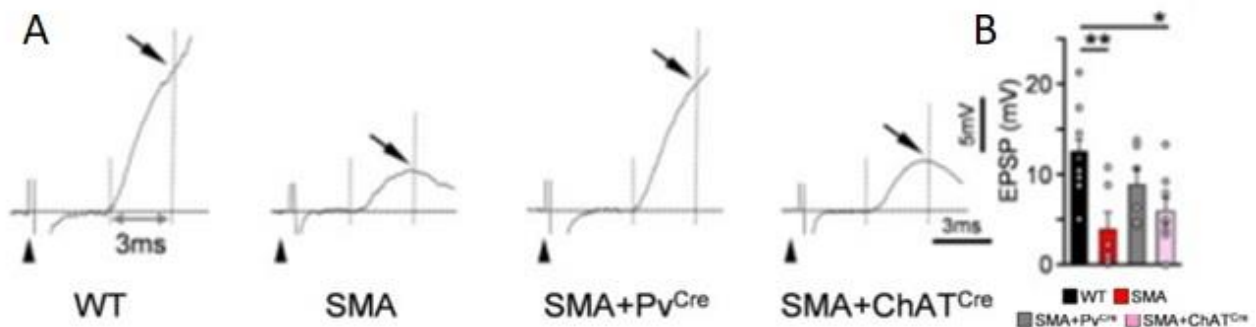
Figure 10. Selective restoration of SMN in proprioceptive neurons in SMA mice restores EPSP amplitude. (A) Intracellular responses of monosynaptic EPSPs following supramaximal stimulation of L2 dorsal root in homonymous motor neurons for WT, SMA, SMA +Pv^{Cre} and SMA+ChAT^{Cre} L2 mice at postnatal day 4 (P4). The peak of EPSP amplitude measured at 3 ms after the onset of response is indicated by arrows. Arrowheads indicate the stimulus artifact. (B) Graph shows the average peak of EPSP amplitude in motor neurons for the experimental groups shown in (A). * P<0.05, ** P<0.01, one-way ANOVA, Tukey's post hoc analysis. Adapted from (Fletcher et al., 2017).

1.2.8. Dysfunction and death of motor neurons are distinct and independent events in SMA

The hallmark of SMA is motor neuron death (Tisdale and Pellizzoni, 2015). Hyperexcitability of motor neurons has been implicated in neuronal death in amyotrophic lateral sclerosis (ALS) (Umemiya et al., 1993) and upon axotomy of facial (Umemiya et al., 1993) and spinal motor neurons (Mentis et al., 2007). These results raised the possibility that synaptic dysfunction might be causally related to motor neuron death in SMA. To address this possibility, Fletcher et al counted the number of vulnerable (L2) motor neurons in mice in which SMN was selectively restored in either motor neurons (SMA+ChAT[Cre]) or in proprioceptive neurons (SMA+Pv[Cre]) as previously described (Mentis et al., 2011). No significant motor neuron loss was observed at postnatal day 2 (P2), whereas 34% of motor neurons were lost at P4 and 42% at P11 (Fletcher et al., 2017) (Figure 11, A-B).
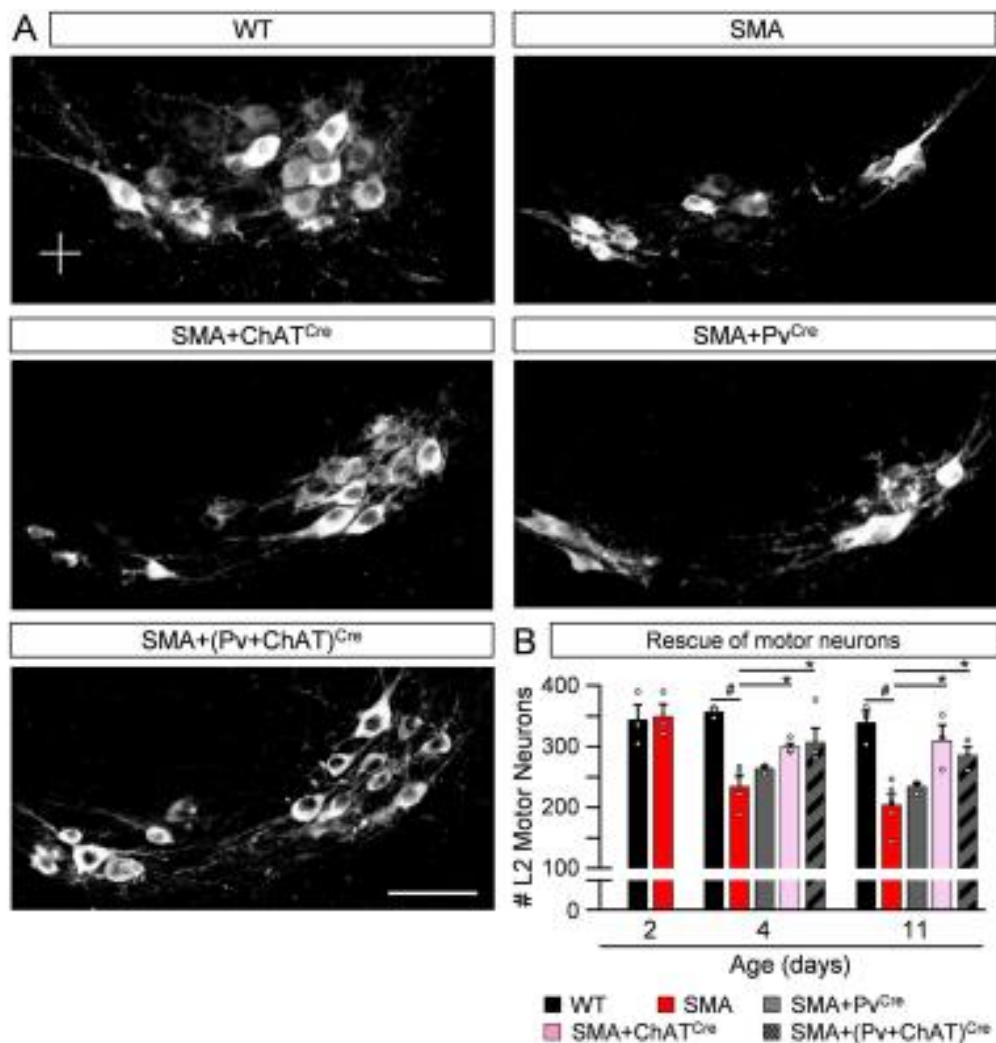
Figure 11. Motor neuron loss in SMA is mediated by cell autonomous mechanisms. (A) Confocal images of L2 motor neurons visualized by ChAT immunoreactivity (and shown in white)

in WT (n=3), SMA (n=4), SMA+Pv^{Cre} (n=3), SMA+ChAT^{Cre} (n=4) and SMA+(Pv+ChAT)^{Cre} (n=4) mice at P4. (B) Time course (P2–P11) of the total L2 motor neurons number for the experimental groups shown in (A). All data are represented as mean ± s.e.m. # P<0.05, one-way ANOVA (WT v SMA); * P<0.05, one-way ANOVA, Tukey's post hoc analysis. Adapted from (Fletcher et al., 2017).

Selective restoration of SMN in proprioceptive neurons (SMA+Pv^{Cre}) did not prevent motor neuron death, whereas SMN restoration in motor neurons (SMA+ChAT^{Cre}) rescued motor neurons both at early (P4) and late (P11) stages of disease. There was no additional motor neuron rescue observed in SMA+(Pv+ChAT)^{Cre} mice (Fletcher et al., 2017) (Figure 11, A-B). Collectively, these results demonstrated that motor neuron death is not induced by SMN-deficiency in sensory neurons, indicating that motor neuron death in SMA is a motor-neuron cell autonomous event due to SMN deficiency in motor neurons *per se*. Furthermore, these results separated death and dysfunction of motor neurons as two independent and distinct events, suggesting that they are driven by different mechanisms.

1.3.   Complement and microglia in CNS development and neurodegeneration

1.3.1.   Complement proteins in the periphery

The complement system consist of ~60 distinct circulating and membrane-bond plasma proteins. They interact with each other to opsonize pathogens, activating array of inflammatory responses which further aid in fighting infection (Medzhitov and Janeway, 2000). In the periphery, complement   is a leading mediator of inflammation. Complement proteins serve as a first line of defense, playing a crucial role in the defense against infection, by a quick elimination of invading pathogens. Complement system have also an important role in regulating adaptive immune response. Furthermore, complement system plays an immune surveillance role through removal of cellular debris and apoptotic cells , thus protecting against autoimmunity (Carroll and Isenman, 2012; Medzhitov and Janeway, 2002; Presumey et al., 2017; Ricklin et al., 2010). Complement proteins interact one with another through a sequential enzymatic cascade which results in elimination of pathogens. Surrounding host cells are normally protected from complement through membrane-bound inhibitors expressed on their cell surface. Soluble complement proteins are inactive zymogens until they encounter the pathogen's cell membrane or a foreign material. Upon binding to a target, complement proteins overgo structural changes, followed by proteolytic

cleavage, and finally assembly into convertases - active enzyme complexes - which will subsequently activate downstream proteins leading to pathogen lysis or phagocytosis (Coulthard et al., 2018; Dunkelberger and Song, 2010; Janeway, 2001; Stephan et al., 2012). Because circulating complement proteins are inactive zymogens, they can be widely distributed until needed locally (Janeway, 2001; Noris and Remuzzi, 2013). Endothelial cells and leukocytes recognize products of complement proteolytic cleavage and aid migration of immune cells to sites of inflammation and complement-opsonized agents (Coulthard et al., 2018; Medzhitov and Janeway, 2000). The complement system can be activated by three separate pathways (Figure 12). They all converge on cleavage of complement component C3 – a central molecule in the complement system, that produces effector complement fragments which drive complement functions, including the elimination of pathogens, debris, and cellular structures. However, all three pathways differ in the way they get activated (Coulthard et al., 2018; Janeway, 2001; Noris and Remuzzi, 2013).
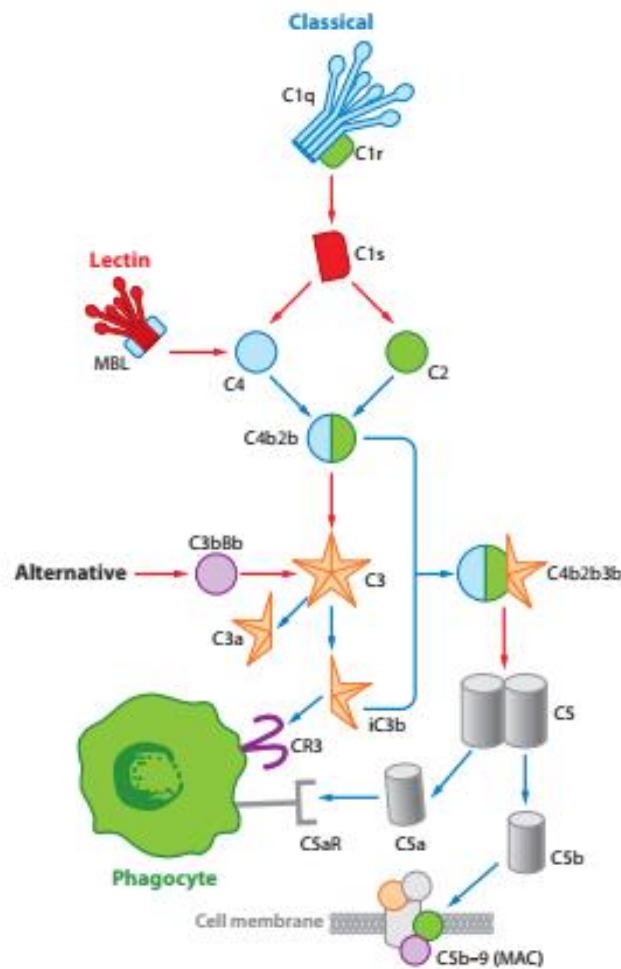
Figure 12. The complement pathway activation: classical, lectin and alternative pathway.
The complement components are activated in a cascade-like manner by one of three major pathways: The classical pathway is initiated when C1q interacts with one of its binding partners

(e.g. antibodies, DNA, RNA, serum pentraxns, apoptotic cells). C1r and C1s proteases bind C1q tail region and form the C1 complex. Binding of C1q complex to target induces conformational change in the C1q leading to enzymatic activity in C1r cleavage of C1s and generation of active serine protease. Activated C1s cleaves C4 and C2 and generates C3 convertase (C3b2b), which cleaves C3 activating downstream components. The lectin pathway is initiated by the binding of mannose binding lectin (MBL) to the residues of mannose on the cell surface. The alternative pathway is spontaneously activated through spontaneous C3 hydrolysis and serves to amplify he pathway initiated by classical or lectin cascade. All three pathways converge on the complement component, C3. C3 cleavage generates opsonin C3b and anaphylactic peptide C3a. C3b/iC3b opsonization leads to elimination of the target by phagocytes expressing C3 receptors. C3b joins C4b2a (the C3 convertase) forming the C5 convertase (C4b2a3b complex) which generates anaphylatoxin C5a, that binds to C5a receptors (C5aR) on phagocytes. Potent complement activation can lead to the terminal complement cascade activation and the target cell lysis through the insertion of membrane attack complex (MAC) - the pore-forming C5b-C9 complex. Adapted from (Stephan et al., 2012).

The classical pathway is activated when C1q - the initiating protein of the pathway, binds to one of its various ligands, including serum pentraxins, antigen-antibody complexes, C reactive protein (CRP), viral membranes, polyanions (RNA, DNA, , and lipopolysaccharides), and apoptotic cells (Gaboriaud et al., 2011; Kang et al., 2006; Kishore and Reid, 2000; Stephan et al., 2012), When C3 is cleaved, activated C3 fragments - C3b and iC3b opsonize targets leading to its elimination by phagocytic cells through C3 receptors (i.e., CR3/Cd11b, Figure 12). Furthermore, potent C3 activation can provoke the terminal activation of classical pathway resulting in cell lysis by formation of the lytic membrane attack complex (MAC) (Figure 12)(Janeway, 2001). The lectin pathway, which is an antibody-independent pathway, is initiated when the mannose binding lectin (MBL) or a group of related proteins binds to terminal sugar moieties that are expressed on glycoproteins or polysaccharides on cell membranes (Degn et al., 2007; Fujita, 2002; Janeway, 2001; Stephan et al., 2012). The alternative pathway is spontaneously activated and can serve as an amplification loop of classical and lectin pathway (Janeway, 2001) acting as an amplifier.

Considering that complement pathways results in such powerful destructive and inflammatory effects they must be tightly regulated. Importantly, when activated, critical complement components are promptly inactivated if they do not bind to the surface (i.e.pathogen) on which their activation was originally initiated. Additionally, there are several check points in pathways at which comlement regulatory proteins act to protect host cells from unintended damage or elimination. Balance between activation and inhibition of the complement activation is critical for a correct complement function as well as for the tissue homeostasis (Janeway, 2001; Kim and

Song, 2006; Zipfel and Skerka, 2009). While, a battery of well described regulatory proteins tightly controls complement cascade in the periphery, little is known about complement regulators in the CNS.

1.3.2. Complement in developmental synaptic pruning

Traditionally, the brain has been viewed as an immune privileged organ. Studies from early and mid 20th century involving transplantation of tumor, fetal tissue and skin grafts into the brain gave rise to this concept. In support of it, are anatomical characteristics of the brain and spinal cord as they are protected by meninges and the cerebrospinal fluid. Additionally, presence of the blood-brain barrier (BBB), protects from the entry of pathogens, harmful factors and circulating immune cells. However, in recent years, this thought of immune privilege has shifted significantly with the growing knowledge that the immune and nervous system interact in various ways. These complex neuroimmune interactions exist under homeostatic as well as under pathological conditions (Louveau et al., 2015; Stephan et al., 2012). Additionally, recent demonstration of Meningeal Lymphatic System existance (Louveau et al., 2018), further modifies the immune privileged view of CNS. Both, central nervous and immune system have a wide array of molecules and signaling pathways with different and comparable functions in each system. Among these immune-nervous system "cross road" molecules are the classical complement pathway components.While the role of the classical complement cascade in the periphery is well known, its function in the central nervous system is under wide-ranging investigation.

At birth, the vertebrate brain contains excess synapses, between neurons. For the establishment of the precise, mature neural circuits, these excess connections must be removed. This process is called synaptic pruning (Hua and Smith, 2004; Katz and Shatz, 1996). Elimination of synapses during circuitry refinement is a developmental process in which certain subsets of synapses are removed while the remaining ones are strengthened and maintained (Paolicelli et al., 2011; Schafer et al., 2012; Stephan et al., 2012; Tenner et al., 2018). Synaptic pruning occurs during postnatal development -a period of remarkable plasticity, but depending on the CNS region and neuronal circuit, during different critical periods.

Rodent visual system has served as a model system to study synaptic pruning in the brain. Recent research revealed an unexpected and remarkable role for the classical complement pathway in the refinement of visual inputs to the lateral geniculate nucleus (LGN) during the early postnatal eye-specific segregation (Stevens et al. 2007). Synaptic pruning is a critical process necessary for correct establishment of neuronal circuits and is thought to be driven by neuronal activity, in such

way that less active or "weak" synapses are removed, which allows for maturation and strengthening of more active ones. Complement proteins are widely expressed in the postnatal brain but during the active circuitry remodeling periods they localize specifically to the subsets of developing synapses. Classical complement pathway components tag synapses for removal by microglia that express complement receptors (Presumey et al., 2017; Schafer et al., 2012; Stevens et al., 2007). There is a growing evidence that related, complement-based mechanisms are involved in synaptic pruning and circuitry refinement in other areas of developing brain (Chu et al., 2010; Coulthard et al., 2018; Stevens et al., 2007). Thus, it is critical to understand when and where are complement components normally expressed in the CNS, as that will help unravel complement functions during normal development as well as in disease. Additionally, it would be important to understand whether complement-dependent synaptic pruning could be a mechanism for developmental synapse elimination in other regions of CNS, as much of the current knowledge is coming from the visual system.

When the synaptic refinement goes wrongly, neuronal circuitries are not properly formed resulting in either too few, too many, or inappropriate synapses. These circuitry perturbations are thought to underlie numerous neurological disorders. Recent studies have indicated involvement of complement proteins in neurodevelopmental disorders, such as schizophrenia and autism (Fagan et al., 2017; Presumey et al., 2017; Sekar et al., 2016). Furthermore, these developmental synaptic pruning mechanisms appear to be reactivated in neurodegeneration and by aging (Presumey et al., 2017).

1.3.3. C1q structure and function

C1q is the first subcomponent of the C1 complex serving as a recognition molecule in the classical complement cascade. However, C1q can act both dependent or independent of classical complement pathway (Janeway, 2001). The human C1q protein weighing 460 kDa is composed of 18 polypeptides and up to 226 amino acid residues each. C1q consists of 6 heterotrimers each of which contains C1qA, C1qB, and C1qC chains. Thus, C1q heterotrimers have collagen-like triple helices structure and associate in their N-terminal portion forming a "stalk", that later separates into individual "stems". Each stem terminates with a C-terminal globular domain (gC1q), each containing a C1qA, C1qB, and C1qC chain (Figure 13) (Gaboriaud et al., 2003; Kishore and Reid, 2000; Mortensen et al., 2017; Sontheimer et al., 2005).
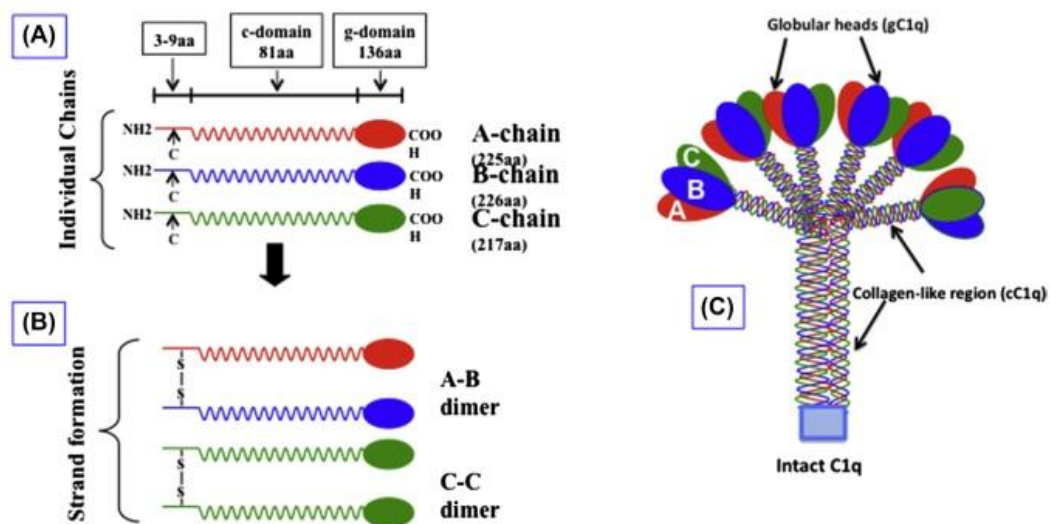
Figure 13. Structural organization of the C1q molecule. (A) C1q molecule is made of 6A, 6B and 6C chains. (B) The chains form six individual strands. Each strand is made up of A-B dimer, noncovalently associated with a C-chain. (C) Two strands are disulphide-bonded through adjacent C-chains and form a doublet. Finally, three doublets are noncovalently linked and form the intact hexameric C1q. Adapted from (Ghebrehiwet, 2018).

While the C-terminal parts form gC1q that allows ligand recognition the N-terminal regions stabilize C1q through interchain disulfide bridges forming (CLR or cC1q). Approximately 35 residues of the N-terminal part of all six C1q heterotrimers have cylinder-shaped organization after which they separate into individual stems following a kink which is in each heterotrimer caused by an imperfect GXY triplet pattern occurring in C1qA and C1qC chains (Kilchherr et al., 1985; Mortensen et al., 2017).The final structure of C1q molecule bears resemblance to a bouquet of tulips (Figure 13). Globular C1q domain, gC1q, at the C-terminus and a short N-terminal collagen-like region represent two unique functional and structural domains (Figure 13) (Brodsky-Doyle et al., 1976; Cho, 2019; Knobel et al., 1975).

They are independent one of another and interact with diverse biological structures which includes cell-associated and pathogen-associated molecules (Cho, 2019). Globular head domains of C1q are responsible for ligand recognition. Each of the three gC1q subunits has particular surface patterns in regards to their hydrophobic and charged residues, thus may be expected to present individual specific recognition properties. In addition, compact trimeric C1q head structure allows recognition of the ligand by residues contributed from two or sometimes even three subunits, which therefor broadens the recognition spectrum of the C1q (Gaboriaud et al., 2003). This may partially

explain the observation that many C1q ligands show significant interaction with several residues of all three globular domain subunits (Kishore et al., 2003).

1.3.4. The classical complement pathway in neurodegeneration

Synapse elimination is mostly considered a developmental process. However, synapse loss and dysfunction have been highly recognized as an early hallmark of numerous neurodegenerative diseases including Alzheimer's disease, Huntington's, Prion diseases, Frontotemporal dementia and Spinal Muscular Atrophy (Lipton et al., 2001; Mallucci, 2009; Mentis et al., 2011; Selkoe, 2002; Smith et al., 2005; Verret et al., 2012). Besides the role of complement proteins in normal brain development recent studies have implicated involvement of the C1q and classical complement pathway in aging process and in neurodegenerative diseases.

Expression and activation of complement has been reported in Alzheimer's patient tissue as well as in mouse models. Furthermore, C1q was found to localize to synapses in mouse models of Alzheimer's disease which implicates complement-mediated synapse loss in Alzheimer's disease A significant upregulation of C1q was found in the retina of a mouse model of glaucoma. Moreover, C1q-deficient mice were found to be protected from the synapse loss and the resulting dendrite atrophy (Presumey et al., 2017; Stevens et al., 2007; Williams et al., 2016). C1q was also found to be upregulated in a mouse model of progranulin-deficient Frontotemporal dementia, where is also involved in the disease progression (Lui et al., 2016). All mentioned neurodegenerative diseases have different ages of onset, affect different CNS regions and have different etiologies, yet complement is upregulated in all and has similar involvement in disease progression. Thus, complement-mediated synaptic loss may be an early characteristic of neurodegenerative diseases in general (Presumey et al., 2017). There is a mounting evidence that implicates complement proteins involvement in other neurodegenerative diseases such as Huntington's disease (HD), Parkinson's disease (PD), and amyotrophic lateral sclerosis (ALS) (Kjaeldgaard et al., 2018; Loeffler et al., 2006; Tenner et al., 2018; Woodruff et al., 2006; Yamada et al., 1992). Beside indications for complement involvement, other common characteristic of these diseases is an increase in microglial and astrocytic activation which further supports that complement factors may be potentially contributing to their pathogenesis (Brennan et al., 2016; Tenner et al., 2018).

Although there seems to be a connection between complement activation and neurodegeneration in Alzheimer's, Glaucoma and Frontotemporal dementia, there are many open questions remained to be answered. Could similar complement-dependent mechanisms be active in

other disease affected CNS regions, where synaptic loss is characteristic of neurodegeneration? Additionally, whether these synapse elimination mechanisms in neurodegeneration represent a reactivation of the developmental program specific for an affected circuitry remains unclear. Importantly, studying the involvement of classical complement cascade will help in uncovering mechanisms involved in synaptic loss and may provide new potential therapeutic targets in order to slow or ameliorate the disease phenotype.

1.3.5. The Role of Microglia in Synapse Elimination

Microglia are immune cells unique to the CNS. They represent resident macrophages in the brain and play critical roles in normal brain development. Microglia are unique among the mononuclear phagocytes as they are the only cells that do not originate from the bone marrow but from the yolk sac's hematopoietic stem cells. From yolk sac microglia migrate early in the development to the brain (Ginhoux et al., 2010; Kierdorf et al., 2013; Presumey et al., 2017). When they populate and get settled in the brain, they are not under normal conditions replenished by peripheral cells from the circulation. It has been demonstrated that microglia are long-lived cells, with approximately half of them surviving the entire life span of a mouse (Füger et al., 2017; Yona et al., 2013).Microglia are highly motile CNS cells which allows them to promptly respond to infections and injuries. Although their functions in the normal brain are not fully elucidated, it is known that microglia in the normal brain development, through the interactions with neurons participate in neuronal migration, neurogenesis, developmental neuronal apoptosis and synaptic development as well as synapse function. Microglia have an important role in brain wiring because they promote synapse development. In support of this are numerous reports of microglia in close relation with spines, small dendritic protrusions enclosing postsynaptic compartment of typically one excitatory synapse (Nayak et al., 2014; Presumey et al., 2017; Tremblay et al., 2011).

Recent research implicates microglia in synaptic pruning in developing brain via complement-dependent and independent mechanisms (Hong et al., 2016; Neniskyte and Gross, 2017; Tenner et al., 2018; Werneburg et al., 2016). Microglia are found to be more phagocytic during the early postnatal period and specifically in regions of active circuitry refinement (Schafer et al., 2012; Tenner et al., 2018). It has been shown, that microglia can - via complement receptor 3 (CR3) - internalize synaptic structures during the development of visual system. Numerous microglia were found to contain in their lysosomes fragments of presynaptic material during the period of circuitry refinement and synaptic pruning. It was also demonstrated in the developing visual system that during the activity-dependent synaptic competition that microglia has preference

to less-active synapses (Schafer et al., 2012). The observed internalization of synaptic material by microglia significantly dropped after the circuitry refinement – synaptic pruning period was over, which highly suggests that microglial engulfment in synapse elimination mechanisms. In support of this is the fact that CR3 (CD11b/CD18, mac-1) expression in the brain is reserved solely to microglia (Presumey et al., 2017; Schafer et al., 2012). These data suggest that microglia mediate synaptic elimination via C3-tagging and CR3 and that this process is regulated through neural activity. In support of this is the observed increase in synaptic engulfment by microglia during neural activity inhibition, suggesting that less active or "weak" synapses are those destined to be eliminated during development (Schafer et al., 2012).

Although synaptic pruning mechanisms have been well studied and described during the development of visual system, synaptic elimination is poorly understood when it comes to developmental circuitry refinement in other CNS regions. In addition to visual system, recent studies have implicated synaptic engulfment by microglia in the visual cortex and hippocampus, but it remain unknown whether this circuitry remodeling is during different developmental stages complement dependent (Paolicelli et al., 2011; Tenner et al., 2018; Tremblay et al., 2010). Furthermore, all these studies focused on different brain regions, but it remains unknown whether spinal cord motor circuits undergo similar microglia and/or complement-mediated synaptic refinement and if so, how would impairment of these refinement mechanisms translate onto the complex motor behavior? Additionally, it is currently unknown whether microglia-mediated synaptic pruning is a shared characteristic of both development and the disease.

Recent studies have implicated complement-mediated synapse elimination via microglia in early synaptic loss observed in Alzheimer's disease (Hong et al., 2016).Similarly, complement-microglia dependent synapse loss may be involved in other neurodegenerative diseases, in which synaptic loss is an early hallmark. In SMA, excitatory glutamatergic synapses are lost early in the disease process. However, it is currently unknown whether this is due to a developmental arrest or, are these synapses actively eliminated. Additionally, contribution of complement and microglia to the pathogenesis of disease is poorly understood. Beside their involvement in synaptic loss it would be essential to unravel whether complement has effect on synapse function or it is a sole mean of synaptic elimination. It is also critical to test whether inhibition of complement activation could prevent circuitry perturbations seen early in the disease and how would that impact the severe SMA phenotype.

2. AIMS

The goal of this study is to investigate the mechanisms involved in spinal sensory-motor circuitry refinement during normal development, as well as the mechanisms that are responsible for sensory-motor circuitry dysfunction in the neurodegenerative disease spinal muscular atrophy (SMA). To achieve these, the following aims have been outlined:

- Determine the molecular mechanisms involved in sensory-motor circuitry pathology in SMA and determine whether they are due to motor neuron autonomous defects or other non-cell autonomous mechanisms.

- Unravel the mechanisms involved in the reduction of proprioceptive synapses in SMA and differentiate between a potential developmental synaptic arrest versus an active synaptic elimination.

- Discover to which extent complement proteins are involved in synaptic loss and dysfunction in SMA.

- Characterize the source of C1q in the spinal cord.

- Identify which cell(s) may mediate elimination of sensory synapses in SMA and determine whether there is selective synaptic vulnerability in the context of disease.

- Determine whether C1q tagging of proprioceptive synapses is driven by SMN deficiency in proprioceptive neurons via cell autonomous mechanisms.

- Demonstrate whether neutralization of C1q by *in vivo* treatment could prevent synaptic loss and confer behavioral benefit in SMA mice.

- Find out if genetic deletion of C1q rescues proprioceptive synapse loss in SMA mice.

- Conclude whether C1q plays a role during normal development and determine the potential role in the refinement of the spinal sensory-motor circuitry during neonatal development.

3.   MATERIAL AND METHODS

3.1.   Materials

3.1.1.   Experimental Model – Mice

Mice used in this study were housed in pathogen-free conditions. All surgical procedures were performed on postnatal mice according to the National Institutes of Health Guidelines on the Care and Use of Animals. Columbia animal care and use committee (IACUC) approved all the performed procedures. Both sexes' mice were used since previously published work in SMA mouse models and patient data do not demonstrate any sex-related difference neither in the onset nor in SMA severity. The original start breeding pairs of SMA mice used in this study ($Smn^{+/-}$ /$SMN2^{+/+}$/$SMN\Delta7^{+/+}$) were obtained from Jackson Mice (Jax stock #005025; background FVB). Dr. M. Botto (Imperial College London, UK) provided under an MTA agreement $C1qa^{-/-}$ mice (background C57BL6) as previously reported (Botto et al., 1998). C1qa-deficient mice (C57BL/6) lack C1q protein, thus have disrupted classical complement pathway (Botto et al., 1998). $C3^{-/-}$ mice (C57BL/6 background), deficient in C3 protein, were purchased from Jackson Laboratory (B6 129S4-C3 < tmCrr > /J; stock No. 003641). In order to generate $Smn^{+/-};SMN2^{+/+};SMND7^{+/+};C1qa^{-/-}$ mice, $C1qa^{-/-}$ mice were crossed with SMA mice. To generate $Pv\text{-}Cre^{+/-};SMN2^{+/+};SMN\Delta7^{+/+}$ mice, SMA mice carrying Smn Cre-inducible allele (Smn^{Res}; JAX stock #007951; (Lutz et al., 2011) were bred with Pv^{Cre} (Jax stock #008069) mice. Cre- SMA mice lacked Cre, they were null for Smn allele and they carried Smn^{Res} allele ($Smn^{Res/-};SMN2^{+/+};SMN\Delta7^{+/+}$). Cre+ SMA mice lacked endogenous mouse SMN, they carried one allele of Smn^{Res} and they were heterozygous for Pv^{Cre} ($PV^{Cre+/-};Smn^{Res/-};SMN2^{+/+};SMN\Delta7^{+/+}$). WT mice were mice homozygous for wild-type allele in which Cre was absent ($Smn^{+/+};SMN2^{+/+};SMN\Delta7^{+/+}$). Similarly $ChAT^{Cre}$ mice were bred with mice carrying Smn Cre-inducible allele (Smn^{Res}) to generate $ChAT^{Cre+/-};Smn^{+/-};SMN2^{+/+};SMN\Delta7^{+/+}$. Cre+ SMA mice carried one allele of SmnRes, they lacked endogenous mouse Smn and they were heterozygous for $ChAT^{Cre}$ ($ChAT^{Cre+/-};Smn^{Res/-};SMN2^{+/+};SMN\Delta7^{+/+}$). Additionally, Pv^{Cre} and $ChAT^{Cre}$ mice were bred with mice carrying Smn^{Res} to generate $PV^{Cre+/-};ChAT^{Cre+/-};Smn^{Res/-};SMN2^{+/+};SMN\Delta7^{+/+}$ mice.

3.1.2. Human Post-Mortem Tissue

Fresh frozen spinal cord tissue (lumbar segments) from one control patient - 3 years old male was obtained from the Brain Center (Columbia University), and fresh frozen spinal cord tissue (lumbar segments) from one SMA type I patient - 7 months old male, was kind gift from Dr. Wendy Chung (Columbia University).

3.2. Methods

3.2.1. Genotyping

Polymerase chain reaction (PCR) genotyping from tail deoxyribonucleic acid (DNA) for SMA-Δ7, Pv^{Cre} and C3$^{-/-}$ mice was performed following Jackson protocols as described on their website (https://www.jax.org). PCR reaction for the Smn, C3 Pv^{Cre} and ChAT^{Cre} alleles was used as follows: 0.5 µl of each primer (25 µM; Sigma), 12.5 µl of GoTaq Hot Start Green Master Mix (Promega) and 4 µl of lysed tail DNA 1:20 diluted. Final volume of reaction - 25 µl was adjusted using ddH2O. Following thermal cycling protocol was used for the amplification of Smn and Smn^{Res} alleles products: 95ºC for 2 minutes was followed by 35 cycles of 95ºC for 1 minute, 55ºC for 1 minute, 72ºC for 1 minute, terminating with 72ºC for 5 minutes. Amplification of Pv^{Cre} alleles products was done following next thermal cycling protocol: 94ºC for 3 minutes was followed by 34 cycles of 94ºC for 30 seconds, 58ºC for 30 seconds, 72ºC for 1 minute and terminating with 72ºC for 5 minutes. Amplification of ChAT^{Cre} allele products was done following next thermal cycling protocol: 95°C for 3 minutes, 97°C for 30 seconds; two step cycles 5 times: 95°C for 15 seconds, 69°C for 1 minute; three step cycles 30 times: 95°C for 15 seconds, 60°C for 15 seconds, 68°C for 1 minute and 68°C for 5 minutes. Amplification of C3 alleles products was performed following next thermal cycling protocol: 94ºC for 3 minutes was followed by 12 cycles of 94ºC for 20 seconds, 64ºC for 30 seconds (0.5ºC increase per cycle), 72ºC for 35 seconds and then followed by 25 cycles of 94ºC for 20 seconds, 58ºC for 30 seconds and 72ºC for 35 seconds, and terminating reaction with 72ºC for 2 minutes. Tail DNA extraction for C1q genotyping was done utilizing KAPA Biosystems Express Extract Kit (cat #KK7103). PCR reaction was performed as per following protocol: 25 µl of 2x Master Mix (2 mM; Promega #: M750B), 0.5 µl of tail DNA, 4 µl of MgCl2 (25 mM; Promega #: A351F), 1 µl of mC1qIN/1 primer, 2 µl of Neo30 primer and 1 µl of mC1qA/50+ primer and adjusted to total volume of 50 µl with 16.5 µl of ddH2O. Amplification of the C1q alleles products was performed using the next thermal cycling protocol: 95ºC for 4 minutes, 94ºC

for 1 minute, and followed by 35 cycles of 94ºC for 1 minute, 57ºC for 30 seconds and 72ºC for 30 seconds, terminating with 70ºC for 10 minutes. All custom-made primers are listed below (Table 1).

Table 1. List of custom-made PCR primers.

C1q knock-out allele forward primer	GGGGATCGGCAATAAAAAGAC
C1q wild-type allele forward primer	GGGGCCTGTGATCCAGACAG
C1q wild-type allele reverse primer	ACCAATCGCTTCTCAGGACC
uninverted SmnRes forward primer	ACGCGTACCGTTCGTATAGC
uninverted SmnRes reverse primer	TGAGCACCTTCCTTCTTTTTG
inverted SmnRes forward primer	CAACCAGTTAAGTATGAGAATTC
inverted SmnRes reverse primer	GTTTGCAGAAGCGGTGGG
PV^{Cre} wild-type allele reverse primer	CGAGGGCCATAGAGGATGG
PV^{Cre} allele reverse primer	GCGGAATTCTTAATTAATCAGCG
PV^{Cre} common forward primer	GGATGCTTGCCGAAGATAAGAGTG
ChAT^{Cre} wild-type allele forward primer	GTTTGCAGAAGCGGTGGG
ChAT^{Cre} allele forward primer	TCGCCTTCTTGACGAGTTCTTCTG
ChAT^{Cre} common reverse primer	GGCCACTTAGATAGATAATGAGGGGCTC

3.2.2. Behavioral Analysis

All experimental mice groups were monitored daily. Their body weight and righting time was recorded. Righting time was measured by placing a mouse on back and recording how long the pup needed to right itself back to an upright position, with cut off test time being 60 seconds to comply with IACUC guidelines. This was repeated 3 times and righting time was averaged for analysis. Mice were euthanized with carbon dioxide per IACUC guidelines if they had both lost 25% of their body weight compared to previous day and were unable to right. Systemic administration anti-C1q antibody (ANX-M1, mouse anti-C1q antibody, Annexon Biosciences) or

its isotype control (mouse IgG1, Annexon Biosciences), was performed under an MTA agreement. Intraperitoneal (IP) injections were done in both WT and SMA mice every second day from birth (P0) and until death with a 100 mg/kg dose. Treated pups were monitored daily for righting times and body weight (average of three trials). Treatment was done in blind manner and mice were injected with either anti-C1q antibody or isotype control antibodies. Mice treated with PLX5622 IP solution were injected intraperitoneally two times a day starting from birth (P0) until P10/11 when tissue was harvested. Systemic administration of PLX5622 IP solution was done at a dose of 50 mg/kg. Treated pups were monitored daily and body weight as well as righting times were analyzed. This treatment had maximal depletion of microglia but at low survival rate was observed in both WT and SMA mice.

3.2.3. Physiology: *Ex vivo* Spinal Cord Preparation

Mice were decapitated and spinal cord was dissected in cold oxygenated (12 ℃, 95%O_2/5%CO_2) artificial cerebrospinal fluid (aCSF) which contained in mM: 4 KCl, 128.35 NaCl, 0.58 $NaH_2PO_4.H_20$, 30 D-Glucose, 21 $NaHCO_3$, 1 $MgSO_4.7H_20$ and 1.5 $CaCl_2.H_20$. Isolated spinal cord was transferred to a custom-made recording chamber which was continuously perfused with oxygenated aCSF at the rate of 10 ml/min, at room temperature (21-24℃). Ventral and dorsal roots were placed in suction electrodes for the stimulation and recording, respectively. Recordings from L1 or L2 ventral root were obtained in response to stimuli from homonymous L1 or L2 dorsal root, respectively. The stimulus threshold was defined as the minimal current which is necessary to evoke a response in homonymous ventral root, in 3 out of total 5 trials. Dorsal roots stimulations were performed at supramaximal intensity (0.2ms, 2-5x threshold) and delivered by constant current stimulus isolator (A365 - WPI, Sarasota, FL). Recordings were 1000x amplified (Cyberamp, Molecular Devices), fed to the A/D interface (Digidata 1320A, Molecular Devices) and acquired at 50kHZ utilizing Clampex (V10, Molecular Devices). Data analysis was done offline using Clampfit (Molecular Devices). Amplitude measurements were obtained by averaging 10 single stimulations responses at 0.1 Hz. Following the recording session, in some experiments, tissue was collected for immunohistochemistry. Spinal cords were immersion fixed overnight in 4% PFA, and then subsequently transferred to 0.01M phosphate buffer saline (PBS) until processed for immunohistochemistry.

3.2.4. Functional Assessment of NMJs

Neuromuscular junctions (NMJs) of Quadratus Lumborum (QL) muscle were functionally assessed at P11. In order to do so a technique was developed in which axons of motor neurons in ventral root L2 (which innervate QL muscle) were stimulated by pulling the ventral root into the suction electrode while having removed spinal cord. The stimulation of L2 ventral root was performed with single stimulus (0.2 ms at supramaximal intensity), at different frequencies which were ranging from 0.1 Hz to 50 Hz to mimic physiological range for firing of neonatal motor neurons (Fletcher et al., 2017). Compound muscle action potentials (CMAPs) of Quadratus Lumborum were recorded utilizing a concentric bipolar electrode which was inserted in the muscle belly. The maximum CMAP amplitude, measured baseline-to-peak, was averaged from 10 stimulations at 0.1 Hz. If tissue was collected for immunohistochemistry, upon the recording session, Quadratus Lumborum muscles were fixed for 20 minutes in 4% PFA and then transferred to PBS until processed for NMJ staining.

3.3. Tracing and Immunohistochemistry

Experimental mice [WT, SMA, SMA+a-C1q Ab, SMA+Ctr Ab, WT+PLX5622, SMA+PLX5622, $C1q^{-/-}$, $C3^{-/-}$, SMA+$C1q^{-/-}$] were used in tracing and immunohistochemistry experiments at birth (P0), P4, or P11.

3.3.1. Somatodendritic labeling of Motor Neurons

The intact but isolated *ex vivo* spinal cord was hemisected to improve oxygenation (for P11 spinal cords). The dissection chamber was perfused with cold oxygenated (10 ºC, 95% O_2 / 5% CO_2) aCSF (which contained in mM: 4 KCl, 128.35 NaCl, 21 $NaHCO_3$, 0.58 $NaH_2PO_4.H_2O$, 30 D-Glucose, 2 $MgSO_4.7H_2O$ and 0.1 $CaCl_2.H_2O$). The L1 or L2 (depending on experiment) ventral root was placed into the suction electrode which was then filled with the fluorescent dextran dye (Texas Red, Alexa Fluor 488 or Cascade Blue) allowing retrograde labeling of motor neurons. After allowing 14 – 20 hours for dye to fill motor neurons, the spinal cord was immersion fixed overnight in 4% paraformaldehyde and subsequently transferred to PBS until processed for immunohistochemistry as described below.

3.3.2. Retrograde Labeling of Muscle-Identified Motor Neurons

C1q$^{-/-}$ and WT motor neurons which supply Tibialis Anterior (TA) and Gastrocnemius (GA) muscles were *in vivo* retrogradely labeled by intramuscular Fluorescinated Dextran or CTb conjugated to Alexa 555 injections. Newborn mice (P0) were anesthetized utilizing isoflurane inhalation. Small incision was made in the right or left TA and GA area to access the muscles. GA muscles were injected with the fluorescinated dextran while TA muscles were injected with the 1 mL of 1% CTb-Alexa 555 in PBS. Injections were performed using a custom made, finely pulled glass micropipette. Dextran and CTb were delivered by pressure to a customized microsyringe. All incisions were sutured. Spinal cords were collected after 7 days (P7) and processed for immunohistochemistry.

3.3.3. Tissue Collection

Mice were anesthetized using 1.2% avertin (300mg/kg, intraperitoneal injection) and transcardially perfused with ice cold PBS to remove blood until tissue was cleared of blood (ie liver blanching). When fixation was required, mice were additionally perfused with 4% PFA. Spinal cord was carefully dissected after transcardial perfusion and immersion fixed in 4% PFA (4 hours to overnight). Subsequently, spinal cord was washed and stored in PBS until being processed for immunohistochemistry

3.3.4. Immunohistochemistry

Embedding of spinal cords was done in warm 5% Agar. Transverse serial sections from L1 or L2 spinal segment (depending on experimental set up) were cut at 75 µm thickness using a Vibratome (Leica). Experiments in which anti-mouse antibodies were used, sections were pre-incubated in M.O.M blocker (Vector Laboratories) for 1 hour, to block endogenous antigens. Blocking was done at room temperature for 1.5 hours using 10% normal donkey serum in 0.01M PBS, 0.1% Triton X-100 (PBS-T, pH 7.4). Following blocking, sections were incubated at room temperature overnight (for C1q antibody 24 hours) in different primary antibodies combinations diluted in PBS-T. The following day, washing was done in PBS-T, followed by 3h secondary antibody incubations at room temperature. Appropriate species-specific secondary antibodies were diluted in PBS-T. Subsequently, sections were washed in PBS, and mounting was done using 30% glycerol in PBS on glass slides and custom cover-slips. All antibodies, except VGluT1 (custom

made), Parvalbumin (custom made), and TMEM119 (Barres lab), were purchased from commercial sources. Production of VGluT1 anti-guinea pig antibody was done with the company Covance. Antibody was designed against the following epitope: (C)GATHSTVQPPRPPPP which is found within n-terminus of a mouse VGluT1 (Fletcher et al., 2017). Specificity of the VGluT1 antibody was confirmed in VGluT1 knock out tissue. Production of Parvalbumin anti-chicken antibody was done by Covance. Antibody was designed against full length bacterial fusion protein. The following primary antibodies were used at the indicated dilutions: rabbit monoclonal anti-C1q (1:1000; Abcam, ab182451), goat polyclonal anti-ChAT (1:100; Millipore, AB144P), rabbit polyclonal anti-human C1q (1:500; Agilent, A013602), rat monoclonal anti-CD45 (1:1000; Millipore, 05-1416), rabbit polyclonal anti-C3d (1:500; Dako, A006302), rat monoclonal anti-CD68 (1:200; AbD Serotec, MCA1957GA), mouse monoclonal anti-GFAP (1:500; Sigma-Aldrich, G3893), rabbit polyclonal anti-GFAP (1:500; Dako, Z0334), goat polyclonal anti-Iba1 (1:500; Abcam, ab5076), rabbit polyclonal anti-Iba1 (1:500; Wako 019-19741), mouse monoclonal anti-NeuN (1:100; Millipore, MAB377) mouse monoclonal anti-TMEM119 (1:3; Barres lab), guinea pig polyclonal anti-Synaptophysin (1:500; Synaptic Systems, 101 004), guinea pig polyclonal anti-VGluT1 (1:2000; custom made), guinea pig polyclonal anti-VGAT (1:200; Synaptic Systems, 131 004). Following are secondary antibodies used at the 1:250 dilution: Alexa Fluor 488 donkey anti-rabbit (Jackson ImmunoResearch, 711-545-152), Alexa Fluor 488 donkey anti-goat (Jackson ImmunoResearch, 705-545-003), Fluor 488 donkey anti—mouse (Jackson ImmunoResearh, 715-545-150), Alexa Fluor 488 donkey anti-guinea pig (Jackson ImmunoResearch, 706-545-148), Alexa Donkey anti-guinea pig-Cy5 IgG (Jackson ImmunoResearch, 706-175-148), Donkey anti-mouse-Cy5 IgG (Jackson ImmunoResearch, 715-175-151), Donkey anti-rabbit-Cy5 IgG (Jackson ImmunoResearch, 711-175-152), Donkey anti-rabbit-Cy3 IgG (Jackson ImmunoResearch, 711 165-152), Donkey anti-goat-Cy3 IgG (Jackson ImmunoResearch, 705-165-147), Donkey anti-guinea pig-Cy3 IgG (Jackson ImmunoResearch, 706-165-148) Donkey anti-rat-Rhodamine Red X IgG (Jackson ImmunoResearch, 712-295-153), Donkey anti-mouse-Cy3 IgG (Jackson ImmunoResearch, 715-165-150).

3.3.5. Human Post-Mortem Tissue Staining

Fresh frozen spinal cord tissue from the control patient (3 years old male) and from the SMA type I patient (7 months old male) was a kind gift from the Brain Center at Columbia University and Dr. Wendy Chung, respectively. Spinal cord tissue was cut on a cryostat at 20 μm thickness. Fixation was done for 2 minutes with 4% PFA upon which, sections were washed in PBS

and subsequently treated as described above. Sections were incubated overnight with primary antibodies against C1q - rabbit polyclonal anti-human (1:500; Dako, A013602-1) and against ChAT - goat polyclonal (1:100; Millipore, AB144P). Following day sections were washed and subsequently incubated with secondary antibodies: Donkey anti-rabbit-Cy3 (Jackson ImmunoResearch, 711-165-152) and Alexa Fluor 488 donkey anti-goat (Jackson ImmunoResearch, 705-545-003). Sections were then washed and mounted using 30% glycerol in PBS.

3.3.6. Staining in Dorsal Root Ganglions (DRGs)

Mice were transcardially perfused at P11 with 2% PFA in a sodium acetate buffer (pH 6). Dorsal root ganglia were collected from L1-L3 spinal segments and immersion fixed for 2 hours. Tissue was cut with a vibratome at 100 µm thickness. Initial blocking was done in M.O.M. blocker (Vector Laboratories) diluted in PBS-T for an hour at room temperature, to prevent non-specific binding of secondary antibody to mouse antigens. Sections were then processed as described above, in previous immunohistochemistry protocol. Following primary antibodies were used: mouse monoclonal anti-SMN (1:50; BD Biosciences, 610646) and chicken polyclonal anti-Parvalbumin (1:2000; custom made). Species specific secondary antibodies used were: donkey anti-mouse-Cy5 IgG (Jackson ImmunoResearch, 715-175-151) and Alexa Fluor 488 donkey anti-chicken (Jackson ImmunoResearch, 703-545-155). Finally, sections were counter-stained with DAPI, washed and mounted using 30% glycerol in PBS.

3.3.7. NMJ Staining

Neuromuscular junctions (NMJs) were studied in the Quadratus Lumborum (QL) muscle. Muscles were collected from P11 mice (from each genotype) and for 20 minutes immersion fixed in 4% PFA which was followed by washing in PBS. Teasing of single fibers was done with fine forceps, which was followed by 30 minutes washing in PBS enriched with 0.1M glycine. Fibers were then incubated with alpha-bungarotoxin-555 for 20 minutes in order to stain postsynaptic part of neuromuscular endplates. Fibers were subsequently washed in PBS and permeabilized in ice cold methanol for 2 minutes. Following permeabilization fibers were washed in PBS and subsequently blocked for an hour with 10% Donkey Serum in 0.3% PBS-T prior to antibodies exposure. Following antibodies were used: guinea pig polyclonal anti-synaptophysin (1:500; Synaptic Systems, 101 004) and rabbit polyclonal anti-Neurofilament (1:500; Millipore). Primary antibodies were incubated overnight at 4 ℃. Following day, fibers were washed in PBS and secondary

antibodies exposure followed for one hour at room temperature. Following secondary antibodies were used: Donkey anti-guinea pig-Cy5 IgG (Jackson ImmunoResearch, 706-175-148) and Alexa Fluor 488 donkey anti-rabbit (Jackson ImmunoResearch, 711-545-152). Following the secondary antibody incubation, fibers were washed and mounting was done using 30% glycerol in PBS.

3.4.   Quantification and Data Analysis

3.4.1. Imaging and Analysis

Imaging was performed using the SP8 Leica confocal microscope. Off-line analysis of images was done using ImageJ (National Institutes of Health) and LASX (Leica Microsystems) software. For all immunohistochemistry experiments analysis, at least three mice from each genotype were used. Motor neuron counts were performed analyzing z-stacks images, which were acquired at 3 µm intervals and collected from each section containing fluorescent signal from L1 or L2 retrogradely labeled MNs and/or ChAT immunostained MNs, as previously described (Mentis et al., 2011; Fletcher et al., 2017). Sections for motor neuron counts were scanned with x20 dry objective. To avoid double counting of motor neurons (ChAT+) from the adjoining spinal cord sections, exclusively motor neurons containing the nucleus were counted. Quantitative analysis of VGluT1 synaptic densities at P11 were performed on L1 motor neurons using z-stacks of optical sections which were scanned with a x40 oil objective throughout the entire section thickness (at 0.35 µm z-step size) in order to include the whole motor neuron cell body as well as proximal dendrites of ChAT+ and/or retrogradely labeled motor neurons. Density estimates were obtained by counting all VGluT1+ inputs on dendritic segments at sequential distances of 50 µm (0-50 µm and 50-100 µm) from the cell body of motor neurons and dividing this number with the total linear length of all dendritic segments in every compartment, as described previously (Mentis et al., 2011; Fletcher et al., 2017). For VGluT1 counts on motor neuron cell bodies, only those motor neurons with an entire soma present within the analyzed z-stack were included. Gamma motor neurons were excluded from analysis, by counting only those motor neurons with a cell bodyperimeter greater than 400 µm^2.

3.4.2. SMN Quantification

DRG sections were scanned throughout the whole section with x40 oil objective at 0.5 µm z-steps. For each studied genotype number of gem negative and positive proprioceptive neurons

was counted. For each genotype three mice were used with a minimum of 30 counted proprioceptive neurons per animal.

3.4.3. NMJs Quantification

The extent of NMJ innervations was determined by analyzing NMJ synapses for different experimental groups. Z stack images of NMJ synapses were acquired with x20 dry objective, scanning at 2 µm z-steps. Offline analysis of images was performed using LASAF software, counting numbers of innervated and denervated synapses. NMJ synapse was considered innervated only if the presynaptic nerve terminal was completely co-localizing with the postsynaptic endplate.

3.4.4. Fluorescent In Situ Hybridization (FISH) combined with Immunohistochemistry

Mice were transcardially perfused and spinal cords were isolated, post-fixed for 24 hours in 4% PFA at 4 ℃, and subsequently cryopreserved overnight in 10%, followed by 20% and finally 30% sucrose solutions. Spinal cord segments L1-L3 were sectioned using a cryostat (Leica) at 20 µm thickness and mounted on super-frost slides. Fluorescent in situ hybridization (FISH) for C1qa was performed with RNAscope probe from Advanced Cell Diagnostics (ACD, #441221-C3) using the RNAscope Multiplex Fluorescent Reagent Kit V2 (ACD, #323110) and following the recommendations from manufacturer. HRPC1 signal was developed using TSA Plus Cyanine 5 System (PerkinElmer, #NEL745E001KT). Slides with sections were briefly washed in PBS following the last wash in RNAscope protocol, and subsequently blocked in 10% normal donkey serum. Primary antibodies were incubated at room temperature overnight in wet chamber. Against ChAT goat polyclonal anti-ChAT antibody was used (1:100; Millipore, AB144P) and against Iba1 rabbit polyclonal anti-Iba1 antibody (1:500; Wako 019-19741) was used. Sections were washed following day in PBS-T and incubated with secondary antibodies for 2 hours at room temperature. Sections were then washed in PBS, mounted using ProLong Gold Antifade Mountant (#P36931) and cover-slipped.

3.4.5. Quantification of Tagged Synapses

Deposition of C1q and C3 on synapses was analyzed and quantified from single optical plane images which were acquired using a x63 oil or x40 oil objectives at resolution of 4096x4096 DPI, using the SP8 Leica confocal microscope and LASX software from Leica Microsystems for subsequent deconvolution and the offline image analyses. Only synapses that were contacting motor neurons on either soma or on dendrites were analyzed. Synapse was defined as ''tagged'' only if C1q or C3 signal clearly colocalized with presynaptic signal. This colocalization was each time confirmed with intensity line profiling tool, where the intensity line profiles of C1q (or C3) and those of synaptic markers overlapped. To obtain percentage of tagged synapses all synaptic contacts were counted on soma and on dendrites of motor neurons and compared against the numbers of tagged synapses on motor neurons soma and on dendrites, respectively.

3.4.6. C1q Binding Assay

Black Costar 3925 plate from Corning was coated with human C1q (Complement Technology Inc) at the concentration of 2 µg/ml in bicarbonate buffer and incubated at 4 ℃ overnight (100 µl/well). Next day, plate was 3x washed with 200 µl/well dPBS. Subsequent locking was done using 3% BSA in PBS, 200 µl/well, at room temperature, for 1 hour. Control isotype antibody or neutralizing anti-C1q antibody (Annexon Biosciences) was added in triplicate serial dilutions (8-12 point titration, 200-400 ng/ml) in dPBS with 0.3% BSA, 0.1% Tween buffer,50 µL/well, and incubated at room temperature for 1 hour. Subsequently, goat anti-mouse-Fc-AP (Jackson ImmunoResearch) at 1:2000 dilution was added, 50 µl/well, diluted in PBS with 0.3% BSA, 0.1% Tween. Plate was then washed 3 times for 10 minutes, with dPBS 0.05%Tween 200 µl/well. Incubation of AP substrate (CDP-Star) followed, for 20 minutes at room temperature. Infinite 200 PRO plate reader (Tecan Life Sciences) was used to read the plate.

3.4.7. RNA Analysis

Spinal segments L1-L2 were isolated at P4 and P11 from WT and SMA mice for RT-qPCR experiments. Phenol-free total RNA isolation was performed using the RNAqueous-Micro Kit (ThermoFisher Scientific). RevertAid First Strand cDNA Synthesis Kit (Thermo Fisher Scientific) was used for reverse transcription of RNA and Power SYBR Green PCR master mix (Applied

Biosystem) was used to perform triplicate reactions in a Realplex4 Mastercycler (Eppendorf). All primers designed for RT-qPCR experiments are listed below (Table 2).

Table 2. List of custom-made primers used in RT-qPCR experiments.

C1qA forward primer:	AAGGATGGGGCTCCAGGAAAT
C1qA reverse primer:	TTCCCCTGGGTCTCCTTTAAAACCT
C3 forward primer:	CCATCACAGTCCGCACCAAGAA
C3 reverse primer:	GAGTTGTGCATAGTGCTGTAGGGA
GAPDH forward primer:	AATGTGTCCGTCGTGGATCTGA
GAPDH reverse primer:	GATGCCTGCTTCACCACCTTCT
C5 forward primer:	CAGTAACAGTCACAGAATCTTCAGGT
C5 reverse primer:	GGAGAGAGGACATATTTGACTCCA
C5aR1 forward primer:	CCAGGACATGGACCCCATAGATA
C5aR1 reverse primer:	CCATCCGCAGGTATGTTAGGA
CD59b forward primer:	TCTCTATGCTGTAGCCGGAAG
CD59b reverse primer:	TTGTATGCCTGCCACGTCTA
IL-1β forward primer:	AGTTGACGGACCCCAAAAG
IL-1β reverse primer:	AGCTGGATGCTCTCATCAGG
IL-6 forward primer:	AGTCCGGAGAGGAGACTTCA
IL-6 reverse primer:	GCCATTGCACAACTCTTTTCTCA
TNF forward primer:	GTCCCCAAAGGGATGAGAAGTT
TNF reverse primer:	TGTGAGGGTCTGGGCCATAG

3.4.8. Western Blot Analysis

WT, SMA+a-C1q antibody and SMA mice spinal cord segments L1–L3 (n = 2) were collected at P11 and homogenized in lysis buffer (150 mM NaCl, 1% Triton, 2 mM EDTA, 50 mM Tris, pH 7.4). Proteins were quantified with Bio-Rad protein assay. Protein extracts, in concentration of 30 µg, were run on 12% SDS–PAGE gels and subsequently transferred for probing

to PVDF membranes. Blocking was done for 1 hour, at room temperature, in 5% milk diluted in TBS/0.2% Tween. Membranes were probed with following primary antibodies: mouse monoclonal Anti-a-Tubulin (1:10000; Sigma-Aldrich, T9026) or mouse monoclonal anti-SMN (1:10000; BD Biosciences, 610646) which were diluted in blocking buffer (5% milk in TBS/0.2% Tween), and incubated at 4 ºC, overnight. Next day, membranes were 3 times washed in TBS/0.2% Tween and incubated at room temperature, for 1 hour, with following secondary antibody diluted in TBS/0.2% Twee: Peroxidase AffiniPure Goat Anti-Mouse IgG (H+L) (Western Blot, 1:10000; Jackson ImmunoResearch, 115-035-003). Membranes were washed 3 times and visualized with enhanced chemiluminescence (GE Healthcare, Lifesciences).

3.4.9. Statistics

PRISM (GraphPad Software, Prism Version 6.04.) was used to perform statistical analysis. Comparisons were performed using Student's t test or One-Way ANOVA when normality and homoscedasticity conditions were respected. When violated, non-parametric Kruskal-Wallis and Mann–Whitney Wilcoxon tests were used. A p-value less than 0.05 ($p < 0.05$) was considered statistically significant. Results are shown as means ± standard error of the mean (SEM).

4. RESULTS

4.1. The origin of sensory-motor circuitry pathology in SMA

4.1.1. Selective restoration of SMN in proprioceptive neurons rescues synaptic loss

In order to accurately quantify proprioceptive synapses on motor neurons across all studied experimental groups, a highly specific vesicular glutamate transporter 1 (VGluT1) antibody had to be produced as all commercially available antibodies were proven to be unreliable and inconsistent upon testing. VGluT1 antibody was designed against the epitope (C)GATHSTVQPPRPPPP on a mouse VGluT1 protein. Selected epitope is located within the n-terminus of a mouse VGluT1. Polyclonal anti-VGluT1 antibody was produced in guinea pig with the company Covance. After being injected with a designed peptide to elicit a primary immune response, guinea pig was given a secondary immunization to achieve higher antibody titers. After each immunization, guinea pig was bled and polyclonal antibodies were obtained straight from the serum and tested on P0, P4 and P11 WT and SMA lumbar spinal cord sections at different serial dilutions, starting at 1:100 and ending at 1:20 000. Processed spinal cord sections were scanned within the 24 hours from the time serum was obtained and decision was made weather to immunize guinea pig again or if satisfied to perform terminal bleed. Specificity of the VGluT1 antibody was confirmed in VGluT1 knock out tissue.

Previous experiments have demonstrated that the reduction of EPSP amplitude observed in SMA motor neurons is successfully restored in SMA+Pv^{Cre} but not in SMA+ChAT^{Cre} motor neurons (Fletcher et al., 2017) suggesting that motor neuron dysfunction is a consequence of SMN loss from proprioceptive neurons. To further examine whether this rescue of the EPSP amplitude in SMA+Pv^{Cre} motor neurons was due to a rescue of the actual number of proprioceptive synapses, the number of VGluT1+ synapses on retrogradely filled motor neurons was quantified. A significant rescue of VGluT1 synapses was found on both soma and dendrites of motor neurons in SMA+Pv^{Cre} mice at P4 (Figure 14, A-C), while no synaptic rescue was noted in SMA+ChAT^{Cre} motor neurons (Fletcher et al., 2017) (Figure 14, A-C;). These results indicate that selective restoration of SMN in proprioceptive neurons rescues the number of synapses that are normally reduced under SMN deficiency conditions.
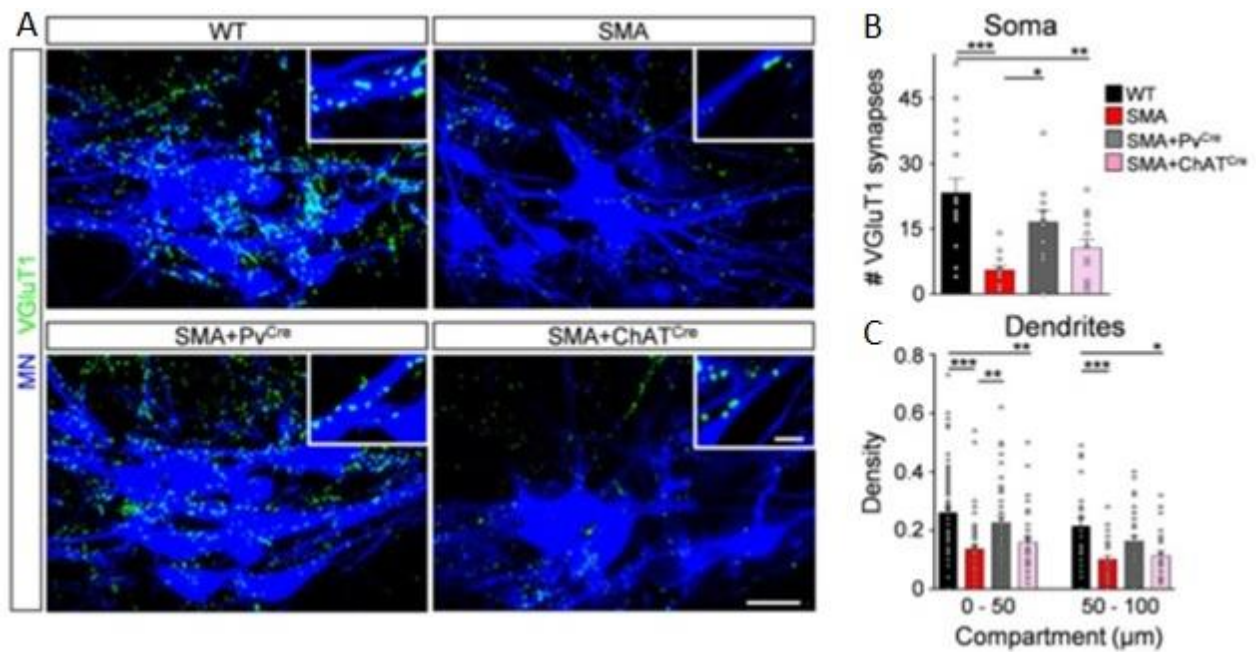
Figure 14. Selective restoration of SMN in proprioceptive neurons in SMA rescues the number of synapses. (A) Z-stack projection of confocal images from L2 retrogradely labeled motor neurons (shown in blue) and VGluT1 immunoreactivity (shown in green) in WT, SMA, SMA+Pv[Cre] and SMA+ChAT[Cre] mice at P4. Insets show at higher magnification VGluT1 synaptic appositions on dendrites. The total distance in the z axis for all images was 7 μm (20 optical planes at 0.35 μm intervals) and 1.5 μm for the insets. (B) The average number of VGluT1 synapses on soma of L2 motor neurons in WT (n=17), SMA (n=14), SMA+Pv[Cre] (n=13) and SMA+ChAT[Cre] (n=15) mice. * $P<0.05$, ** $P<0.01$, *** $P<0.001$, one-way ANOVA, Tukey's post hoc analysis. (C) VGluT1 synaptic density at 50 μm dendritic compartments from soma, for the same groups shown in (A) and (B). * $P<0.05$, ** $P<0.01$, *** $P<0.001$, one-way ANOVA, Tukey's post hoc analysis. Adapted from (Fletcher et al., 2017).

Additionally, the number of VGluT1 synapses in SMA+Pv[Cre] motor neurons remained comparable to those observed in WT mice motor neurons at a late stage of disease – P11 (Fletcher et al., 2017) (Figure 15, A-C;), which demonstrates that VGluT1 synapses continue to develop at older ages. Thus, SMN restoration in proprioceptive neurons rescues synaptic loss. Taken together with physiological findings (Fletcher et al., 2017), these results strongly argue that motor neuron dysfunction is a non-cell autonomous event driven by SMN deficiency in proprioceptive neurons.
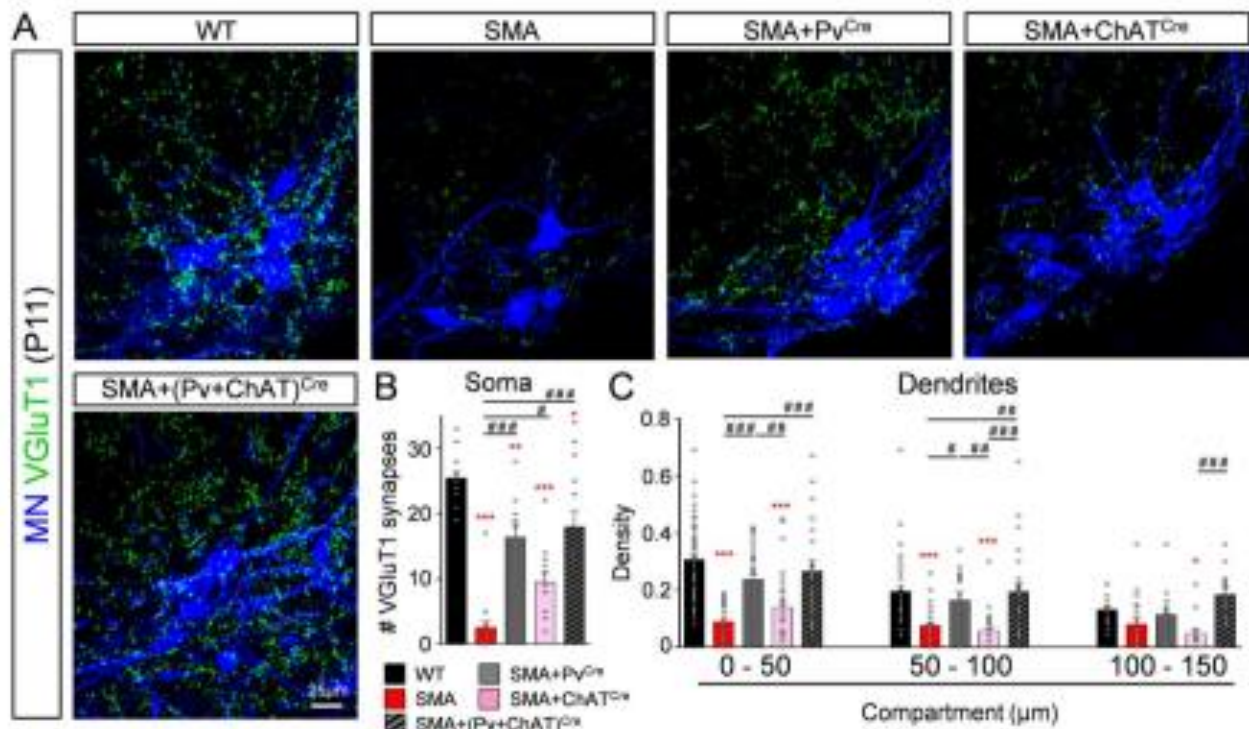
Figure 15. Maintenance of rescued VGluT1 synapses at P11. (A) Z-stack projection of confocal images from L2 retrogradely labeled motor neurons (shown in blue) and VGluT1 immunoreactivity (shown in green) at P11 in WT, SMA, SMA+Pv^{Cre}, SMA+ChAT^{Cre} and SMA+(Pv+ChAT)^{Cre} mice. The total distance in the z-axis for all images was 7 μm (20 optical planes at 0.35 µm intervals). (B) The average number of VGluT1 synapses on soma of L2 motor neurons at P11 in WT, SMA, SMA+Pv^{Cre}, SMA+ChAT^{Cre} and SMA+(Pv+ChAT)^{Cre} mice. * $P<0.05$, ** $P<0.01$, *** $P<0.001$, one-way ANOVA, Tukey's post hoc analysis. (C) VGluT1 synaptic density at 50 μm dendritic compartments from soma, for the same groups as shown in (A) and (B). * $P<0.05$, ** $P<0.01$, ***$P<0.001$, one-way ANOVA, Tukey's post hoc analysis. Adapted from(Fletcher et al., 2017).

4.1.2. BDNF does not contribute to motor neuron dysfunction

Fletcher et al addressed the possibility that other factors such as Brain-Derived Neurotrophic Factor (BDNF), which can be released by proprioceptive neurons (Betley et al., 2009; Mende et al., 2016) could also contribute to motor neuron dysfunction (Fletcher et al., 2017). Physiological assays revealed similar physiological properties in SMA motor neurons compared to SMA + BDNF^{proprio} motor neurons (SMA motor neurons in mice in which BDNF was overexpressed in proprioceptive neurons) (Fletcher et al., 2017). To confirm BDNF release from proprioceptive SMA synapses upon the AAV9-GFPmBDNF based overexpression of BDNF (Fletcher et al., 2017), VGluT1, glutamic

acid decarboxylase 65-kilodalton isoform (GAD65) and 67-kilodalton isoform (GAD67) immunohistochemistry was performed (figure 16A, C). An increase in GAD65, and not GAD67 in Gamma-aminobutyric acid (GABA)pre synapses demonstrated that BDNF is released from SMA proprioceptive synapses (Figure 16B, D) similarly as what was previously reported for VGluT1−/− mice (Mende et al., 2016).
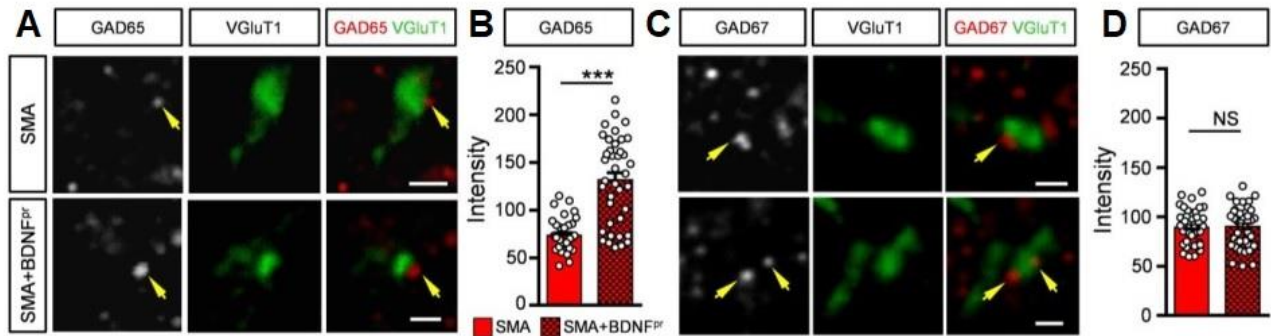

Figure 16. BDNF is released from SMA proprioceptive synapses. (A) GAD65 immunoreactivity (shown in red) in GABApre terminals contacting VGluT1 (shown in green) proprioceptive afferent terminals in SMA and SMA+AAV9-BDNF mice at P5. GABApre terminals are indicated by arrows. (B) Synaptic marker intensity measurements (shown in arbitrary units) in GAD65+ GABApre terminals in mice at P5. (total numbers for GAD65: 39 terminals, n=3 mice per experimental group). *** P<0.001, Mann-Whitney test. (C) GAD67 immunoreactivity (shown in red) in GABApre terminals contacting VGluT1 (shown in green) proprioceptive afferent terminals in SMA and SMA+AAV9-BDNF mice at P5 mice. GABApre terminals are indicated by arrows. (D) Synaptic marker intensity measurements (shown in arbitrary units) in GAD67+ GABApre terminals in mice at P5. (total numbers for GAD67: 39 terminals, n=3 mice per experimental group). NS: not significant (P=0.72, Mann-Whitney test) Adapted from (Fletcher et al., 2017).

Together with electrophysiological assays which revealed very similar physiological properties of SMA + BDNF[proprio] motor neurons compared to SMA motor neurons (Fletcher et al., 2017) this data indicates that changes in SMA motor neuron function are unlikely mediated by release of BDNF from proprioceptive neurons. In summary, these results demonstrate that presynaptic impairment is responsible for motor neuron dysfunction in SMA further supporting that motor neuron dysfunction is a non-cell autonomous event driven by SMN deficiency in proprioceptive neurons.

4.2. The mechanisms of synaptic loss in SMA

4.2.1. Proprioceptive synapses are eliminated at the onset of SMA

Proprioceptive synapses reach motor neurons at late embryonic stages (Chen et al., 2003) and continue proliferating during postnatal development (Kudo and Yamada, 1987; Li and Burke, 2002; Mentis et al., 2011). Proprioceptive synapses in SMA have reduced numbers compared to age-matched wild type (WT) mice at late stages of disease (Mentis et al., 2011). It is currently unknown whether this is due to synaptic arrest occurring during development, or are these synapses physically eliminated in SMA. This question was addressed by performing temporal analysis of the synaptic density of proprioceptive synapses on the somata and proximal dendrites in SMA motor neurons in the L1 spinal segment which is also a vulnerable spinal segment in SMA. Analyses were done on proximal dendrites (at distance from soma 0-100μm) of motor neurons, as the large majority (>80%) of proprioceptive synapses expressing the vesicular glutamate transporter 1 (VGluT1) are found on these sites (Fletcher et al., 2017; Rotterman et al., 2014). Analysis revealed that at birth (P0), there is no significant difference in the number of proprioceptive synapses between WT and SMA mice (Vukojicic et al., 2019) (Figure 17, A-C). This suggests that in SMA sensory synapses are formed normally. However, a significant progressive loss of SMA VGluT1+ synapses in proximal dendrites of motor neurons was observed at later ages, P11 and P13, compared to P4. Synaptic counts were analyzed at dendritic compartments 0-50μm and 50-100μm from the soma (Vukojicic et al., 2019) (Figure 17B, C).
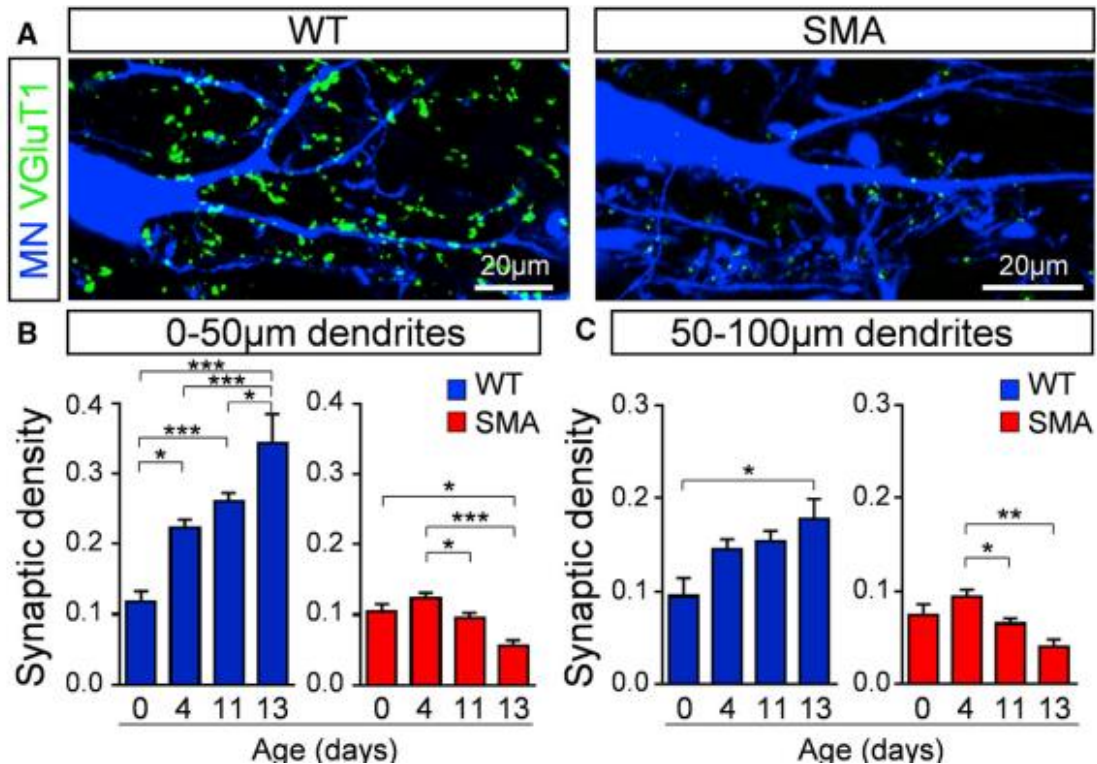
Figure 17. Vulnerable proprioceptive synapses are actively eliminated in SMA. (A) z-stack projection of confocal images from L1 motor neurons (MNs) retrogradely labeled (shown in blue) and VGluT1 synapses (shown in green) in P11 WT and SMA mice. Total distance in the z axis: 6 µm. (B) VGluT1+ synaptic density (number of synapses per 50 µm of dendritic length) in proximal dendritic compartments (0–50 µm) of WT (shown in blue) and SMA (shown in red) motor neurons at P0, P4, P11, and P13; N ≥ 3 mice per group. In WT number of dendrites: n = 11 (P0), n = 51 (P4), n = 35 (P11), and n = 18 (P13); in SMA: n = 9 (P0), n = 42 (P4), n = 33 (P11), and n = 10 (P13). (C) VGluT1+ synaptic density in 50–100 µm proximal dendritic compartments in WT (shown in blue) and in SMA (shown in red) motor neurons at P0, P4, P11, and P13; N ≥ 3 mice per group. In WT number of dendrites: n = 15 (P0), n = 44 (P4), n = 36 (P11), and n = 15 (P13); in SMA: n = 9 (P0), n = 34 (P4), n = 31 (P11), and n = 11 (P13). $*p < 0.05$, $**p < 0.001$, $***p < 0.001$; one-way ANOVA with Tukey's test. Adapted from (Vukojicic et al., 2019).

Intriguingly, there was no significant difference in the number of eliminated synapses on the soma of motor neurons at different ages in SMA (Vukojicic et al., 2019) (Figure 18), suggesting that the proprioceptive synapses on the soma may be more resilient to synaptic loss as compared to those synapses making contact on dendritic compartments of motor neurons.
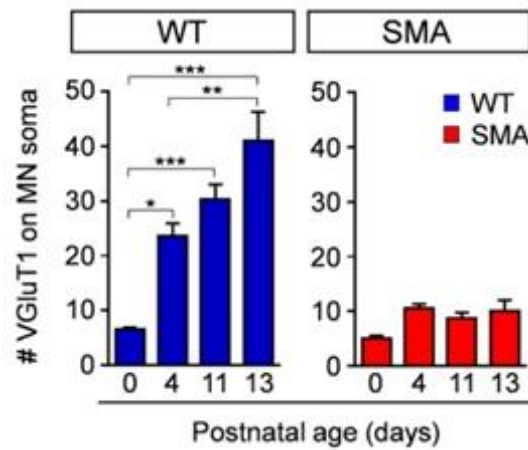
Figure 18. Proprioceptive synapses on the motor neurons soma may be more resilient to synaptic loss Graphs are showing temporal difference in the somatic number of VGluT1 synapses on L1 motor neurons in WT (shown in blue) and SMA (shown in red) mice at P0, P4, P11 and P13. * $p<0.05$, ** $p<0.001$, *** $p<0.001$ with One-way ANOVA and Tukey's test. Adapted from (Vukojicic et al., 2019).These results indicate that proprioceptive synapses in SMA are formed normally, but subsequently eliminated, starting at the onset of disease phenotype in mouse models of disease.

4.2.2. C1q is expressed during normal spinal cord development and upregulated in SMA

C1q, the initiating protein of the classical complement pathway, has been implicated in synapse elimination in Alzheimer's disease models (Hong et al., 2016), in glaucoma (Howell et al., 2011; Stevens et al., 2007), and frontotemporal dementia models (Lui et al., 2016). These observations have raised the possibility that classical complement pathway may also be involved in SMA. To investigate the molecular mechanisms underlying synaptic loss in SMA, the involvement of the C1q – the initiating protein of the classical cascade, was explored in this phenomenon. Immunoreactivity experiments revealed presence of C1q at similar levels in WT and SMA mice at birth (Vukojicic et al., 2019) (Figure 19). In striking contrast, a strong upregulation of C1q was observed in vulnerable SMA spinal cord segments at the onset of disease - (P4) and at late stages - (P11) compared to the age-matched WTs (Vukojicic et al., 2019) (Figure 19).
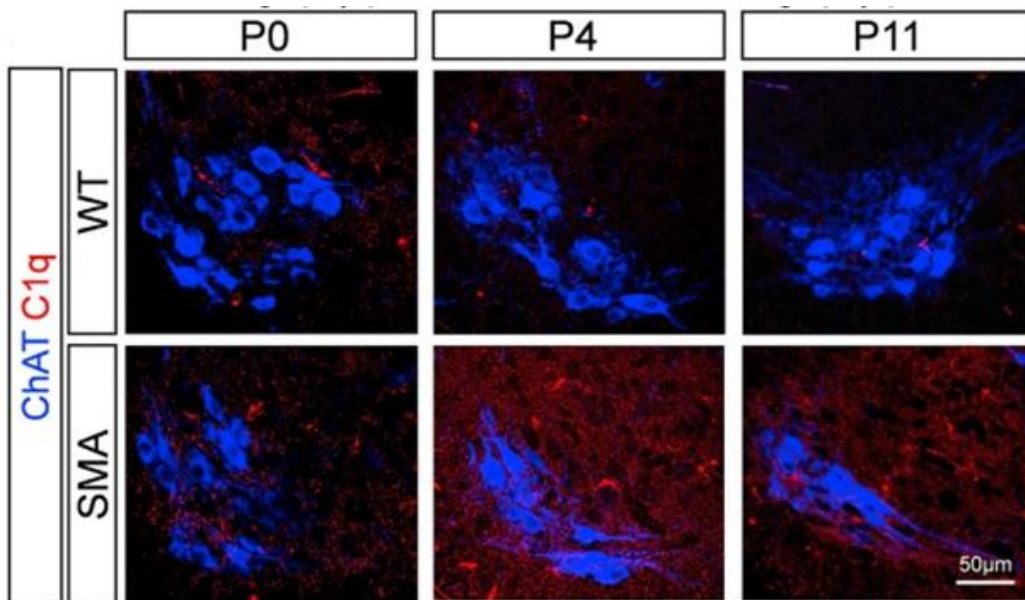
Figure 19. Increased C1q expression coincides with the onset of SMA when vulnerable synapses are eliminated. Z stack projection of confocal images from L1 motor pools visualized with ChAT (shown in blue) and C1q (shown in red) immunoreactivity from P0, P4, and P11 WT and SMA mice. Total distance in the z axis: 4.9 µm. Adapted from (Vukojicic et al., 2019).

An increased C1q immunoreactivity was noted around, but not within motor neurons (Vukojicic et al., 2019) (Figure 20), suggesting that C1q was not expressed in motor neurons.
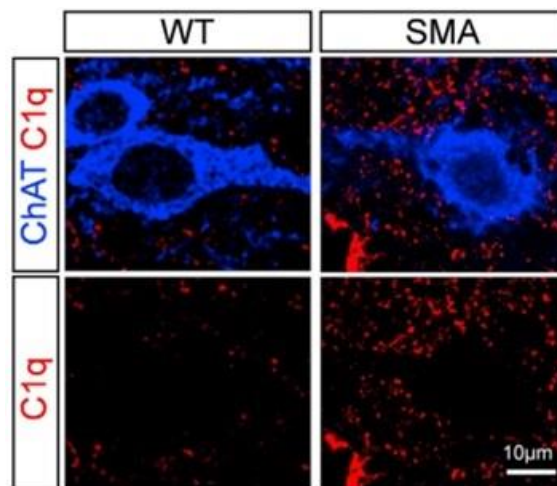
Figure 20. C1q is found around but not within motor neurons. Confocal images of motor neurons (ChAT: shown in blue) and C1q (shown in red) immunoreactivity in WT and SMA mice at P4. Adapted from (Vukojicic et al., 2019).

Importantly, C1q antibody specificity was validated in C1q knockout (C1q-/-) mice (Vukojicic et al., 2019) (Figure 21).
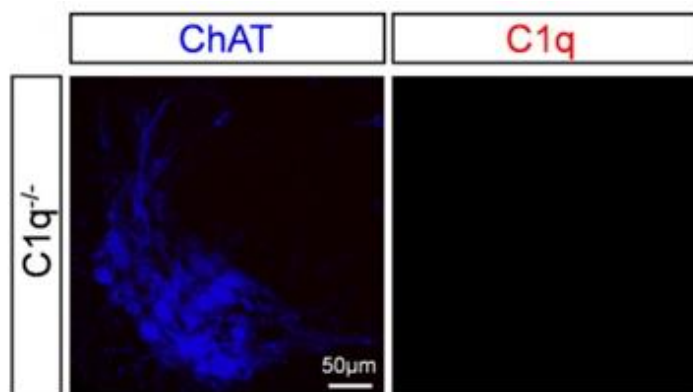
Figure 21. Validation of C1q antibody specificity. Z-stack projection of confocal images from the L1 spinal cord segment of C1q-/- mice showing motor neurons labeled with ChAT in blue and C1q in red. Total distance in the z-axis: 9.1 µm. Adapted from (Vukojicic et al., 2019)

Furthermore, quantitative reverse transcription polymerase chain reaction (RT-qPCR) experiments revealed that C1qA mRNA was also significantly increased at the onset of disease - P4 in vulnerable SMA spinal segments L1-L2 compared to those in WT mice (Vukojicic et al., 2019) (Figure 22A).
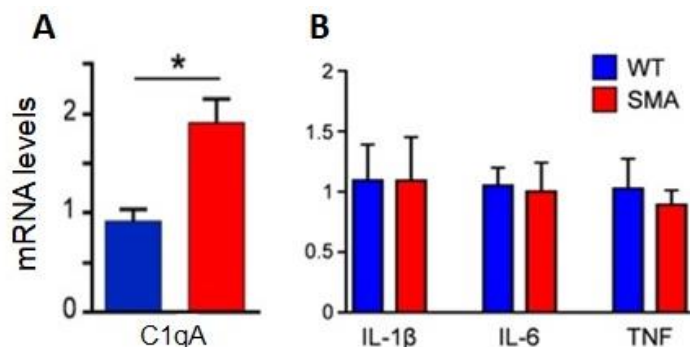

Figure 22. C1qA gene expression is increased at the onset of disease while the main proinflammatory cytokines remain unchanged. (A) qRT-PCR analysis of C1qA mRNA levels at P4 in the spinal cord segments L1–L2 of WT (n = 3, shown in blue) and SMA (n = 3, shown in red) mice. $*p < 0.05$; t test. (B) RT-qPCR analysis of IL-1β, IL-6 and TNF mRNA levels at P4, in the spinal cord segments L1-L2 of WT (n=3, shown in blue) and SMA (n=3, shown in red) mice. No significant difference was observed, t-test. Adapted from (Vukojicic et al., 2019).

While C1q levels were elevated, there was no significant difference in the mRNA levels of the proinflammatory cytokines tumor necrosis factor (TNF), interleukin 1 beta (IL-1β), and interleukin 6 (IL-6) in WT and SMA L1-2 spinal cords at P4 (Vukojicic et al., 2019) (Figure 22B) suggesting that increased C1q expression in SMA was not associated with the activation of inflammatory pathways as seen in neuroinflammatory diseases or in CNS injury. In addition to the increase in a mouse model of SMA, increased C1q immunoreactivity was also observed in human post-mortem spinal cord tissue from SMA Type I patient compared to a control (Vukojicic et al., 2019) (Figure 23), suggesting that similar mechanisms operate in both animal models and in SMA patients.
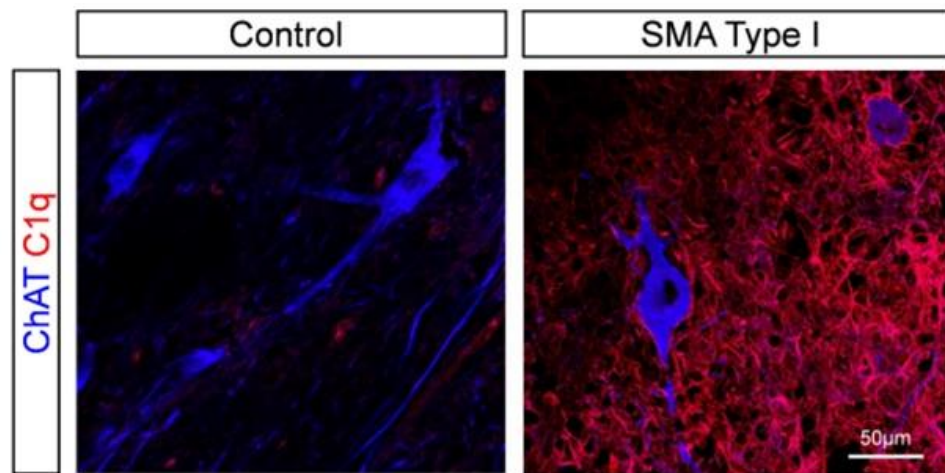
Figure 23. C1q expression is increased in SMA Type I human spinal cord. Z-stack projection of confocal images visualized with ChAT (shown in blue) and C1q (shown in red) immunoreactivity from post-mortem control and SMA patient's spinal cord lumbar segment. Total distance in the z-axis: 6μm. Adapted from (Vukojicic et al., 2019).

Taken together, these results suggest that there is a local production of C1q in close proximity to motor neurons and demonstrate a transient expression of C1q during early normal postnatal development in WT spinal cords as well as an aberrant upregulation of C1q at the onset of SMA.

4.2.3. Vulnerable SMA synapses are tagged by C1q and C3

To determine C1q localization at the synaptic level and particularly whether it is associated with proprioceptive sensory synapses, putative interactions between VGluT1+ synapses and C1q were investigated using confocal microscopy and high resolution imaging, followed by deconvolution

and image analysis in WT and SMA spinal cords at P4. Analysis revealed a close association of C1q with VGluT1synapses in both WT and SMA mice (Vukojicic et al., 2019) (Figure 24, A-D). However, this "tagging" of proprioceptive synapses occurred at significantly higher percentage (~25%) on proximal dendrites of L1 motor neurons in SMA compared to WT counterparts (~4%) (Vukojicic et al., 2019) (Figure 24E), which is in correlation with previously described findings that proprioceptive synapses are actively lost from proximal dendrites but not form the soma of vulnerable L1 motor neurons. Intensity line profiling was used as a quantifiable measure for overlap between the two signals (C1q and VGluT1) to confirm each tagging event (Vukojicic et al., 2019) (Figure 24C,D).
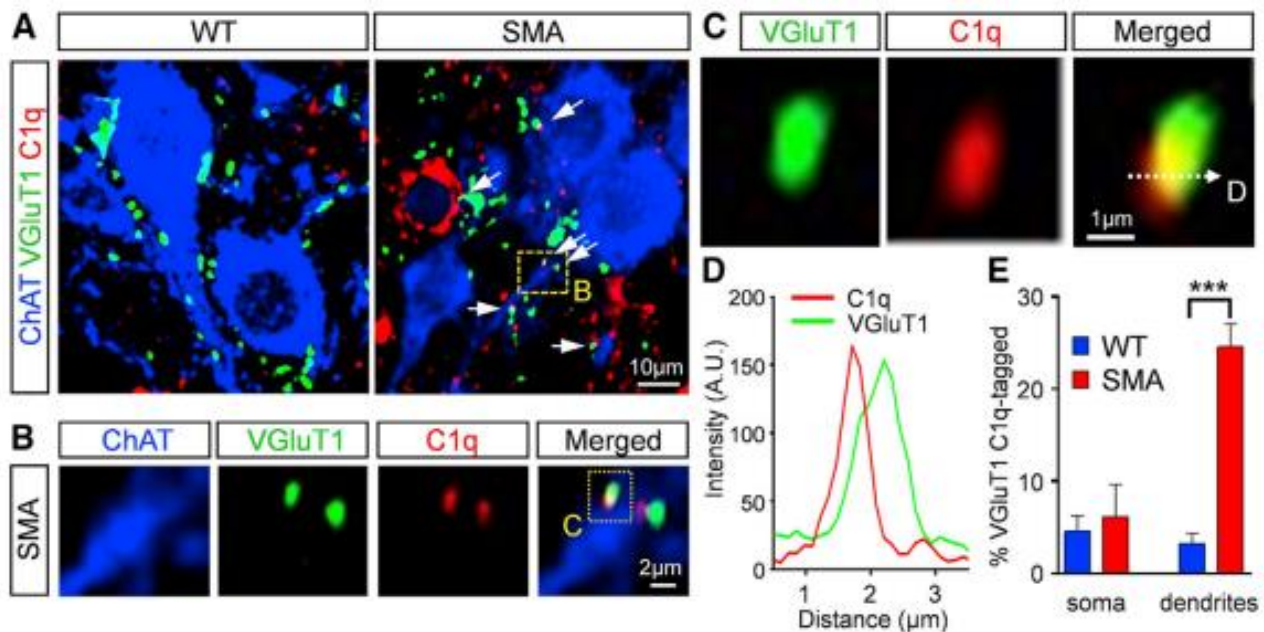
Figure 24. C1q tags vulnerable VGluT1 SMA synapses at the onset of disease. (A and B) Confocal images of ChAT (shown in blue), C1q (shown in red), and VGluT1 synapses (shown in green), at P4 in WT and SMA mice. Arrows indicate tagged synapses. (B) Higher magnification of dotted-line box from (A). (C) Higher magnification of the dotted-line box in (B), indicating the line in which the fluorescence profile is measured. (D) Fluorescence intensity profile (arbitrary units) for C1q signal (shown in red) and VGluT1 signal (shown in green) across the line which is shown in (C). (E) Percentage of VGluT1 synapses tagged by C1q on the soma and dendrites of spinal segment L1 motor neurons in WT (2,170 synapses from 76 motor neurons) and SMA (1,580 synapses from 86 motor neurons) at P4. ***p < 0.001; t test. Adapted from (Vukojicic et al., 2019).

To address whether C1q tagging is a selective event targeting specific synapses or alternatively all synapses indiscriminately in the context of the neurodegenerative disease, immunohistochemistry was employed against a pan-synaptic marker – synaptophysin. A

widespread C1q tagging of SMA synapses contacting MNs was discovered (Vukojicic et al., 2019) (Figure 25A, B) suggesting possibly C1q tagging beyond proprioceptive synapses in SMA.
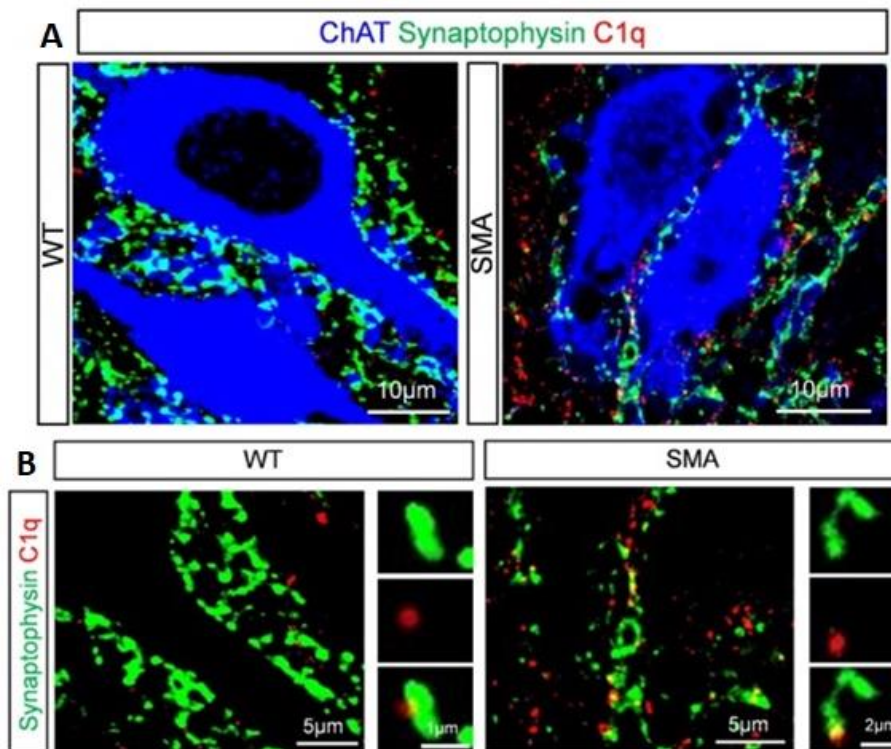
Figure 25. C1q might be tagging different types of synapses. (A) Confocal images of ChAT (shown in blue), Synaptophysin (shown in green) and C1q (shown in red) at P4 in WT and SMA motor neurons. (B) Higher magnification images of synaptophysin (shown in green) and C1q (shown in red) in WT and SMA spinal cords. Adapted from (Vukojicic et al., 2019).

To explore the possibility that C1q tagging is random in SMA and irrespective of the utilized synaptic neurotransmitter immunohistochemical experiments using antibodies against inhibitory synapses were performed. GABAergic synapses were labeled with the vesicular GABAergic transporter (VGAT). There was no difference between WT and SMA mice in the extent of C1q tagged synapses (Vukojicic et al., 2019) (Figure 26A, B). These results are in agreement with previous reports that GABAergic and glycinergic synapses are not affected in SMA (Ling et al., 2010a; Mentis et al., 2011).
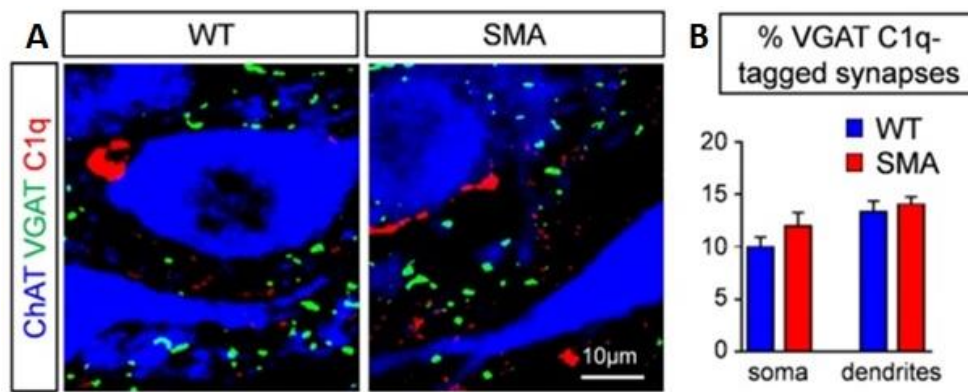
Figure 26. C1q does not preferentially tag inhibitory synapses in SMA. (A) Confocal images of ChAT (shown in blue), VGAT (shown in green) and C1q (shown in red) immunoreactivity at P4 in WT and SMA motor neurons. (B) Percentage of VGAT synapses tagged by C1q on the soma and dendrites in WT (shown in blue, n=55) and SMA (shown in red, n = 29) L1 motor neurons at P4. Adapted from (Vukojicic et al., 2019).

These results point out that increased synaptic tagging by C1q is specific for excitatory proprioceptive synapses, the numbers of which are significantly reduced in SMA (Mentis et al., 2011). Therefore, these results suggest that C1q might be tagging those synapses destined to be eliminated in the context of SMA.

At birth (P0) aberrant tagging of proximal proprioceptive synapses in SMA was not evident (Vukojicic et al., 2019) (Figure 27), which was in agreement with the finding that there was no statistical difference in the number of proprioceptive synapses on motor neurons between WT and SMA mice.

Figure 27. At birth aberrant tagging of SMA synapses is absent. Percentage of C1q-tagged VGluT1 synapses on the soma and dendrites of L1 motor neurons in WT (shown in blue, 454 synapses from 56 MNs) and SMA (shown in red, 487 synapses from 46 MNs) mice at birth (P0). Adapted from (Vukojicic et al., 2019).

These results indicate that in SMA, aberrant C1q tagging occurs after birth, at the onset of the disease which correlates with the time synaptic loss occurs, suggesting C1q involvement in synaptic elimination.

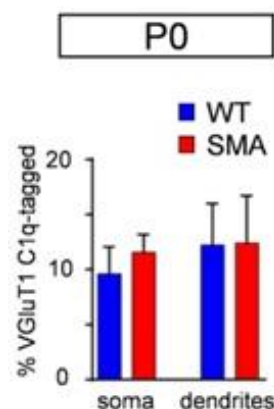To test whether C1q deposition on synapses, triggers classical complement pathway activation, localization and the expression of the downstream complement component C3 was next investigated. A significant increase in C3 gene expression in SMA compared to WT spinal cords at P4 (Vukojicic et al., 2019) (Figure 28A) was revealed with RT-qPCR experiments. Additionally, immunohistochemistry against C3 was performed, followed by high resolution confocal imaging, deconvolution and image analysis, to determine C3 localization in the context of vulnerable synapses in SMA. Analysis showed that C3 associates with WT and SMA VGluT1+ synapses (Vukojicic et al., 2019) (Figure 28B, C). However, in SMA mice, C3 is associated with a significantly higher number of proprioceptive synapses compared to WT controls (Vukojicic et al., 2019) (Figure 28D).
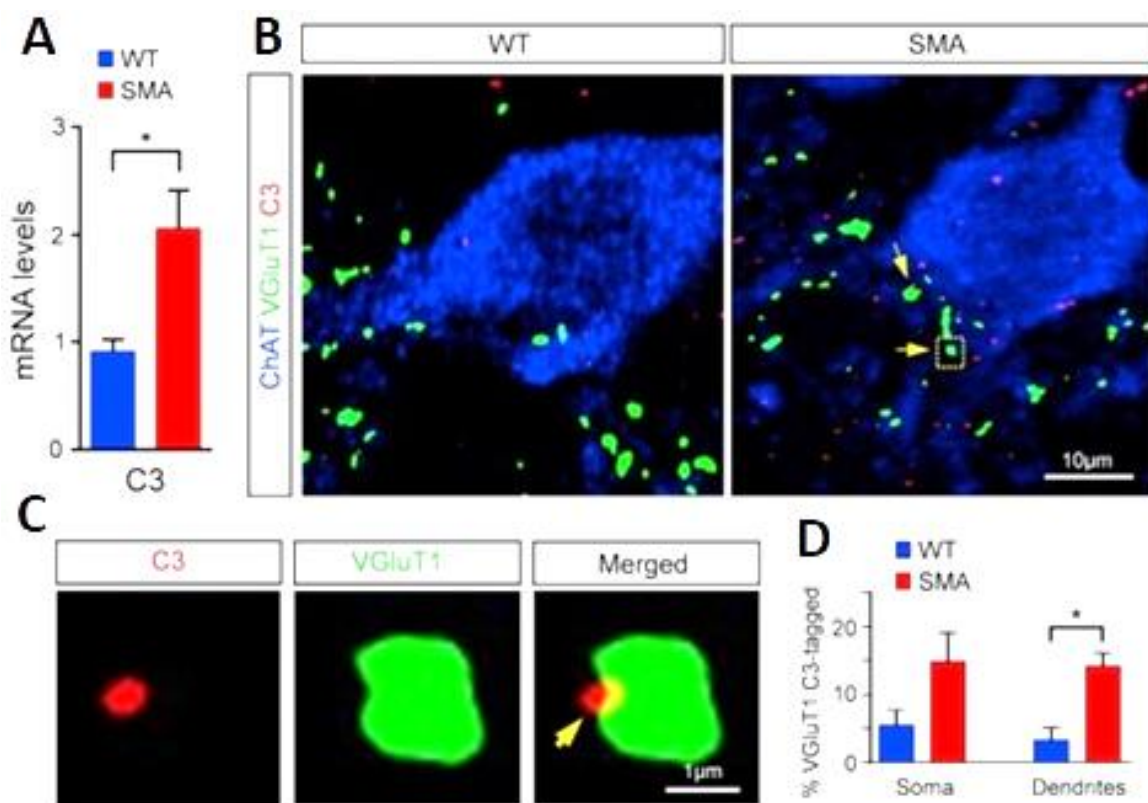
Figure 28. Aberrantly increased C3 tags vulnerable synapses in SMA. (A) qRT-PCR analysis of C3 mRNA levels at P4 in the spinal cord L1–L2 segments of WT (shown in blue, n = 3) and SMA (shown in red, n = 3) mice. *p < 0.05; t test. (B) Confocal images of motor neurons visualized with ChAT (shown in blue), C3 (shown in red), and VGluT1 synapses (shown in green) immunoreactivity at P4 in WT and SMA mice. The arrows indicate C3 deposited on synapses. (C) Confocal image at a higher magnification of a C3 (shown in red) deposited on a VGluT1 synapse

(shown in green) indicated by the dotted-line box in (B; SMA image). (D) Percentage of VGluT1 C3-tagged synapses on the soma and the proximal dendrites of L1 motor neurons in WT (1,155 synapses from 27 MNs) and SMA (1,305 synapses from 22 MNs) mice at P4. *p < 0.05; t test. Adapted from (Vukojicic et al., 2019).

C3immunoreactivity specificity was validated in C3$^{-/-}$ (C3 knockout) mice (Vukojicic et al., 2019) (Figure 29).
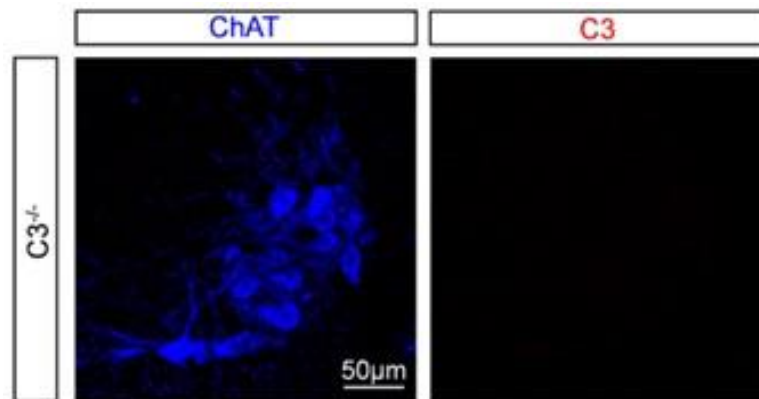
Figure 29. Validation of C3 antibody specificity. Z-stack projections of confocal images of motor neurons visualized with ChAT (shown in blue) and C3 (shown in red) immunoreactivity in L1 motor neurons of C3-/- at P4. Total distance in the z-axis: 9.1 μm. Adapted from (Vukojicic et al., 2019).

Together, these results indicate that similar percentage of proprioceptive synapses on proximal dendrites associated with C3 to those observed with C1q tagging, suggesting that early in the disease process the classical complement pathway is triggered and activated.

4.2.4. Microglia are responsible for synaptic removal in the spinal cord

Microglia have been implicated in synaptic pruning through the complement receptor 3 (Schafer et al., 2012; Stevens et al., 2007; Wu et al., 2015) which is the major phagocytic receptor on microglia (Ehlers, 2000). To determine the cell type responsible for the synapse elimination in SMA, the presence of microglia was investigated initially, since they express complement receptor 3 (CR3) (Tremblay et al., 2011). Immunohistochemistry utilizing ionized calcium-binding adapter molecule 1 (Iba1) as a marker for microglia revealed increased presence of Iba1+ cells in SMA mice, within the motor neuron nucleus, compared to the WT mice at P4 (Vukojicic et al., 2019)

(Figure 30A and 34B). Importantly, VGluT1+ synapses remnants were found within microglia profiles in WT and SMA motor neuron pools (Vukojicic et al., 2019) (insets in Figure 30A). However, quantification of the number of VGluT1+ synapses remnants within microglia revealed significantly higher incidence in SMA mice (Vukojicic et al., 2019) (Figure 30B).
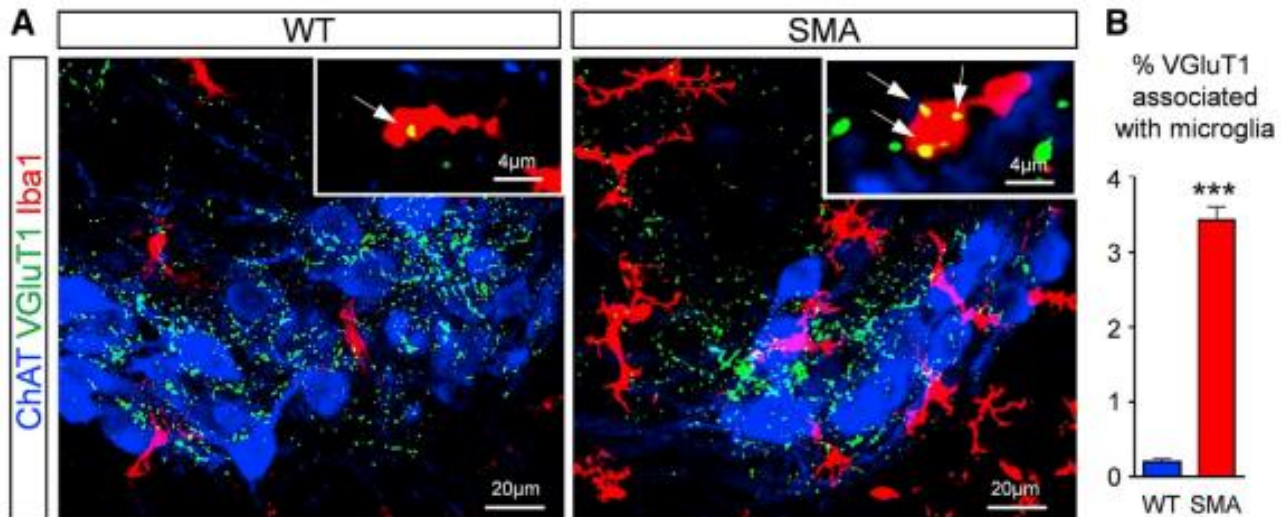
Figure 30. VGluT1+ synapse remnants are found within microglia suggesting of microglia-mediated synaptic elimination. (A) Z-stack projections of confocal images of motor neurons with ChAT (shown in blue), VGluT1 (shown in green), and Iba1 (shown in red) immunoreactivity at P4 in WT and SMA L1 motor neuron pools. Total distance in the z-axis: 10 µm. Insets show single optical planes in which areVGluT1 remnants (indicated by arrows) found within Iba1+ cells. (B) Percentage of VGluT1 synapses engulfed by microglia at P4 in WT and SMA mice. *p < 0.001; t test (n = 3). Adapted from (Vukojicic et al., 2019).

Most of the VGluT1 remnants within microglia were localized within the internal lysosomal compartments labeled by CD68 (Cluster of Differentiation 68) antibody (Vukojicic et al., 2019) (Figure 31) suggesting active phagocytosis of engulfed synapses.
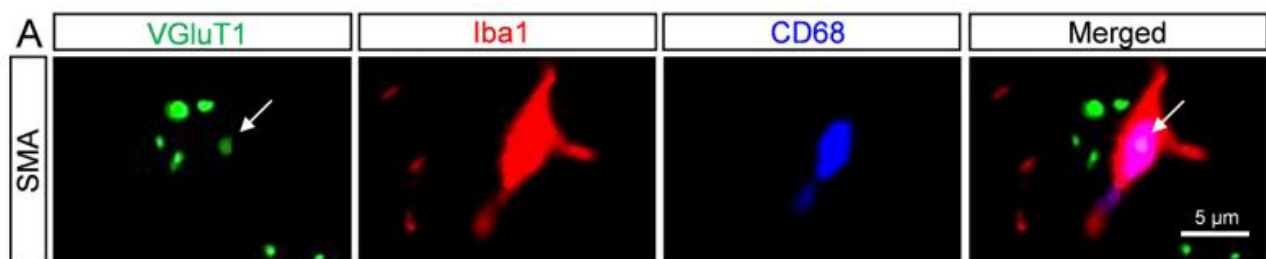
Figure 31. VGluT1 remnants are found within microglia lysosomes. Single optical plane confocal images of SMA microglia within the L1 spinal segment motor neuron nucleus at P4,

visualized by Iba1 (shown in red) and CD68 (shown in blue) as well as VGluT1 (shown in green) immunoreactivity. VGluT1 signal within microglial lysosome is indicated by arrows. Adapted from (Vukojicic et al., 2019).

Additionally, in both WT and SMA, every Iba1+ cell revealed low expression of cluster of differentiation 45 (CD45). At the same time CD45+/Iba1- cells were not observed, suggesting that there is no infiltration of leukocytes (Vukojicic et al., 2019) (Figure 32) which further supports that, beside complement activation, other inflammatory pathways are likely not activated.
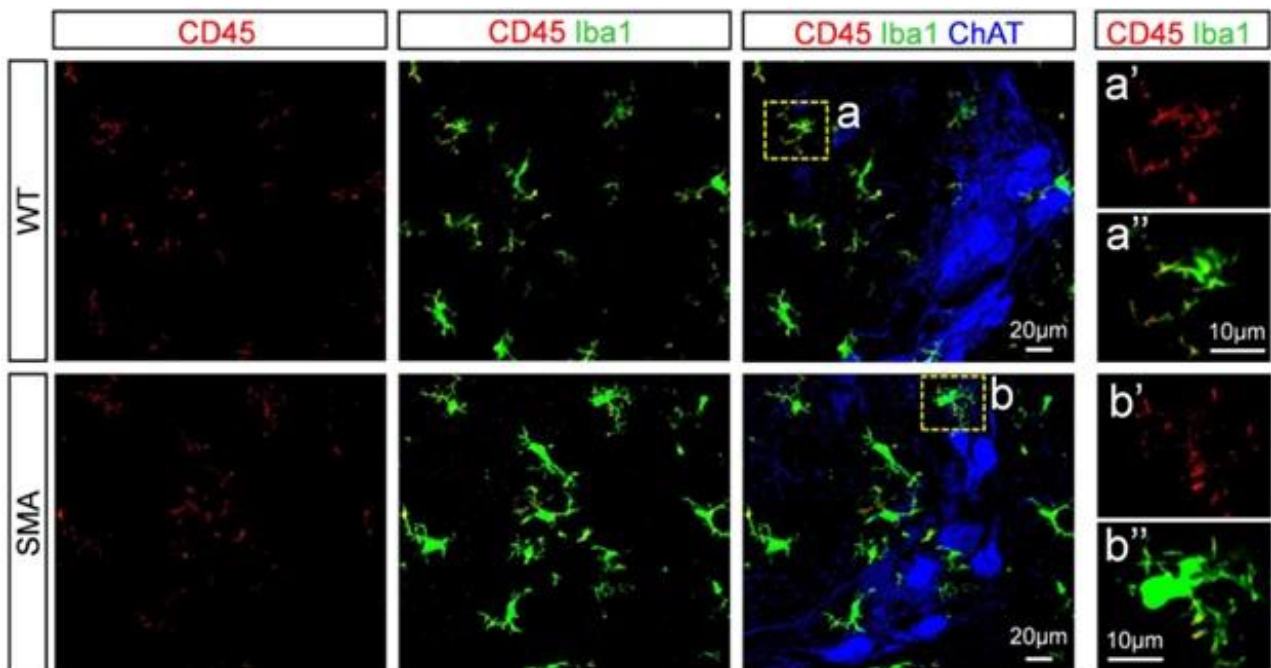
Figure 32. Low CD45 expression in WT and SMA spinal cord is restricted to Iba1+ cells. (B) Z-stack projections of confocal images of WT and SMA spinal cord L1 segments visualized by CD45 (shown in red), Iba1 (shown in green) and ChAT (shown in blue) immunoreactivity at P4. Total distance in the z-axis: 5.4 μm. Dotted boxes are shown at higher magnification on the right side for CD45 (shown in red) immunoreactivity in WT and SMA (a' and a'') and for Iba1 (shown in green) immunoreactivity in WT and in SMA (b' and b''). Adapted from (Vukojicic et al., 2019).

Collectively, these results suggest that VGluT1 synapses are phagocytosed by resident macrophages within the central nervous system – microglia, upon activation of the classical complement cascade.

To test whether activation of other components of the classical complement pathway occurs, gene expression level of the downstream C5 and its receptor C5aR1 was tested in WT and SMA

mice at P4, when complement tagging of vulnerable synapses has been initiated. RT-qPCR experiments revealed no difference between WT and SMA L1-2 spinal cord mRNA levels of either C5 or C5aR1 (Vukojicic et al., 2019) (Figure 33A,B). Additionally, potential differences in the expression of membrane attack complex (MAC) inhibitor - CD59b between WT and SMA mice were tested since studies in Amyotrophic Lateral Sclerosis and Alzheimer's disease noted low expression of CD59 coupled with high levels of downstream complement component (Lee et al., 2013; Yang et al., 2000). It has been demonstrated that CD59b is a key complement regulator in mice (Qin et al., 2003).WT and SMA mice, L1-2 spinal segments, at P4 revealed no difference in CD59b expression (Vukojicic et al., 2019) (Figure 33C).
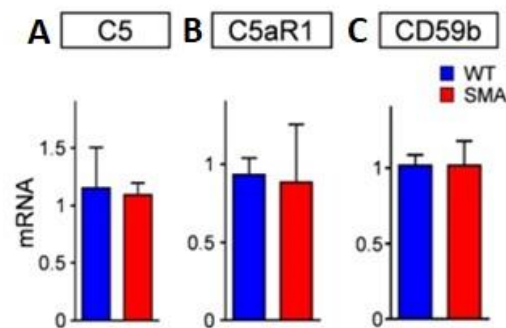
Figure 33. The downstream classical complement components are not activated in SMA mice. RT-qPCR analysis of C5 (A), C5aR1 (B) and CD59b (C) mRNA levels at P4 in the spinal cord L1-L2 segments of WT (shown in blue, n=3) and SMA (shown in red, n=3) mice. No significant difference was observed, t-test. Adapted from (Vukojicic et al., 2019).

The gene expression experiments for C5, C5aR1 and CD59b in WT and SMA suggest that the activation of the downstream components of the classical complement pathway and the membrane attack complex (MAC) is unlikely to be involved in synaptic elimination in SMA. These results suggest that resident microphage of CNS – microglia are responsible for synapse elimination in SMA mice. Collectively, this data indicates that vulnerable SMA synapses are removed upon complement tagging and classical pathway activation via microglia-mediated mechanisms which appear to be triggered independent of other inflammatory pathways or MAC activation.

4.2.5. Depletion of microglia rescues vulnerable synapses in SMA mice

To provide the evidence that microglia are causally responsible for synaptic elimination in SMA, both WT and SMA mice were treated with PLX5622 – a drug that inhibits the colony stimulating factor 1 receptor (CSF1R) (Elmore et al., 2018). Microglia originate from stem cells in the yolk sac (Kierdorf et al., 2013). These pluripotent cells develop into microglia precursor cells that will migrate to CNS and become microglia. Their development depends on Pu.1 and Irf8 (Kierdorf et al., 2013) and on the CSF1R (Elmore et al., 2014; Erblich et al., 2011; Ginhoux et al., 2010). Genetic evidence indicate that CSF1R plays a role in regulating the proliferation, viability and density of microglia (Cecchini et al., 1994; Michell-Robinson et al., 2015; Oosterhof et al., 2018). In adult mice treatment with selective CSF1R inhibitors eliminate up to ~99% of microglia brain-wide (Elmore et al., 2014; Elmore et al., 2018; Najafi et al., 2018; Spangenberg et al., 2019), confirming high efficacy of the drug and that microglia physiologically depend on CSF1R signaling in adult brain. While adult mice are treated with CSF1R inhibitor enriched breeder chow, SMA and WT mice were treated two times a day from birth until P10 with 50 mg/kg of PLX5622, as recommended by the provider - Plexxikon Inc. Morphological analysis of the untreated SMA and WT mice ventral horn revealed significantly higher number of microglia in SMA mice compared to age-matched WT controls (Vukojicic et al., 2019) (Figure 34A and B) an active proliferation of microglia in the close proximity to SMN-deficient motor neurons. In addition to this, microglia surrounding motor neurons in SMA mice appeared "activated" as indicated by larger cell body with strong Iba-1 immunoreactivity and thicker shorter processes (Davis et al., 1994). In support of this is the observation from another study in which increased association of activated microglia with motor neurons in SMAΔ7 mice has been reported (Ling et al., 2010a). PLX5622 treatment during the first 10 postnatal days resulted in approximately 90% reduction of microglia in WT as well as in SMA mice (Vukojicic et al., 2019) (Figure 34B) confirming that administration of PLX5622 resulted in successful microglia depletion.
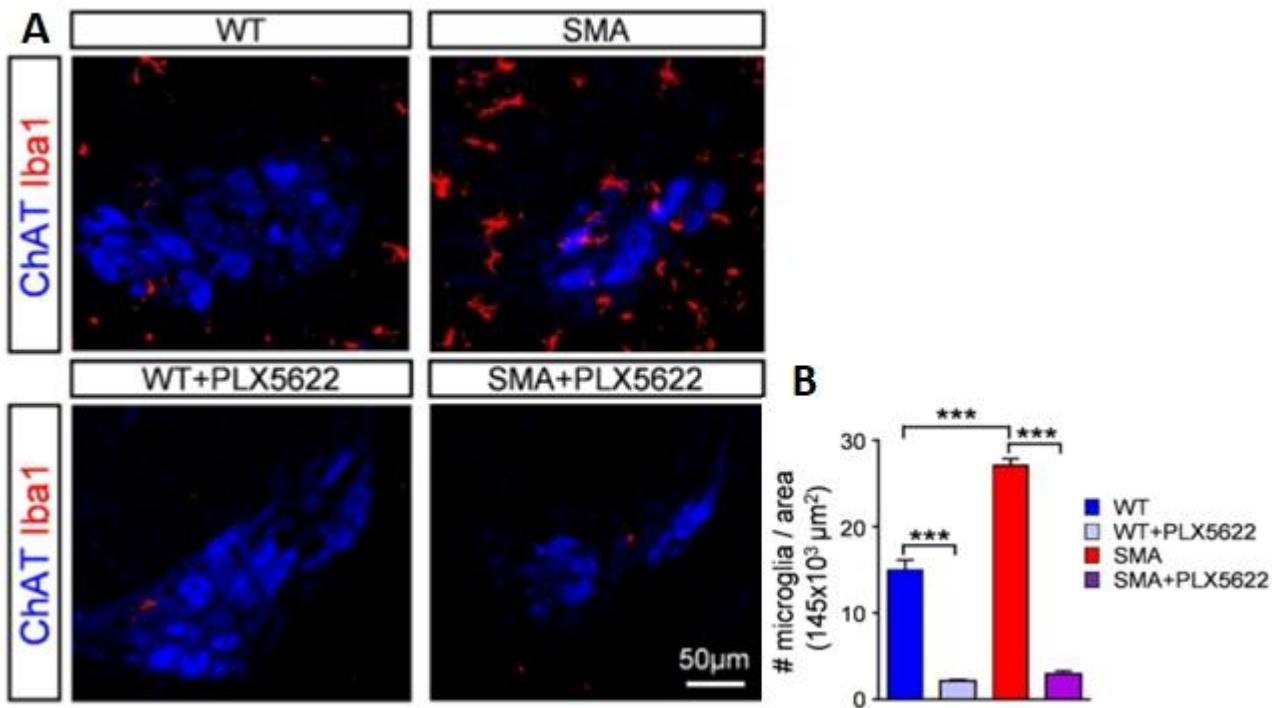
Figure 34. Microglia is successfully depleted from WT and SMA mice upon treatment with PLX5622.
(A) Confocal images of motor neurons within L1 motor neuron nuclei labeled with ChAT (shown in blue) and microglia labeled with Iba1 (shown in red) in WT, SMA, WT+PLX5622 and SMA+PLX5622 at P11. (B) Total number of microglia (Iba1+ cells) per 145x103 μm2 area and within motor neuron area in WT (shown in blue, n=5), WT+PLX5622 (shown in light blue, n=3), SMA (shown in red, n=7) and SMA+PLX5622 (shown in purple, n=3) mice at P11. *** p<0.001, One-way ANOVA, with Tukey's test. Adapted from (Vukojicic et al., 2019).

Strikingly, microglia depletion correlated with a significant rescue of VGluT1+ proprioceptive synapses on proximal dendrites of motor neurons in SMA mice treated with PLX5622 compared to untreated ones (Vukojicic et al., 2019) (Figure 35C,D). No difference was observed in somatic synaptic counts, supporting the observation that proprioceptive synapses contacting soma of motor neurons are partially lost very early (i.e. already at P2) (Fletcher et al., 2017) in the disease process.
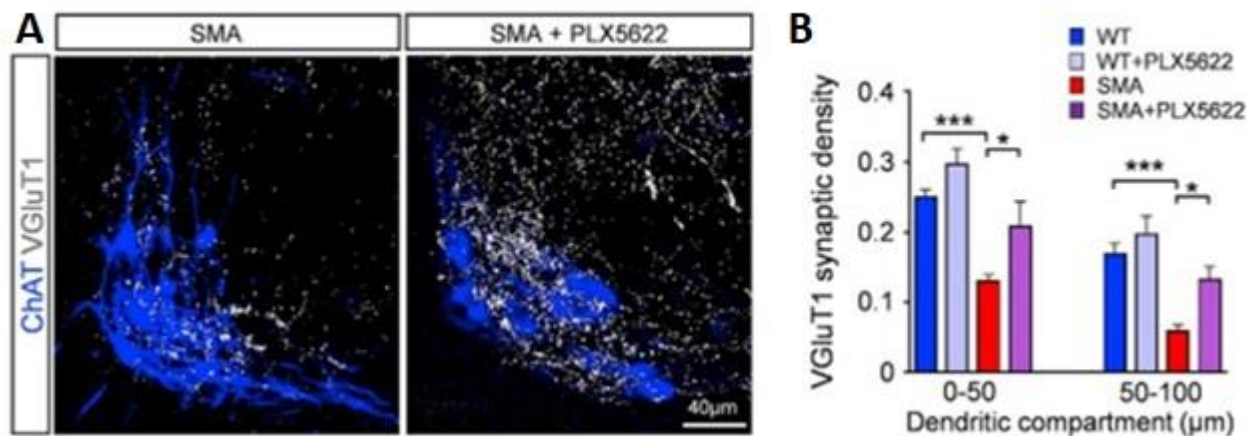
38. Depletion of microglia in SMA mice rescues vulnerable synapses. (A) Z-stack projections of confocal images of motor neurons at P11, labeled with ChAT (shown in blue) and VGluT1 synapses (shown in white) from untreated SMA and PLX5622-treated SMA mice. Total z stack distance: 20 µm. (B) VGluT1 synaptic density - number of synapses in 50-µm from soma dendritic compartments at P11 for WT (shown in blue, n = 41), WT+PLX5622 (shown in light blue, n = 17), SMA (shown in red, n = 43), and SMA+PLX5622 (shown in purple, n = 9) dendrites. *p < 0.05, ***p < 0.001; One-way ANOVA with Tukey's test. Adapted from (Vukojicic et al., 2019).

To test whether the rescue of synapses had any effect on behavior, the righting reflex was monitored daily in SMA and WT mice treated with PLX5622 In addition to synaptic rescue, a significant behavioral benefit correlated with the depletion of microglia in SMA treated mice, shown by a gradual improvement in time mice take to right after being placed on their back (righting time) (Vukojicic et al., 2019) (Figure 36).
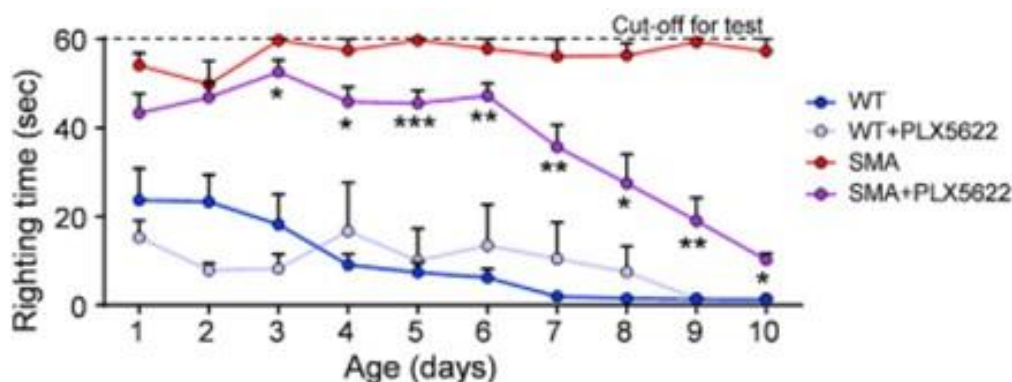
Figure 36. Depletion of microglia in SMA mice leads to motor behavior improvement. Righting times for WT (shown in blue, n = 10), WT+PLX5622 (shown in light blue, n = 9), SMA (shown in red, n = 8), and SMA+PLX5622 (shown in purple, n = 18) mice. *p < 0.05, **p < 0.01,

***p < 0.001; t test for SMA versus SMA+PLX5622 for individual ages. Adapted from (Vukojicic et al., 2019).

Control experiments showed that PLX5622 treated WT and SMA mice had no significant differences in body weight gain (Figure 37A) but a significant improvement in righting behavior in SMA, but not WT mice (Figure 36) (Vukojicic et al., 2019).
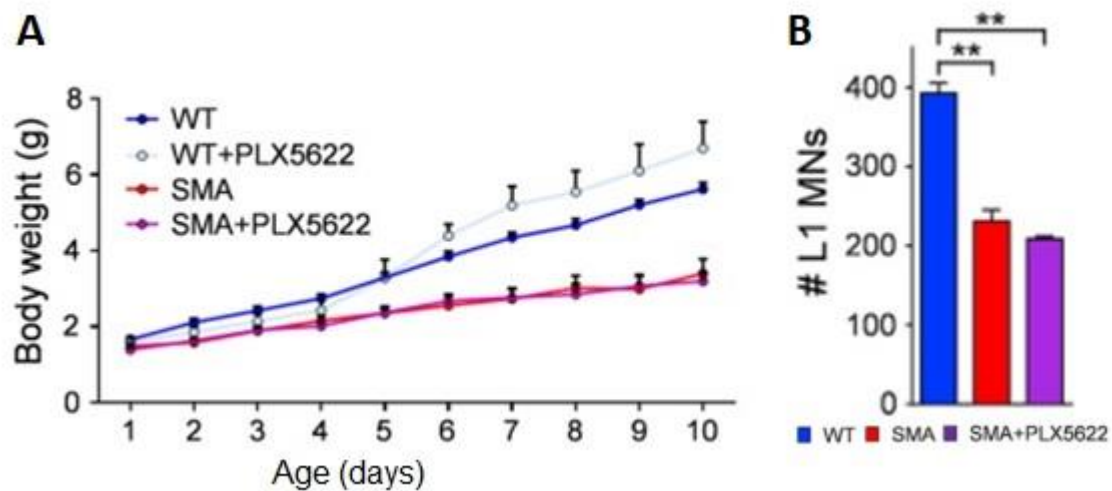
Figure 37. Depletion of microglia in SMA does not affect body weight nor does it rescue motor neurons from dying. (A) Body weights for WT (shown in blue, n=10), WT+PLX5622 (shown in light blue, n=9), SMA (shown in red, n=8) and SMA+PLX5622 (shown in purple, n=18) mice. (B) Total number of motor neurons in spinal L1 segment for WT (shown in blue, n = 3), SMA (shown in red, n = 4), and SMA+PLX5622 (shown in purple, n = 3) mice, at P11. **p < 0.01; one-way ANOVA with Tukey's test. Adapted from (Vukojicic et al., 2019).

PLX5622 treatment did not rescue motor neuron death in SMA mice (Figure 37B), which is consistent with previous results which demonstrate that motor neuron death and synaptic loss as well as dysfunction are two independent events (Fletcher et al., 2017). While motor neuron loss is driven by SMN deficiency in motor neurons *per se,* which leads to activation of intrinsic mechanisms responsible for their degeneration (Simon et al., 2017; Van Alstyne et al., 2018), sensory motor circuitry dysfunction and synaptic loss are consequence of SMN deficiency in proprioceptive neurons (Fletcher et al., 2017). Taken together, these results provide the evidence that microglia play an important role in the pathogenesis of SMA. These data demonstrate that activated and aberrantly increased microglia are responsible for synaptic elimination in SMA, potentially providing another therapeutic target point.

4.2.6. SMN deficiency in proprioceptive neurons drives C1q tagging of proprioceptive synapses

In order to identify what triggers C1q deposition at VGluT1 synapses, SMN was selectively restored in proprioceptive neurons in SMA mice. An SMA mouse model harboring two transgenic alleles and a single targeted mutation which resuls in the following genotype *Smn*[+/*Res*]*;SMN2*^{+/+}*;SMNΔ7*[+/+]was used (Fletcher et al., 2017). The allele that carries targeted mutation (*Smn*[*Res*]) reverts to a fullyfunctional *Smn*allele consequent to Cre-mediated recombination (*Cre*^{+/-}*;Smn*[*Res/-*]*;SMN2*^{+/+}*;SMNΔ7*[+/+]) (Lutz et al., 2011).*SMN2* is the human gene whereas*SMNΔ7*is the human SMN cDNA without exon 7. These mice have phenotype similar to the SMNΔ7 SMA mice in the absence of the Crerecombinase (Cre^{-/-};Smn[Res/-];SMN2^{+/+};SMNΔ7[+/+]) (Fletcher et al., 2017). In order to restore SMN protein selectively inproprioceptive neurons these conditional inversion SMA mice were crossed with Parvalbumin::Cre (Pv[Cre]) mice as has mentioned before, which label only proprioceptive neurons(during the first 10 postnatal days), as previously shown (Fletcher et al., 2017;Mendelsohn et al., 2015). SMA::Pv[Cre]mice show significant reduction of C1q deposition on VGluT1+ proprioceptive synapses located at the proximal dendrites of SMA vulnerable motor neurons (Vukojicic et al., 2019) (Figure 38A,B). Previous results have demonstrated that loss of SMN from proprioceptive neurons drives sensory-motor circuitry dysfunction and synaptic loss (Fletcher et al., 2017). Now, results of these experiments indicate that upon specific restoration of SMN in proprioceptive neurons, C1q tagging of VGluT1 synapses in SMA is comparable to that in WT mice (Vukojicic et al., 2019), suggesting that presynaptic SMN deficiency drives C1q-mediated mechanisms of synaptic loss in SMA.
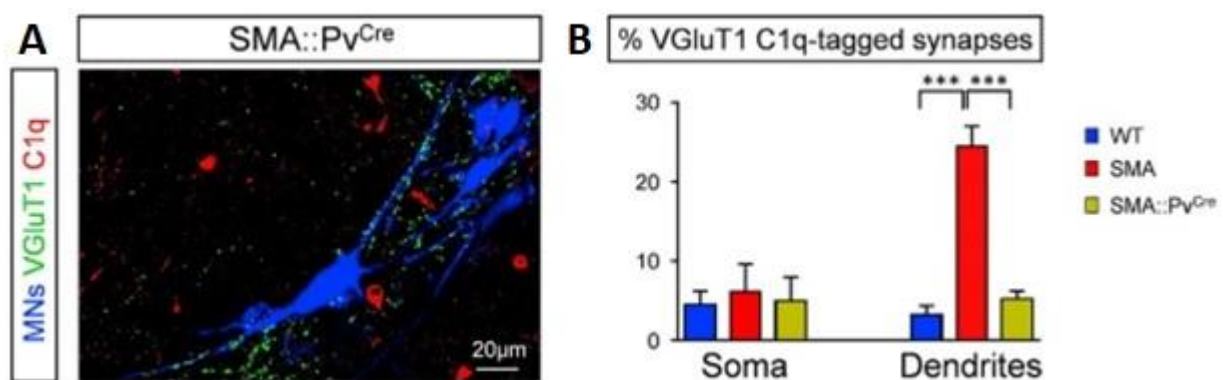
Figure 38. Selective restoration of SMN in proprioceptive neurons prevents C1q-tagging proprioceptive synapses. (A) z stack projection of confocal images of motor neurons retrogradely labeled (shown in blue), VGluT1 synapses (shown in green), and C1q (shown in red) from a P4 SMA::PvCre motor neuron pool. Total distance in the z-axis: 4.2 µm. (B) Percentage of C1q-tagged VGluT1 synapses on the soma and dendrites of spinal segment L1 motor neurons in WT (shown in

blue, 2,170 synapses from 76 MNs), SMA (shown in red, 1,580 synapses from 86 MNs), and SMA::PvCre (shown in yellow, 921 synapses from 52 MNs) at P4. ***p < 0.001; one-way ANOVA with Tukey's test. Adapted from (Vukojicic et al., 2019).

4.2.7. The local source of C1q in spinal cord are microglia

Possible local source of C1q in spinal cord was next investigated considering that previous results suggest that there is no infiltration of leukocytes in SMA spinal cord as well as the fact that through transcardial perfusion preceded all immunohistochemical experiments, meaning all blood derived complement was eliminated. Since C1q signal was not present within motor neurons and morphology of large C1q accumulations resembled the shape of microglia, immunohistochemistry experiments utilizing C1q antibody in combination with the antibodies against transmembrane protein 119 (TMEM119) and Iba1 were performed. While Iba1 labels microglia and microphages and is upregulated during the activation of these cells (Ohsawa et al., 2004), TMEM119 is a specific marker for microglia only and it is not expressed by macrophages or other neuronal or immune cell types (Bennett et al., 2016). All double positive Iba1+/TMEM119+ cells (n=128 from 3 WT mice n=215 from 3 SMA mice) showed a strong C1q signal in both WT and SMA mice (Vukojicic et al., 2019) (Figure 39A, B). These results suggest that C1q in spinal cord could be produced locally by microglia.
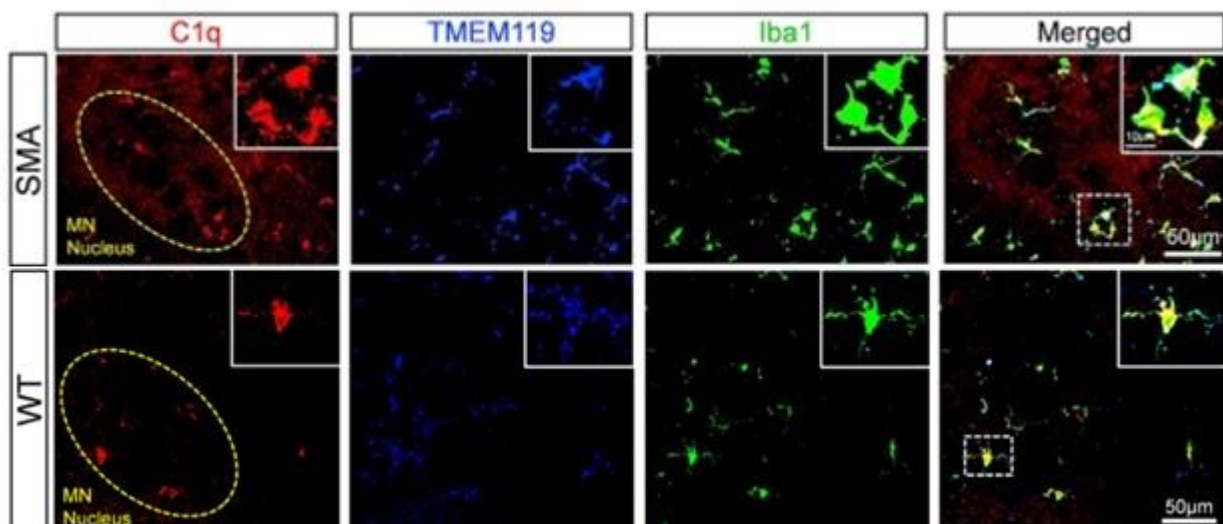
Figure 39. All spinal cord microglia expresses C1q. Z-stack projections of confocal images of C1q (shown in red), TMEM119 (shown in blue), and Iba1 (shown in green) in P4 SMA (upper images) and WT (lower images) in the L1 spinal ventral horn. Total distance in the z-axis: 5.25 µm. The circled area indicates the motor neuron nucleus. The area shown in the insets is indicated by

dotted-line box The insets show at higher magnification the colocalization of microglia (Iba1+/TMEM119+ cells) and C1q. Adapted from (Vukojicic et al., 2019).

Additionally, all Iba1+ cells (n=135 from 3 WT mice; n=252 from 3 SMA mice) were positive for cluster of differentiation 68 (CD68) (Vukojicic et al., 2019) which is highly expressed by the monocyte lineage cells and by both circulating and tissue macrophages and microglia (Holness and Simmons, 1993). This result together with the previous observation that all Iba1+ cells were TMEM119+, suggests that infiltration of macrophages or monocytes does not occur in WT or SMA mice, further supporting idea that C1q is locally produced by microglia. Additionally, these data also support previous observation that in SMA spinal cord there is no leukocyte infiltration as seen in classically defined neuroinflammatory conditions (e.g. multiple sclerosis) or after CNS injury. Importantly, to probe further whether C1q is produced by microglia, fluorescent in situ hybridization (FISH) in combination with immunohistochemistry was performed.
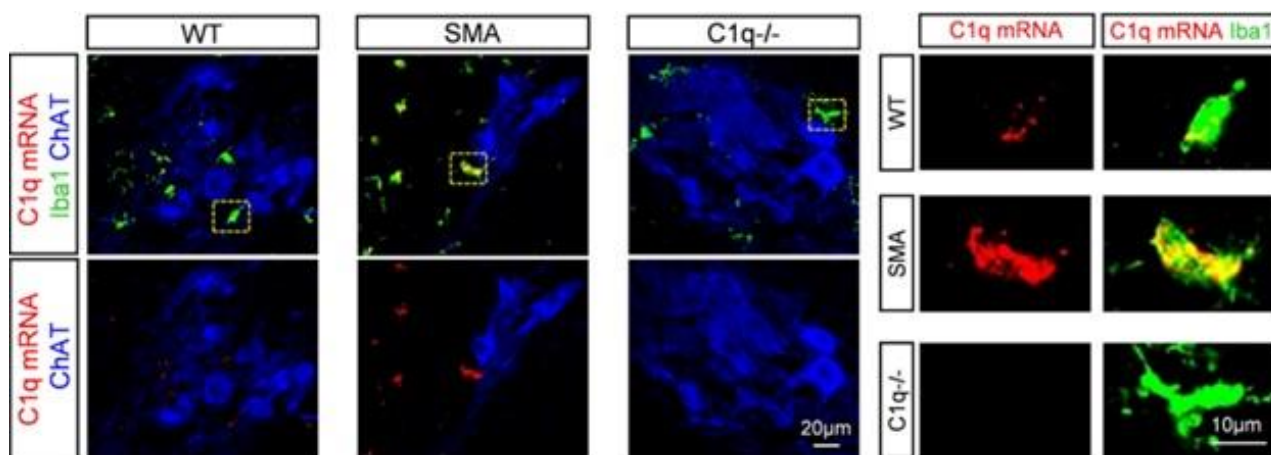
Figure 40. Microglia are the source of C1q in the spinal cord. Single optical plane confocal images from FISH C1q mRNA (shown in red) combined with Iba1 (shown in green) and ChAT (shown in blue) immunoreactivity at P4 in WT, SMA and C1q-/- mice. Dotted boxes are presented at higher magnification on the right side for C1q mRNA (shown in red) and Iba1 (shown in green) immunoreactivity in WT, SMA and C1q-/- mice. Adapted from (Vukojicic et al., 2019).

These experiments revealed C1qA mRNA presence within Iba1-antibody labeled microglia, but not inside motor neurons, which were labeled with ChAT antibody (Vukojicic et al., 2019) (Figure 40). FISH results confirmed that indeed microglia produces C1q both during normal development and in SMA. While all Iba1+ cells expressed C1qA, none was found inside of motor neurons. Additionally, SMN deficient microglia had significantly higher expression of C1qA which

is in correlation with previous results that C1q has increased expression in SMA mice compared to WT (Vukojicic et al., 2019). Together, these results demonstrate that during early development the major source of C1q in the spinal cord is microglia.

4.2.8. Postnatal neutralization of C1q tagging confers synaptic rescue and behavioral benefit in SMA mice

To further confirm the role of C1q in synaptic loss in SMA, mouse monoclonal anti-C1qantibody (a-C1q) (Lansita et al., 2017) was used to block postnatally C1q in SMA mice. The globular domain of C1q which is responsible for the recognition properties of C1q has compact, close to spherical heterotrimeric assembly of C1qA, C1qB and C1qC. This organization of subunits appears to be responsible for C1q's wide recognition properties (Gaboriaud et al., 2003). The exact binding target of C1q on a synapse is unknown. It is also not known which C1q subunit(s) are involved in its synaptic localization. The neutralizing a-C1q antibody binds to a conformational epitope which spans two of the three subunits of C1q globular head domains. It has been demonstrated that a-C1q antibody blocks interaction between C1q and diverse ligands, including phosphatidyl serine, IgM and CRP. Additionally, Lansita and colleagues (Lansita et al., 2017) showed in multiple animal species that functional activation of the classical pathway can be fully blocked by a-C1q antibody. Efficient C1q blockage by a-C1q antibody was also shown in animal models of antibody-independent neurodegeneration (Dejanovic et al., 2018; Hong et al., 2016) and antibody-mediated disease (McGonigal et al., 2016). C1q binding assay, utilizing plate coated with human C1q and both C1q neutralizing and control antibody in triplicate serial dilutions, was used to validate the specificity and affinity of the a-C1q antibody versus the isotype control – mouse immunoglobulin G1 (mIgG1) (Vukojicic et al., 2019) (Figure 41). This result confirmed high specificity and affinity of neutralizing a-C1q antibody used in *in vivo* experiments. SMA mice were treated from birth (P0) with either a-C1q antibody or isotype control antibody at a dose of 100mg/kg, every other day (Vukojicic et al., 2019).
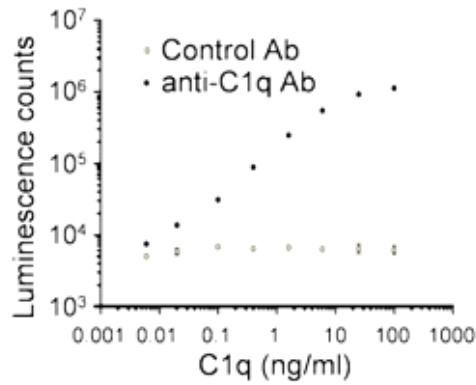
Figure 41. Validation of the specificity and affinity of the a-C1q antibody. C1q binding assay – ELISA of anti-C1q neutralizing antibody (shown in black), and Isotype control antibody (shown in gray) to human C1q. Adapted from (Vukojicic et al., 2019).

SMA mice which were treated with a-C1q antibody (SMA+a-C1q Ab) had a significant increase in VGluT1+ synapses on both soma and proximal dendrites of L1 MNs at P10. SMA mice treated with control antibody (SMA+Ctr Ab) did not show any increase in VGluT1+ synapses (Vukojicic et al., 2019) (Figure 42A-C). Additionally, there was no difference in VGluT1 synaptic density between isotype control treated and untreated SMA mice (Vukojicic et al., 2019) (Figure 42B, C). Strikingly, in a-C1q treated SMA mice, nearly complete synaptic rescue of VGluT1+ synapses on proximal dendrites of MNs was observed (Vukojicic et al., 2019) (Figure 42C).
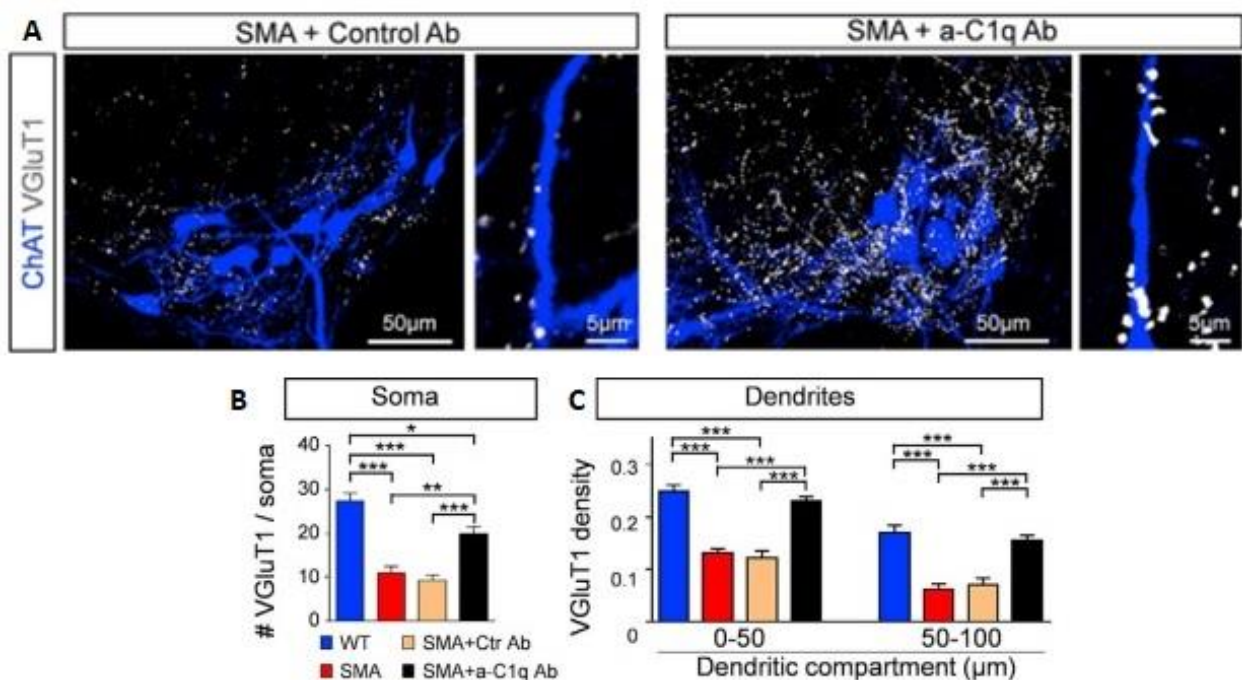
Figure 42. Postnatal *in vivo* neutralization of C1q in SMA mice rescues VGluT1 synapses (A) Z-stack projections of confocal images of L1 moto neurons retrogradely labeled (shown in blue)

and VGluT1 (shown in white) in SMA mice treated with isotype control antibody (left) and with anti-C1q antibody (right) at P11. Total distance in the z axis: 22.4 µm. Higher-magnification confocal images of individual motor neuron dendrites with VGluT1 synapses are shown at right. (B) The total number of VGluT1 synapses on the entire soma in WT (shown in blue, n = 10), SMA (shown in red, n = 10), SMA+Ctr Ab (shown in orange, n = 10), and SMA+a-C1q Ab (shown in black, n = 6) L1 motor neurons. *p < 0.05, **p < 0.01, ***p < 0.001; one-way ANOVA with Tukey's test. (C) Synaptic density in 50-µm from the soma dendritic compartments in WT (shown in blue, n = 41), SMA (shown in red, n = 43), SMA+Ctr Ab (shown in orange, n = 31), and SMA+a-C1q Ab (shown in black, n = 54) L1 motor neurons . ***p < 0.001; One-way ANOVA with Tukey's test. Adapted from (Vukojicic et al., 2019).

To test whether treatment with a-C1q antibody upregulated SMN in spinal cord, western blot was used to asses SMN levels in spinal cords from treated SMA mice compared to untreated WT and SMA mice. Results of these experiments revealed that SMN levels remain unchanged in SMA mouse spinal cord upon a-C1q antibodies treatment (Vukojicic et al., 2019) (Figure 43A). To also address this possibility of SMN upregulation in DRGs upon treatment, immunohistochemistry against SMN and parvalbumin was performed. Similarly to spinal cord observations, SMN levels did not increase in DRGs upon treatment, as no increase of Gems (nuclear structures containing SMN) (Liu and Dreyfuss, 1996) was observed in proprioceptive neurons (Vukojicic et al., 2019) (Figure 43 B, C).
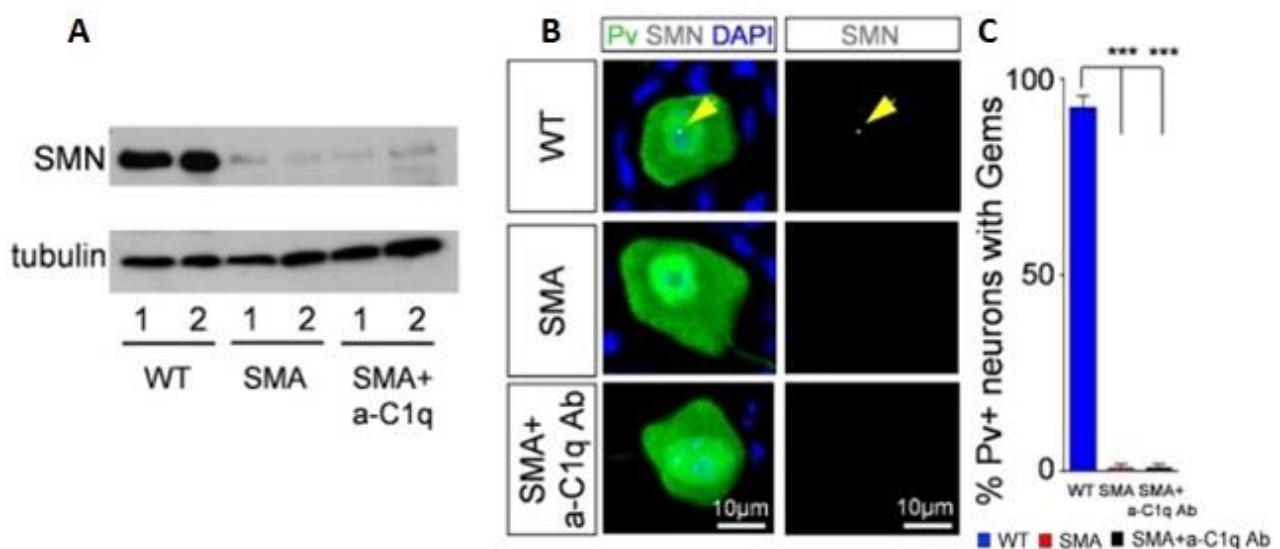
Figure 43. Postnatal *in vivo* neutralization of C1q in SMA mice does not upregulate SMN protein. (A) Western blot analysis for SMN and β-tubulin protein expression from L1-L3 spinal cord segments of two WT, two SMA and two SMA+a-C1q Ab at P11. (B) Confocal images of

Parvalbumin (shown in green), SMN (shown in white) and nuclei stained with 4′,6-diamidino-2-phenylindole (DAPI, shown in blue) in P11 DRGs from WT, SMA and SMA+a-C1q Ab. Arrow points on gem, visualized by SMN (shown in white) immunoreactiity. (C) Percentage of parvalbumin neurons containing gems in P11 DRGs from WT (shown in blue, n=50), SMA (shown in red, n=50) and SMA+a-C1q Ab (shown in orange, n=50). *** p<0.01, One-way ANOVA with Tukey's test. Adapted from (Vukojicic et al., 2019).

Furthermore, to test whether a-C1q antibody treatment rescues motor neurons, all L1 spinal segment motor neurons were counted in untreated WT and SMA mice and compared against treated SMA mice. SMA mice treated with a-C1q antibody did not have any rescue of SMA motor neurons (Vukojicic et al., 2019) (Figure 44), suggesting that C1q does not play a role in motor neuron death. This is not surprising as it has been demonstrated that motor neuron death is cell autonomous event driven by SMN deficiency which leads to activation of intrinsic mechanisms responsible for motor neurons degeneration (Simon et al., 2017; Van Alstyne et al., 2018). Additionally, previous results show that synaptic loss and sensory motor circuitry dysfunction are due to SMN deficiency in proprioceptive neurons (Fletcher et al., 2017), indicating that these events are independent from motor neuron death.
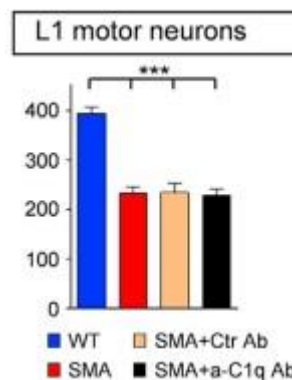
Figure 44. Postnatal *in vivo* neutralization of C1q in SMA mice does not rescue motor neurons from dying. Total number of L1 motor neurons at P11 in WT (shown in blue, n = 3), SMA (shown in red, n = 4), SMA+Ctr Ab (shown in orange, n = 5), and SMA+a-C1q Ab (shown in black, n = 8) mice. ***p < 0.001; one-way ANOVA with Tukey's test. Adapted from (Vukojicic et al., 2019).

Furthermore, to test whether neutralization of C1q has any effects on neuromuscular junction (NMJ) denervation, the extent of denervation was investigated in the vulnerable muscle Quadratus Lumborum (QL) (Fletcher et al., 2017).
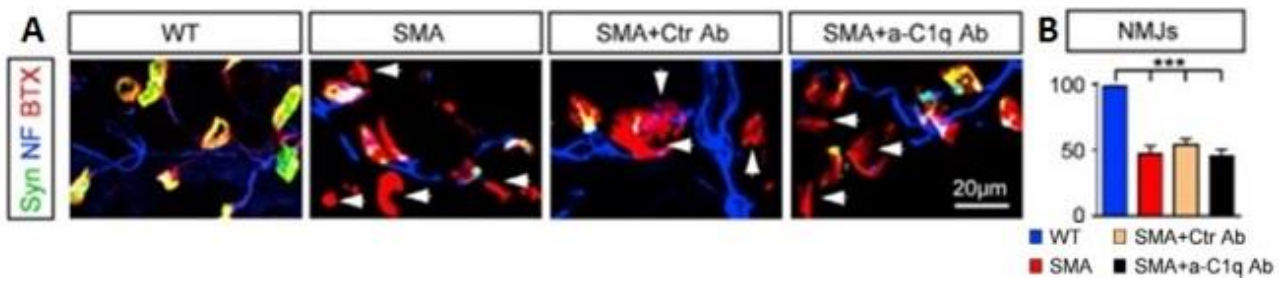
Figure 45. Postnatal *in vivo* neutralization of C1q in SMA mice does not rescue NMJs. (A) Z-stack projections of confocal images of synaptophysin (shown in green), neurofilament (NF) (shown in blue) and a-bungarotoxin (BTX) (shown in red) to label pre- and postsynaptic elements of neuromuscular junctions (NMJs) in the QL muscle at P11 in WT, SMA, SMA+Ctr Ab, and SMA+a-C1q Ab mice. The arrows indicate denervated NMJ. total distance in thez-axis:7 µm. (B) Percentage extent of QL muscle innervation in WT (shown in blue, n = 3 mice), SMA (shown in blue, n = 3), SMA+Ctr Ab (shown in orange, n = 3), and SMA+a-C1q Ab (showan in black, n = 5). ***p < 0.001; One-way ANOVA with Tukey's test. Adapted from (Vukojicic et al., 2019).

No difference was found between isotype control-treated, untreated SMA and SMA mice treated with a-C1q antibody (Vukojicic et al., 2019) (Figure 45A, B). This is most likely due to the absence of C1q around neuromuscular junctions (NMJs), as no C1q signal was detected in close proximity to NMJs of vulnerable QL muscle in SMA mice (Vukojicic et al., 2019) (Figure 46A,B). Although the number of NMJ synapses was not rescued, to further investigate whether anti-C1q antibody treatment had any physiological benefit in vulnerable muscle performance, in collaboration with Dr. Nicolas Delestree in the Mentis Lab, physiological assays were performed on vulnerable QL muscles. Following stimulation of the L1 ventral root, tested compound muscle action potentials (CMAPs) in QL muscle of SMA a-C1q antibody treated mice did not reveal any improvement compared to isotype control treated or untreated SMA mice (Vukojicic et al., 2019) (Figure 46C). This was not surprising considering that NMJ denervation was not rescued with C1q neutralization.
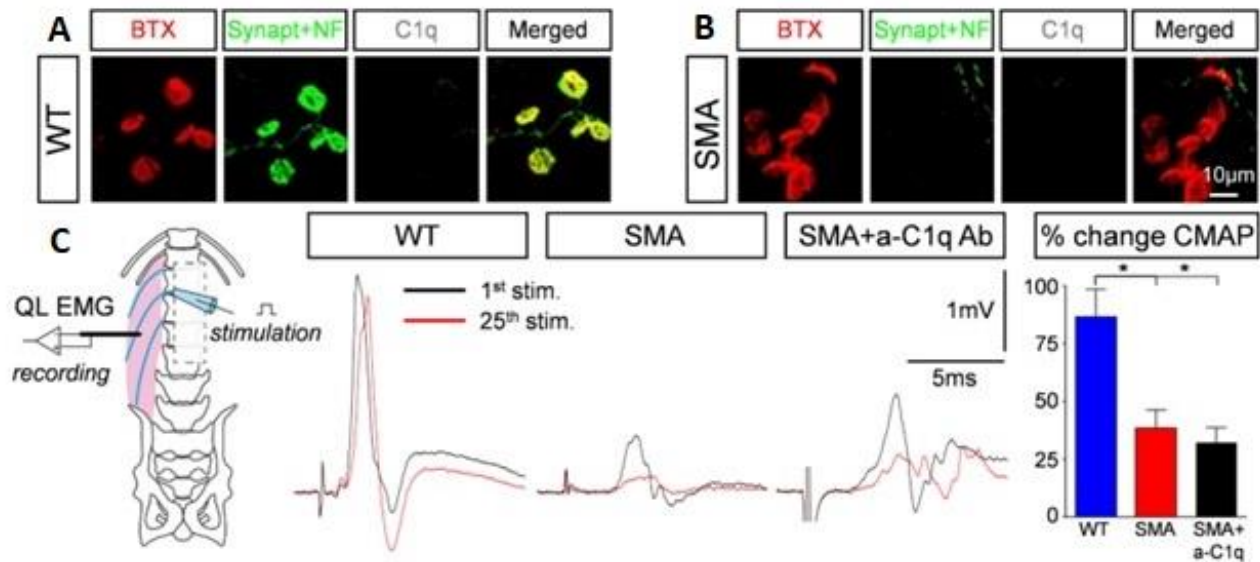
Figure 46. C1q does not tag NMJs and postnatal *in vivo* neutralization of C1q in SMA mice does not have any effect on NMJ denervation and function. Z-stack projections of confocal images of NMJs from the Quadratus Lumborum (QL) muscle visualized with α-bungarotoxin (BTX, shown in red), synaptophysin and neurofilalment (shown in green) and C1q (shown in white) immunoreactivity at P5 in WT (A) and SMA (B) mice. Total z stac distance: 7 μm. (C) Schematic illustration of ex vivo experimental setup for assessment of Compound Muscle Action Potentials (CMAPs) in the QL muscle in mice. Superimposed traces of the 1st (shown in black) and 25th (shown in red) CMAPs during 25 Hz stimulation of the L2 ventral root in WT, SMA and SMA+a-C1qAb mice. Graph shows the percentage change in CMAP amplitude (baseline-to-peak) of the 25th response normalized to the 1st CMAP following 25 Hz stimulation of the ventral root in WT (shown in blue, n=5), SMA (shown in red, n=5) and SMA+a-C1qAb (shown in back, n=5) mice. * p<0.05, One-way ANOVA with Tukey's test. Adapted from (Vukojicic et al., 2019).

Collectively, these results demonstrate that while C1q is involved in central synapse elimination, it plays no role in peripheral synapse elimination in SMA. Importantly, to address whether rescued VGluT1+ synapses in SMA mice treated with a-C1q antibody were functional, the *ex vivo* spinal cord preparation (Vukojicic et al., 2019) (Figure 47) was employed and dorsal-to ventral root reflexes were performed in collaboration with Dr. Nicolas Delestree, in L1 segment at P11.
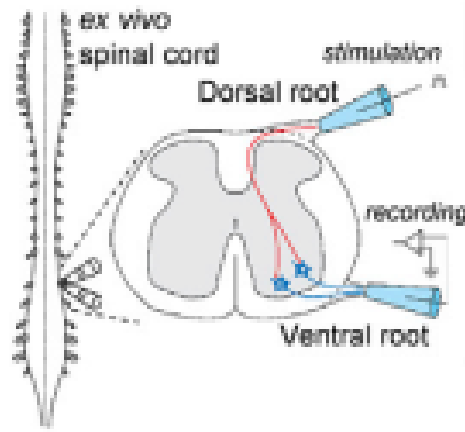
Figure 47. The ex vivo spinal cord physiological assay. Schematic illustration of the ex vivo spinal cord physiological assessment. Stimulation of the L1 dorsal root elicits a response on the homonymous L1 ventral root. Adapted from (Vukojicic et al., 2019).

In SMA mice treated with a-C1q antibody the amplitude of the reflex response showed a significant increase compared to isotype control treated or untreated SMA mice (Vukojicic et al., 2019) (Figure 48A, B,). These results indicate that more motor neurons can be activated following proprioceptive synapse activation in those mice treated with C1q neutralizing antibody. In addition, to test synaptic reliability of the synapses rescued by treatment, we challenged proprioceptive synapses at different frequencies in order to investigate presynaptic from postsynaptic mechanisms. These experiments demonstrated that synaptic reliability of rescued synapses in treated mice is similar to synaptic reliability of WT mice, following the high frequency stimulation (20Hz) (Vukojicic et al., 2019) (Figure 48C). Thus, although the number of motor neurons in treated SMA mice remains similar to the one in untreated, their function and output are significantly improved due to the restoration of sensory-motor circuitry. Importantly, the synaptic reliability test does not depend on the number of synapses present nor on the number of MNs present, since the motor neuron response amplitude at high frequency is normalized to the first stimulus, meaning that presynaptic function is being tested.
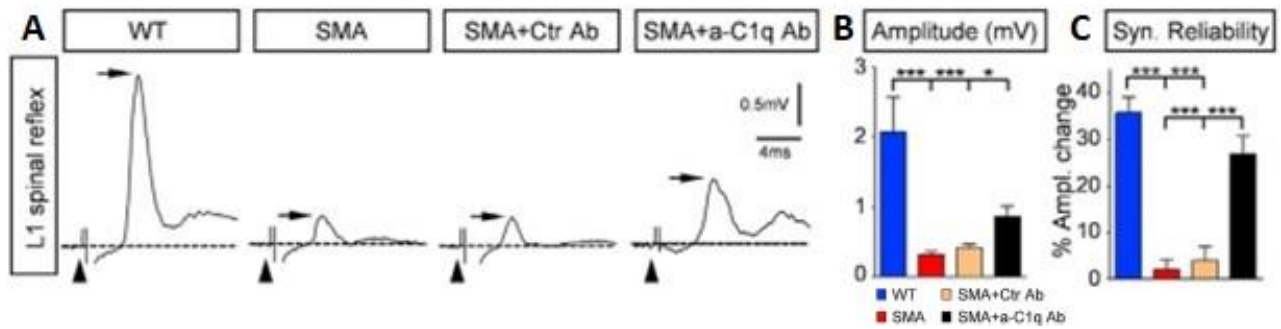
Figure 48. Postnatal *in vivo* neutralization of C1q in SMA mice improves motor output by rescuing synaptic function. (A) Ventral root responses to L1 dorsal root stimulation in WT, SMA, SMA+Ctr Ab, and SMA+aC1q Ab at P10. The dotted line indicates baseline. The arrowheads point to the stimulus artifacts. The arrows indicate the maximal amplitude of the monosynaptic responses. (B) The maximum amplitude of the monosynaptic response in WT (shown in blue, n = 6), SMA (shown in red, n = 9), SMA+Ctr Ab (shown in orange, n = 7), and SMA+a-C1q Ab (shown in black, n = 7) mice. *p < 0.05, ***p < 0.001; One-way ANOVA with Tukey's test. (C) Percentage of the amplitude change for the 5th response (normalized to the 1st) following 20-Hz stimulation in WT (shown in blue, n = 6), SMA (shown in red n = 9), SMA+Ctr Ab (shown in orange, n = 7), and SMA+aC1q Ab (shown in black, n = 7) mice at P11. ***p < 0.001; One-way ANOVA with Tukey's test. Adapted from (Vukojicic et al., 2019).

Together, these results demonstrate that *in vivo* neutralization of C1q by a-C1q antibody treatment from birth results in increased number and function of proprioceptive synapses in SMA mice. This suggests that beside the role for complement in selective synaptic elimination, complement also play a role early in synaptic dysfunction. To test whether all these observations upon a-C1q antibody treatment translate into behavioral improvement, body weight and righting time were monitored daily in the isotype control treated, untreated SMA and a-C1q antibody treated SMA mice. SMA mice treated with a-C1q antibody showed a significant improvement in the survival by the lifespan increase of ~25 % (Figure 49A), but minimal body weight gain (Figure 49B) (Vukojicic et al., 2019).
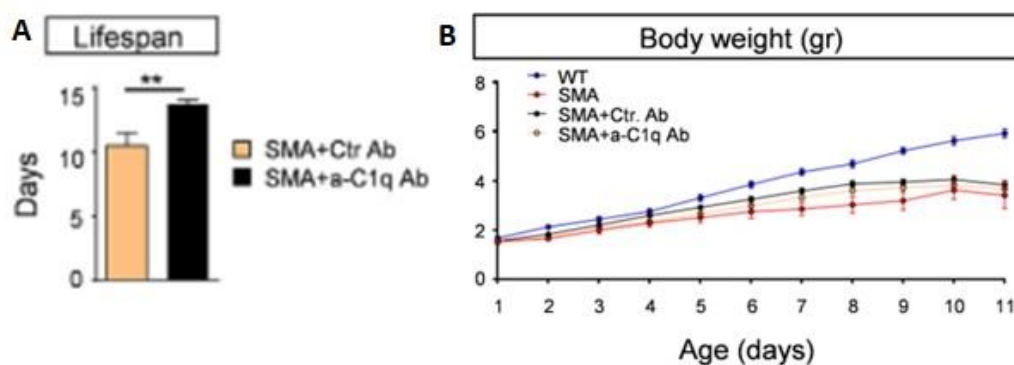
Figure 49. Postnatal *in vivo* neutralization of C1q in SMA mice improves survival but results in minimal body weight gain. (A) Lifespan of SMA+Ctr Ab (n = 8) compared to SMA+a-C1q Ab (n = 10) mice. **$p < 0.01$; t test. (B) Body weights gain in WT (shown in blue), SMA (shown in red), SMA+Ctr. Ab (shown in orange) and SMA+a-C1q Ab (shown in black) mice. Adapted from (Vukojicic et al., 2019).

Importantly, a-C1q antibody treated SMA mice showed a significant improvement in righting time compared to controls (Vukojicic et al., 2019) (Figure 50). This improvement in treated SMA mice was improving progressively over time, with the striking ability to right and even walk in second postnatal week.
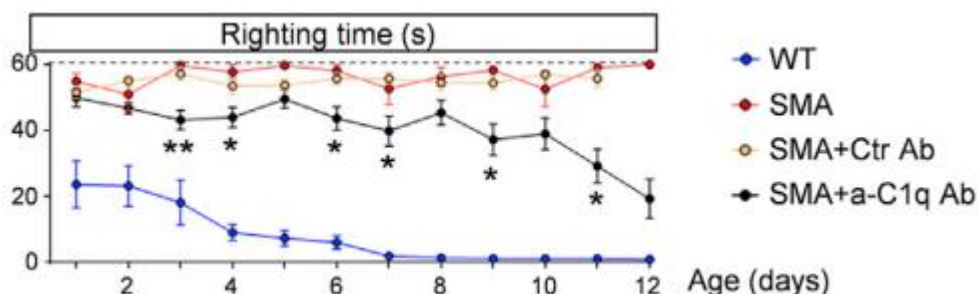
Figure 50. Postnatal *in vivo* neutralization of C1q in SMA mice has a striking effect on motor behavior. Righting times of WT (shown in blue, n = 10), SMA (shown in red, n = 9), SMA+Ctr Ab (shown in orange, n = 15), and SMA+a-C1q Ab (shown in black, n = 24). *$p < 0.05$, **$p < 0.01$; t test for individual ages. Adapted from (Vukojicic et al., 2019).

Collectively, these results demonstrate that *in vivo* postnatal treatment of SMA mice with a-C1q antibody rescues both number and the function of proprioceptive synapse which further confirms the essential role for C1q in active synaptic elimination in SMA mice. Importantly, rescued synaptic function indicates that C1q does not tag dysfunctional synapses and suggests involvement of complement proteins in synaptic dysfunction. Furthermore, synaptic rescue and

improved sensory-motor circuitry function in treated mice provided remarkable behavioral benefit, underlying importance of contribution of other neuronal types to motor neuron dysfunction and motor deficit seen in SMA. Thus, neutralization of C1q could be a potential therapeutic approach combinatorial to SMN upregulation in SMA patients.

4.2.9. Genetic deletion of C1q in SMA mice rescues proprioceptive synapses

To test whether complete elimination of C1q during embryonic development might also be beneficial, since postnatal neutralization of C1q resulted in significant synaptic rescue and behavioral benefit, C1q was removed from SMA mice through genetic manipulations. This was achieved by crossing mice harboring ubiquitous deletion of *C1qa* (Botto, 1998) with SMA mice. SMA::C1q-/- mice showed significant rescue of proprioceptive synapses on the somata as well as on proximal dendrites of L1 motor neurons in comparison to SMA mice at P10 (Vukojicic et al., 2019) (Figure 51A-C).
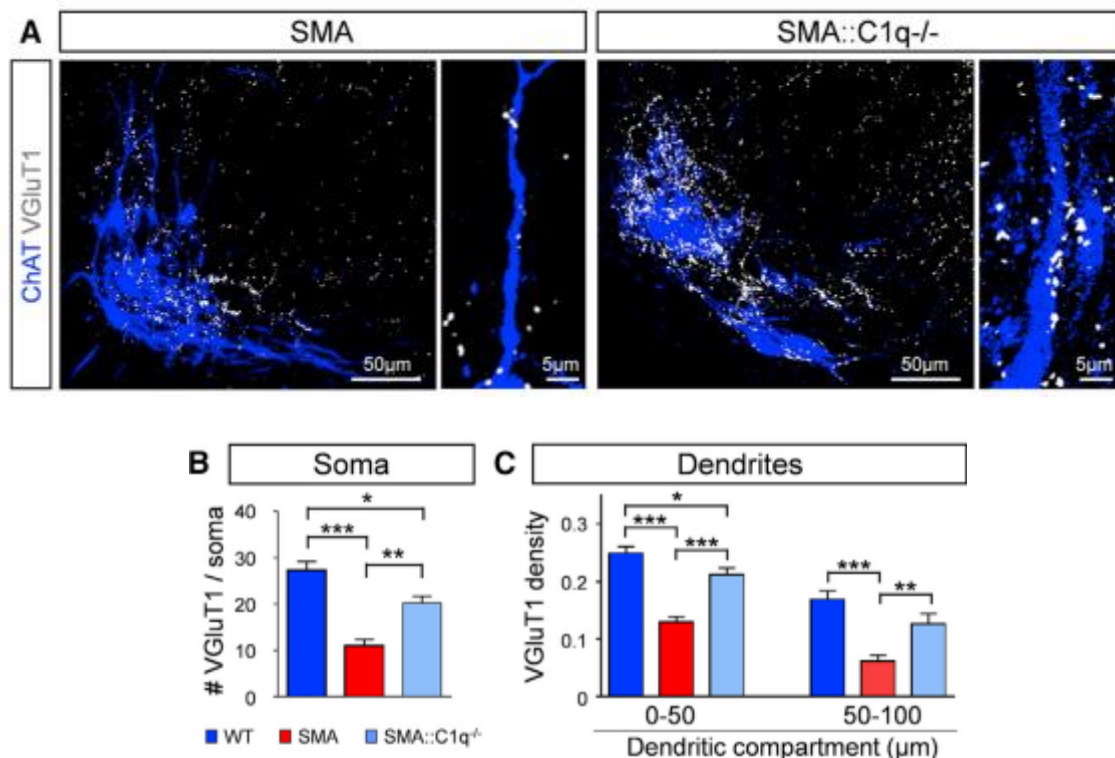
Figure 51. Genetic deletion of C1q in SMA mice rescues proprioceptive synapses. (A) z-stack projections of confocal images motor neurons visualized with ChAT (shown in blue) and VGluT1 (shown in white) immunoreactivity in SMA and SMA::C1q$^{-/-}$ motor neurons at P11. Total distance in the z-axis: 22.4 µm. Inset shows at higher magnification motor neuron dendrites (shown in blue) with VGluT1 synapses (shown in white). (B) The total number of VGluT1 synapses on the entire

soma in WT (shown in dark blue, n = 10), SMA (shown in red, n = 10), and SMA::C1q$^{-/-}$ (shown in light blue, n = 10) L1 motor neurons at P11. *p < 0.05, **p < 0.01, ***p < 0.01; One-way ANOVA with Tukey's test. (C) VGluT1 synaptic density – number of synapses in 50-µm from the soma dendritic compartments for WT (shown in dark blue, n = 41), SMA (shown in red, n = 43), and SMA::C1q$^{-/-}$ (shown in light blue, n = 29) motor neurons. *p < 0.05, **p < 0.01, ***p < 0.01; one-way ANOVA with Tukey's test. Adapted from (Vukojicic et al., 2019).

Similar to C1q neutralization, there was no rescue of L1 motor neurons in SMA::C1q-/- mice (Vukojicic et al., 2019) (Figure 52), further supporting that C1q does not play a role in motor neuron death. These results are not surprising considering recent studies demonstrating that motor neuron death is a cell autonomous event in which SMN deficiency leads to activation of intrinsic mechanisms involved in motor neuron degeneration (Simon et al., 2017; Van Alstyne et al., 2018). Additionally, since previous results demonstrated that synaptic loss is not due to cell-autonomous mechanisms but rather due to proprioceptive-autonomous mechanisms (Fletcher et al., 2017), it is expected that synaptic rescue and motor neuron death are independent events in SMA::C1q-/- mice.
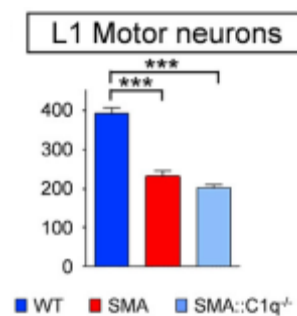
Figure 52. Genetic deletion of C1q in SMA mice does not rescue motor neurons. Total number of L1 motor neurons in WT (shown in dark blue, n = 3), SMA (shown in red, n = 4), and SMA::C1q$^{-/-}$ (shown in light blue, n = 4) mice. ***p < 0.01; one-way ANOVA with Tukey's test. Adapted from (Vukojicic et al., 2019).

To address whether rescued synapses are functional, in collaboration with Dr. Delestree the *ex vivo* spinal cord preparation was utilized to measure the monosynaptic reflex amplitude recorded in the L1 ventral root upon the stimulation of the L1 dorsal root SMA::C1q-/- mice showed a significant increase in the reflex amplitude compared to the age matched SMA mice (Vukojicic et al., 2019) (Figure 53A, B). No difference was recorded in the reflex latency (Vukojicic et al., 2019) (Figure 53C).
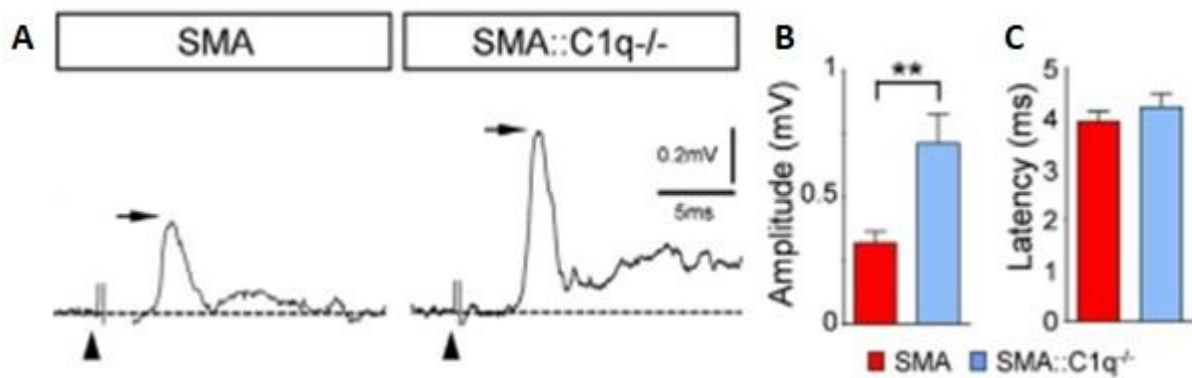
Figure 53. Genetic deletion of C1q in SMA mice improves motor output by rescuing synaptic function. (A) The monosynaptic response (indicated with arrows) in SMA and SMA::C1q$^{-/-}$ mice at P10 are shown. The arrowheads indicate stimulus artifacts. (B) The amplitude of the monosynaptic reflex responses at P10, in SMA (shown in red, n = 9) and in SMA::C1q$^{-/-}$ (shown in light blue, n = 4) mice. **p < 0.01; t test. (C) The latency of the monosynaptic response onset for the same groups. Adapted from (Vukojicic et al., 2019).

These results demonstrate that genetic removal of C1q in SMA mice rescues number and the function of proprioceptive synapses which indicates that C1q mediated synaptic elimination is an active aberrant pathogenic process.

4.3.   C1q mediates sensory-motor circuits refinement during normal development

Surprisingly, genetic removal of C1q, unlike postnatal C1q neutralization with anti-C1q antibody, did not result in any behavioral improvement in SMA mice, despite very similar rescue of proprioceptive synapses. While SMA mice treated with a-C1q antibody from birth had striking improvement in time to right SMA::C1q-/- mice lacked any improvement in righting reflex (Vukojicic et al., 2019) (Figure 54A). Their body weight gain and time to right across all ages were comparable to those of SMA mice (Vukojicic et al., 2019) (Figure 54B,A). These results were intriguing considering a seeming sensory-motor circuitry restoration, as both synapse numbers and function were rescued. These results opened the possibility of C1q involvement in synaptic elimination during the spinal sensory-motor circuit refinement during the prenatal development. Proprioceptive neurons synapse onto motor neurons innervating the homonymous muscle, but not the antagonistic muscle. However, during early development motor neurons do receive proprioceptive inputs originating from antagonistic muscles (Seebach and Ziskind-Conhaim, 1994),

that will be eliminated at postnatal ages (Poliak et al., 2016) to achieve proper motor function. The molecular mechanisms involved in this sensory-motor circuitry refinement are currently unknown.
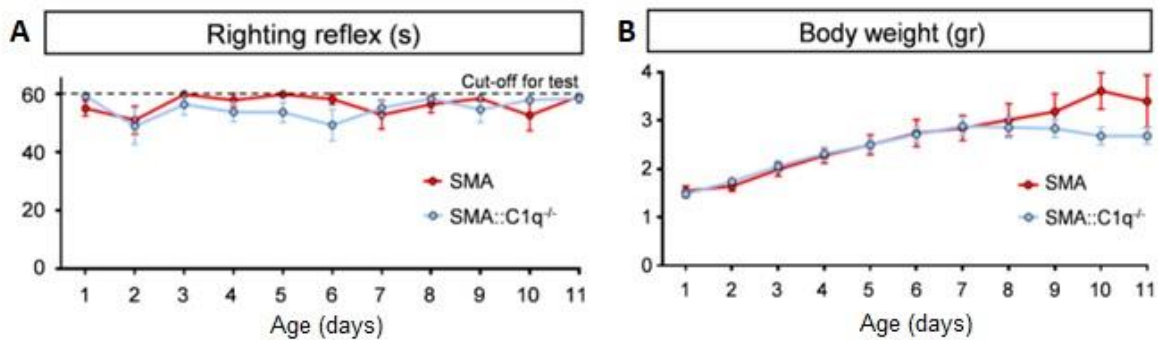
Figure 54. Genetic deletion of C1q in SMA mice does not confer behavioral benefit. (B) Righting time and (B) body weight gain during postnatal development in SMA (shown in red, n=9) and SMA::C1q$^{-/-}$ (shown in light blue, n=10) mice. Adapted from (Vukojicic et al., 2019).

To explore whether C1q is involved in synaptic refinement early during development, the synaptic numbers of VGluT1+ proprioceptive synapses on soma and proximal dendrites of motor neurons in C1q-/- mice were investigated. Synaptic density analysis revealed ~25% of excessive VGluT1 synapses, on the soma and proximal dendrites of C1q-/- motor neurons in comparison to WT counterparts at P11 (Vukojicic et al., 2019) (Figure 55A-C).
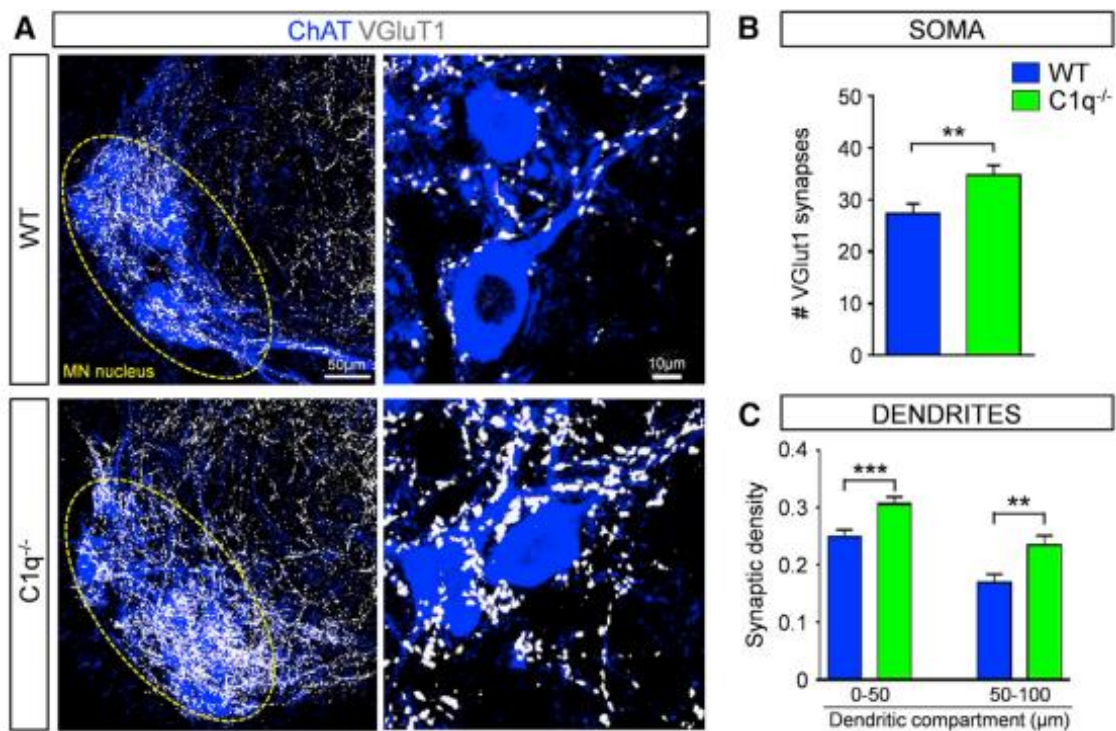
Figure 55. Genetic deletion of C1q in SMA mice results in an increased number of proprioceptive synapses during normal development. (A) Z-stack projections of confocal images

83

of L1 motor neurons visualized with ChAT (shown in blue) and VGluT1 synapses (shown in white) in WT and C1q$^{-/-}$ mice at P11. Total distance in the z-axis: 25.2 µm. Circled areas indicate MN nuclei. Higher magnification images (right) of z stack projections from single motor neurons in WT and C1q$^{-/-}$ mice. Total distance in the z-axis: 2.1 µm. (B) The total number of VGluT1 synapses on the entire soma from WT (shown in blue, n = 10) and C1q$^{-/-}$ (n = 12) L1 motor neurons. **$p < 0.01$; t test. (C) VGluT1 synaptic density – number of synapses in 50-µm from the soma dendritic compartments in WT (shown in blue, n = 41) and C1q$^{-/-}$ (shown in green, n = 35) motor neurons. **$p < 0.01$, ***$p < 0.001$; t test. Adapted from (Vukojicic et al., 2019).

To test whether these supernumerary synapses were functional, in collaboration with Dr. Delestree, dorsal root-to-ventral root reflexes were measured in the L1 lumbar segment, *ex vivo,* at P11.The monosynaptic reflex amplitude was significantly increased compared to WT counterparts (Vukojicic et al., 2019) (Figure 56A, B). Furthermore, to probe the synaptic efficacy of these excessive synapses in C1q-/- mice, synaptic neurotransmission was challenged under high frequency (20Hz) stimulation. Electrophysiological recordings revealed that the change in reflex amplitude during repetitive stimulation, was similar to the one observed in WT mice (Vukojicic et al., 2019) (Figure 56C, D).
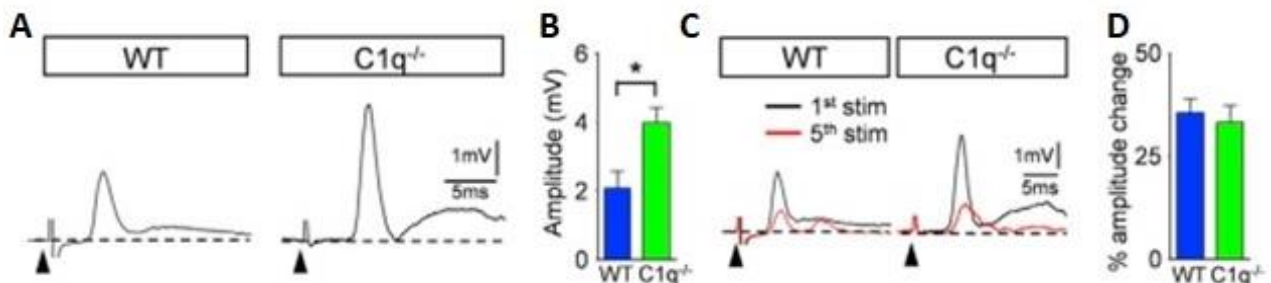
Figure 56. Supernumerary synapses in C1q$^{-/-}$ mice are functional. (A) Ventral root responses to supramaximal stimulation of the homonymous L1 dorsal root in WT and C1q$^{-/-}$ spinal cords at P10. The arrowheads indicate the stimulus artifacts. (B) The amplitude of the monosynaptic reflex responses for WT (n = 6) and C1q$^{-/-}$ (n = 7) mice at P11. *$p < 0.05$; t test. (C) Superimposed traces of the 1st (shown in black) and 5th (shown in red) responses following 20-Hz stimulation of the dorsal root in WT and C1q$^{-/-}$ mice. (D) Percentage of the amplitude change of the 5th response normalized to the 1st response, following a 20-Hz stimulation in WT (n = 6) and C1q$^{-/-}$ (n = 7) mice. Adapted from (Vukojicic et al., 2019).

Additionally, there was no difference in the numbers of motor neurons in WT and C1q$^{-/-}$ mice (Vukojicic et al., 2019) (Figure 57A,B) which together with previous observation indicates that supernumerary synapses in C1q-/- mice are functional.
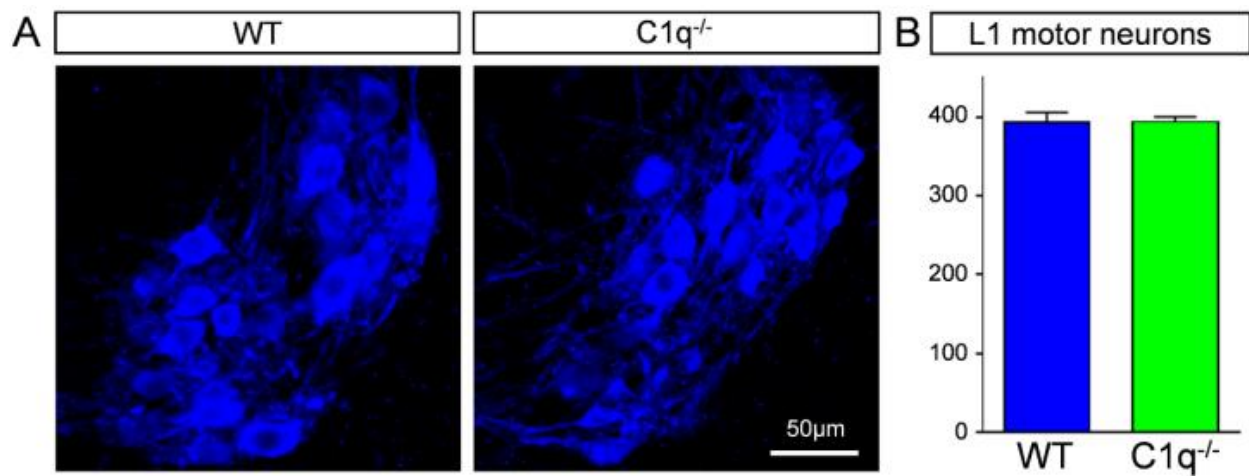
Figure 57. Genetic deletion of C1q does not result in motor neuron death. (A) Confocal images of L1 motor neurons labeled with ChAT (shown in blue) in WT and C1q$^{-/-}$ mice at P11. (B) The total number of L1 spinal segment motor neurons in WT (shown in blue) and C1q$^{-/-}$ (shown in green) mice. Adapted from (Vukojicic et al., 2019).

Behavioral analysis revealed a mild underweight condition for C1q-/- mice compared to the WT controls (Vukojicic et al., 2019) (Figure 58).
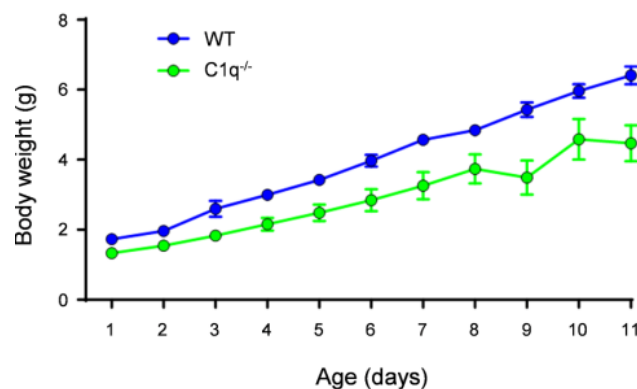
Figure 58. Genetic deletion of C1q results in mild under-weight gain. Body weight gain in WT (shown in blue, n=10) and C1q$^{-/-}$ (shown in green, n=10) mice. Adapted from (Vukojicic et al., 2019).

Strikingly, C1q$^{-/-}$ mice exhibited remarkable differences in time they took to right (Vukojicic et al., 2019) (Figure 59). They showed a significant delay in righting, very prominent at birth and with progressive improvement during the second postnatal week (Vukojicic et al., 2019) (Figure 59). This is not surprising as previous results demonstrated involvement of proprioceptive sensory synapses in the righting ability during the first postnatal week (Fletcher et al., 2017). In the second postnatal week, however, descending pathways mature and especially vestibulospinal pathways play a more prominent role in the righting reflex. This could explain why sensory-motor circuitry perturbations caused by the lack of C1q will not have strong effect after the first postnatal week.
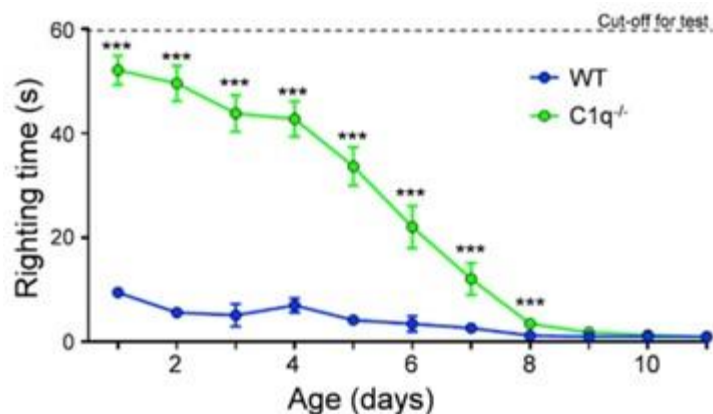
Figure 59. C1q$^{-/-}$ mice show a significant delay in righting. Righting times in WT (n = 10) and C1q$^{-/-}$ (n = 18) mice during the first 12 postnatal days. ***p < 0.001; t test for the individual ages. Adapted from (Vukojicic et al., 2019).

The righting inability of C1q-/- mice coupled with the increased numbers of proprioceptive synapses on MNs raised the question whether sensory motor circuits may have been inadequately established during the late embryonic and early postnatal development. Therefore, the connectivity pattern between two antagonistic motor pools, Gastrocnemius (Gastro) and the Tibialis Anterior (TA) muscles were investigated. An assay that utilizes the transganglionic transport properties of cholera toxin β-subunit (CTb) conjugated to Alexa-555 was used. Upon muscle injection, CTb accumulates in approximately 40% of proprioceptive synapses, which can be independently and selectively marked by the presynaptic VGluT1 expression (Mendelsohn et al., 2015). The TA muscle was injected with CTb-Alexa-555 which labels TA motor neurons as well as proprioceptive synapses. At the same time Gastro muscle was injected with fluorescein dextran (Dext) which labels only motor neurons (Vukojicic et al., 2019) (Figure 60A, B). This distinction allowed binary

density comparison of proprioceptive synapses labeled with CTb in contact with either homonymous CTb-labeled or Dextran labeled antagonistic MNs (Mendelsohn et al., 2015).
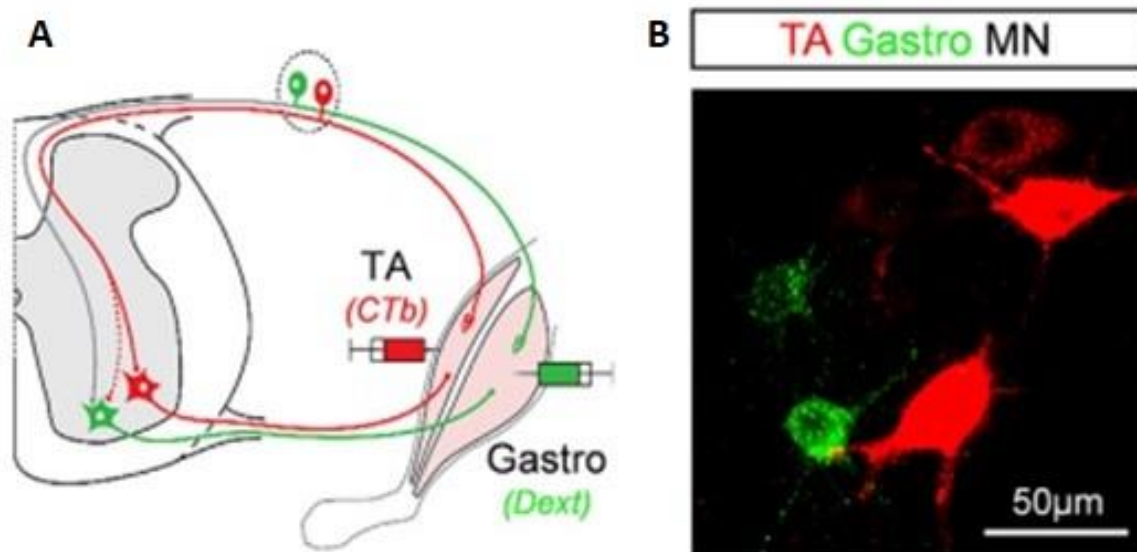
Figure 60. Experimental set up for binary density comparison of proprioceptive synapses in contact with either homonymous CTb-labeled or Dextran labeled antagonistic motor neurons. (A) Schematic illustration for retrograde labeling of Tibialis Anterior (TA) motor neurons and their proprioceptive synapses with CTb-555 (shown in red) and gastrocnemius (Gastro) motor neurons only with fluorescinated dextran (shown in green). The dotted red line indicates inappropriate Tibialis Anterior synapses onto gastrocnemius motor neurons. (B) Tibialis Anterior and gastrocnemius motor neuronss labeled with CTb-555 and fluorescinated dextran correspondingly. Adapted from (Vukojicic et al., 2019).

Synaptic density was analyzed 6-7 days after injection which is the minimum time needed for labeling both motor neurons and proprioceptive synapses (Mendelsohn et al., 2015). C1q-/- mice had approximately 22% of Gastro motor neurons which received inappropriate sensory synapses originating from proprioceptive neurons in antagonistic TA muscle compared to none in WT mice (Vukojicic et al., 2019) (Figure 61A, B).
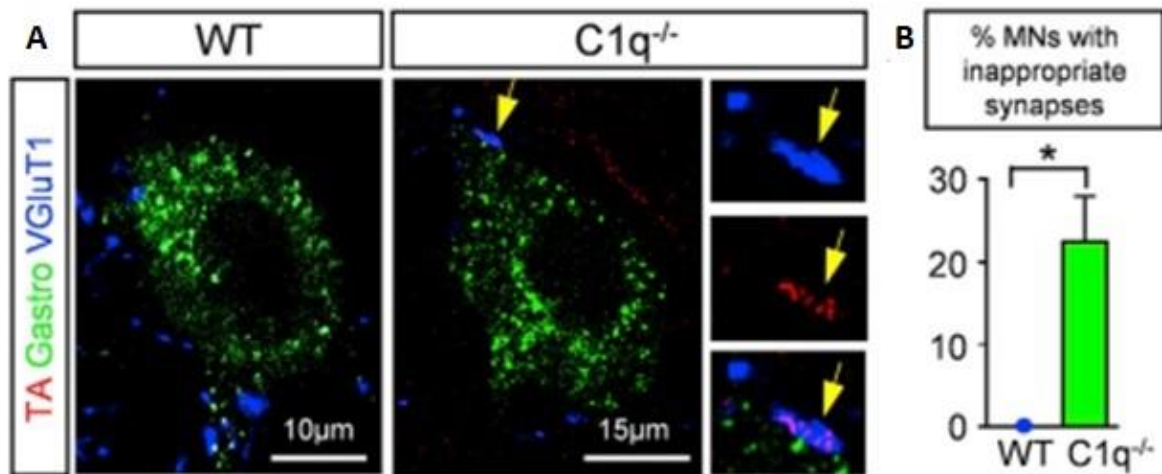
Figure 61. C1q mediates sensory-motor circuitry refinement during normal development. (A) Single optical planes of confocal images with the tracers fluorescinated dextran (shown in green), CTb-555 (shown in red) and VGluT1 (shown in blue) immunoreactivity from gastrocnemius motor neurons in a WT and a C1$^{-/-}$ mouse at P7. Inset shows an example of inappropriate synapse – tibialis anterior-originating proprioceptive synapse (arrow) on a gastrocnemius motor neuron. (B) Percentage of motor neurons receiving inappropriate synapses in WT (n = 3) and C1q-/- mice (n = 4). *p < 0.05; t test. Adapted from (Vukojicic et al., 2019).

These results provide evidence that sensory-motor circuitry refinement occurs early during development, likely during late embryonic and early postnatal period, and that it is C1q-dependent. Although these data demonstrate that ~ 22% of Gastro motor neurons receives inappropriate sensory synapses, this percentage is likely higher but due to experimental limitations cannot be assessed prior to P7. These results may also offer the explanation for the lack of motor improvement in SMA::C1q-/- mice, as these inappropriate synapses contributed to seemingly rescued VGgluT1 density on vulnerable SMA motor neurons in the absence of C1q. Importantly, these results indicate a major role for C1q in the refinement of spinal sensory-motor circuits during the normal development.

5. DISCUSSION

5.1. Sensory-motor circuitry dysfunction in SMA is driven by non-motor neuron autonomous mechanisms

Dysfunction and death of vulnerable neurons are common characteristics of neurodegenerative diseases. Behavioral deficits are often thought to be due to dysfunction of vulnerable neurons driven by cell-autonomous mechanisms. Deciphering the mechanisms behind these events is key in understanding and determining their contribution to pathology of disease. Importantly, since vulnerable neurons are located within neuronal circuits, the mechanisms by which their synaptic partners contribute to the disease process may play important roles in disease pathology. Neuronal dysfunction is often described by changes in physiological properties in disease vulnerable neurons (Kuo et al., 2004; Mentis et al., 2011).

This study confirms, in a mouse model of spinal muscular atrophy (SMA), that non-cell autonomous mechanisms drive motor neuron dysfunction. It has been shown that the reduction of EPSP amplitude observed in SMA motor neurons is restored in SMA+Pv[Cre] (restoration of SMN in proprioceptive neurons only) but not in SMA+ChAT[Cre] motor neurons (Fletcher et al., 2017) indicating that motor neuron dysfunction is a consequence of SMN loss from proprioceptive neurons. Following SMN restoration in proprioceptive neurons (SMA+Pv[Cre]), synaptic loss is rescued. Taken together with physiological findings (Fletcher et al., 2017), this suggests that SMN-deficiency from proprioceptive neurons causes sensory-derived motor neuron dysfunction leading to motor behavior impairments.

Motor neuron dysfunction can be seen as a non-motor neuron autonomous consequence of SMN deficiency in proprioceptive neurons which is further exacerbated at later stages by progressive synaptic loss from motor neuron dendrites (Redman, 1979), which comprise nearly 80% of the total synaptic number (Rotterman et al., 2014). Dendritic synapses are also largely responsible for the activation of motor neurons (Redman, 1979). Thus, to decipher the mechanisms behind the SMA pathology it was critical to understand how are these synapses lost.

5.2. Loss of vulnerable synapses in SMA is induced by aberrantly activated classical complement pathway

Results of this study in neurodegenerative disease SMA indicate involvement of C1q in synaptic dysfunction and its role in selective elimination of proprioceptive synapses. Dysfunction of the vulnerable motor neuron synapses is coupled with deposition of C1q and the subsequent activation of classical complement cascade, which leads to progressive microglia-mediated synaptic elimination in SMA. Inhibition of classical complement pathway after birth with an anti-C1q antibody *in vivo* treatment, rescues the number and the function of vulnerable synapses, while also extending moderately the lifespan and conferring significant behavioral benefit in a mouse model of SMA. Thus, protecting vulnerable synapses from elimination by neutralizing aberrant C1q may serve as an applicable therapeutic approach complementary to upregulation of SMN. This study uncovers previously unknown roles for classical complement pathway in synaptic pathology of SMA.

SMA is a neurodegenerative disease in which a deficiency in the SMN protein leads to selective loss of motor neurons, but the course of disease does not involve CNS injury. Additionally, there is a limited knowledge on neuroinflammation, if any present, in either human patients or mouse models of disease (Deguise et al., 2017; Papadimitriou et al., 2010). Furthermore, the loss of blood-brain barrier integrity has not been reported in SMA patients or in mouse models of SMA, nor the influx of lymphocytes and myeloid cells, which would be the case in classically defined neuroinflammatory conditions such as multiple sclerosis or during CNS infections or following CNS injury. Importantly, results from this study demonstrate absence of infiltrating macrophages in SMA mouse spinal cord tissue , since all Iba1+ cells were positive for TMEM119, a marker specific to microglia but not expressed by either macrophages or other immune or neuronal cell types (Bennett et al., 2016). Furthermore, in CD68 experiments, all Iba1+ cells were positive for CD68, suggesting that there is no infiltration of monocytes or macrophages. Additionally, immunohistochemistry against CD45 in L1 spinal cords of WT and SMA mice at P4 – when complement proteins are highly expressed and synaptic tagging occurs, revealed low expression of CD45, while no CD45+/Iba1- cells were observed, suggesting that there is no infiltration of leukocytes. Although influx of leukocytes was not observed, it is possible that microglia as well as astrocytes and endothelial cells could locally produce cytokines in response to homeostatic imbalance in SMA, as seen in some neurodegenerative diseases. However, gene expression levels of few important pro-inflammatory cytokines (IL-1β, IL-6 and TNF) from mouse L1/L2 spinal segments - which show significant pathological changes early in the course of disease, showed no significant difference between WT and SMA at the onset of the disease when synaptic

loss occurs and complement proteins are highly expressed. All these observations, suggest that the aberrant upregulation of C1q by local microglia production does not occur in response to activation of inflammatory pathways but as a direct consequence of SMN-deficient conditions which are driving neurodegeneration in SMA. How does loss of SMN leads to increased C1q expression is an intriguing question left to be solved. Several genes have been recently implicated in the sensory neuron dysfunction in SMA (Ackermann et al., 2013; Shorrock et al., 2018). However, a precise mechanistic bridge that connects the loss of SMN with the increased C1q expression reported in this study remains unknown. It is possible that microglia under its own SMN deficient conditions changes gene expression profile, which includes upregulation of C1q. However, since this upregulation happens at specific time point, around the time when synaptic loss occurs, it is more likely that microglia is upregulating C1q in response to signals from other SMN deficient cell type(s). SMN deficiency in motor neurons leads to their dysfunction which could cause a release of yet unknown factor(s) from motor neurons, that could be recognized either directly by microglia or through signals from other glial cell(s) triggering the overexpression of C1q in microglia. Overall, there has been very limited information on the contribution of glia to SMA pathology. However, some reports have highlighted the involvement of astrocytes in the disease. Increased astrogliosis was observed in postmortem tissues of SMA patients (Dachs et al., 2011; Kuru et al., 2009; Rindt et al., 2015; Tarabal et al., 2014) and in the SMA-Δ7 mouse model at both early and late disease stages (McGivern et al., 2013). Astrocytes are known to control formation, maturation and function of synapses through various contact-mediated and secreted signals (Clarke and Barres, 2013). It is possible therefore that astrocytes "sense" SMN deficient synapses and then signal to microglia which in turn upregulates expression of C1q, an initiating protein that mediates synaptic elimination in SMA.

SMA has been used as a model disease which allows studying the role of synaptic dysfunction in neurodegenerative diseases (Shorrock et al., 2019; Tisdale and Pellizzoni, 2015). It has been shown that loss of motor neurons follows sensory synapse dysfunction (Mentis et al., 2011). Additionally, restoration of SMN selectively in proprioceptive sensory neurons, restores number of sensory synapses as well as their function, which results in the spiking frequency improvement of SMA motor neurons, while not having an effect on the survival of motor neurons (Fletcher et al., 2017). This finding revealed that in SMA, motor neuron survival and synaptic dysfunction are two independent events (Fletcher et al., 2017). Similarly, SMN restoration in spinal interneurons and sensory neurons in Drosophila models of SMA was reported to improve behavioral phenotype (Imlach et al., 2012). All these studies had one thing in common - sensory synapses were identified as primary neuronal target which contributes to the disease phenotype.

However, the mechanisms by which sensory synapses are lost in SMA remained elusive. Results of this study demonstrate that synaptic loss in SMA is due to an active elimination of proprioceptive sensory synapses contacting motor neurons. These vulnerable synapses are tagged by the imitating protein of classical complement pathway - C1q, as well as with the downstream C3 protein, both of which are aberrantly expressed in SMA. C1q and C3 are found to localize to proprioceptive synapses both in WT and in SMA mice, but to a significantly higher extent in SMA. Furthermore, VGluT1 remnants found within microglia suggest that upon C1q deposition on proprioceptive synapses activation of the classical complement pathway is triggered leading to their subsequent elimination. Microglia mediates synaptic elimination likely via complement receptor 3 (CR3) considering that C3 deposits on synapses and that microglia are the only cell type in CNS carrying receptor for cleaved C3 protein. Additionally, results of this study show that microglia have another important role in developing and diseased spinal cord. C1q production in the spinal cord of WT and SMA mice is reserved exclusively to microglia, which is also consistent with a recent study in the brain (Fonseca et al., 2017). Importantly, C1q protein as well as C1q mRNA were not observed within motor neurons, as previously suggested (Zhang et al., 2013). Considering these findings microglia may be an important target in combinatorial SMA therapy. Pharmacological neutralization of C1q or genetic ablation in SMA mice results in a rescue of vulnerable synapses, which indicates that dominant mechanism of synaptic elimination in SMA is activation of the classical complement pathway. Additionally, microglia depletion *in vivo* with PLX5622 from birth, resulted in a significant synaptic rescue in treated SMA mice. Coupled with the rescue of vulnerable synapses was a significant phenotypic benefit observed in these mice, further confirming the role for C1q and microglia in synaptic elimination. The focus of this study was the loss of VGluT1+ synapses, but VGluT2+ synapses have also been reported to be reduced in SMA (Ling et al., 2010b; Simon et al., 2016). Although not investigated, complement proteins and microglia could also be involved in their removal. This study therefore demonstrates that aberrant activation of classical complement cascade triggers loss of proprioceptive synapses and indicates that microglia are responsible for elimination of synapses in SMA. However, what is the trigger for this selective elimination of proprioceptive synapses in SMA, remains to be answered.

It is unlikely that preferential C1q tagging of glutamatergic synapses in SMA is due to the type of neurotransmitter, since inhibitory synapses are selectively removed via C1q in a mouse model of FTD (Lui et al., 2016). It is possible that neuronal activity may be a driving factor for the selective elimination of synapses. It has been shown (Fletcher et al., 2017) that in SMA, proprioceptive synapses dysfunction to a certain extent very early (P2) in the disease process. It is possible that C1q can ''sense'' these early synaptic changes, tag synapses and further propagate

their dysfunction leading to demise of motor function. Furthermore, if SMN is selectively restored in proprioceptive neurons or if neuronal activity is pharmacologically induced, synaptic function will be rescued and synaptic elimination is prevented in SMA mice (Fletcher et al., 2017). Results of this study demonstrate that restoration of SMN selectively in proprioceptive neurons of SMA mice abrogates synaptic tagging by C1q to nearly WT levels. This is in the support of the idea that C1q somehow senses changes in synaptic activity and that tagging by C1q is mediated by synaptic mechanisms that arise from proprioceptive neurons. Considering the tagging role for C1q in synaptic elimination, there must be a way for tight regulation of this process, by which all properly active synapses remain protected from complement proteins. It has been reported that CD47 is localized at synapses (Mi et al., 2000; Toth et al., 2013). CD47, also termed integrin-associated protein (IAP), is widely expressed transmembrane protein which provides a "do not eat me" signal. It has been demonstrated recently that in the developing lateral geniculate nucleus (LGN) CD47 localizes preferentially in more active synapses, to which it may provide protective signal against the complement proteins. Therefore, microglia get to eliminate dysfunctional or weak synapses (Lehrman et al., 2018). It is possible that vulnerable proprioceptive synapses in SMA, may have downregulated CD47 expression, thus became available to complement and microglia-mediated elimination.

5.3.   The role of the C1q in the Normal Development of Spinal Sensory-Motor Circuits

This study has uncovered a previously unknown role for the C1q and classical complement pathway in the refinement of spinal sensory-motor circuit during normal development. The monosynaptic spinal sensory-motor arc reflex includes proprioceptive sensory neurons which directly synapse onto motor neurons which innervate homonymous muscle. It has been shown during embryonic development that 30% of motor neurons are being innervated by proprioceptive afferents originating from antagonistic muscles (Seebach and Ziskind-Conhaim, 1994). Additionally, it has been demonstrated that this persists during the first postnatal week (Poliak et al., 2016). However, proprioceptive afferents which connect motor neurons that supply antagonistic muscles are being removed during postnatal development (Mears and Frank, 1997; Mendelsohn et al., 2015). However, molecular mechanisms behind elimination of these inappropriate synapses had long remained elusive. This study shows that removal of these inappropriate synapses requires C1q and likely the activation of the classical complement cascade. Results of this study demonstrate that genetic removal of C1q from WT mice results in increased number of proprioceptive synapses, for approximately 25%, on both soma and proximal dendrites of WT motor neurons. These results

indicate that in the absence of C1q 25% of proprioceptive synapses fail to be pruned and suggest its involvement in sensory-motor circuitry refinement. Additionally, tracing experiments demonstrate involvement of C1q in refinement of proprioceptive synapses which contact motor neurons that originate from antagonistic muscles. This result reveals a C1q-mediated mechanism behind the synaptic refinement in developing spinal cord. During this early postnatal period, proprioceptive synapses play a major role in righting behavior (Fletcher et al., 2017). It has been demonstrated that descending pathways, such as vestibule-spinal inputs have more impact in this behavior than proprioceptive after the first postnatal week (Bignall, 1974; Pellis and Pellis, 1994; ten Donkelaar, 2000). The amplitude increase of the homonymous dorsal to ventral root reflex in C1q$^{-/-}$ mice compared to WT mice revealed that supernumerary synapses in C1q deficient mice are functional. However, observed deficits in motor behavior which are illustrated through the impaired righting behavior during the first postnatal week could be explained by the absence of pruning of inappropriate synapses. In support of this are also the results from SMA mice in which C1q was removed genetically. Unlike postnatal neutralization of C1q with anti-C1q antibody, there was no behavioral benefit in SMA mice lacking C1q, despite the similar level of synaptic rescue. Furthermore, results of this study show an increased C1q expression at birth compared to later postnatal days. Taken together, these results suggest the role for C1q in pruning of inappropriate proprioceptive synapses during development. However, the intriguing question is how does C1q mediate elimination of inappropriate proprioceptive synapses? The assembly of selective connections between sensory and motor neurons has been demonstrated to depend on their surface recognition features as well as on the position at which will motor neurons settle in ventral spinal cord (Fukuhara et al., 2013; Pecho-Vrieseling et al., 2009; Surmeli et al., 2011). Microglia are known to interact with synapses as a response to sensory experience or neurotransmitter release (Nimmerjahn et al., 2005; Ransohoff and Perry, 2009; Wake et al., 2009). In addition, it has been demonstrated that early during development, microglia engulf synapses in lateral geniculate nucleus. This engulfment is dependent on neural activity and complement tagging, and it is mediated through microglia-specific CR3 (Schafer et al., 2012). It is likely that inappropriate proprioceptive synapses are being less active, which could be sensed by microglia, leading to C1q deposition, subsequent activation of the classical complement cascade and finally microglia-mediated elimination of improper synapses via CR3. In support of this are following observations: C1q and C3 tagging of VGluT1 synapses early in postnatal WT mice and VGluT1 remnants within microglia. This suggest that a portion, if not all, inappropriate proprioceptive synapses tagged by C1q are eliminated via classical complement cascade and microglia-mediated mechanism and unfolds their previously unsuspected role in spinal sensory-motor circuits refinement during normal development.

In summary, this study shows that refinement of spinal sensory-motor circuits during early development is mediated by C1q-depndent mechanisms. In neurodegenerative disease SMA aberrantly activated classical complement cascade contributes to the synaptic dysfunction and induces elimination of proprioceptive synapses early in the disease pathology, propagating the demise of motor function. Future studies should determine whether pruning of other synapses in the spinal motor circuit is mediated by similar mechanisms during their developmental refinement. It will be also interesting to resolve mechanism behind the C1q upregulation in SMA and to answer the intriguing question of what exactly C1q binds to on the synapse. Importantly, future work should examine the therapeutic potential of C1q neutralization in SMA patients, as part of the combinatorial strategy for the treatment of this devastating neurodegenerative disease.

6. CONCLUSIONS

Based on the results of this study, the following conclusions can be drawn:

1.) This study confirms, utilizing a mouse model of spinal muscular atrophy (SMA), that presynaptic impairment driven by SMN deficiency in proprioceptive neurons is responsible for motor neuron dysfunction in SMA. Thus, results of this study indicate that non-cell autonomous mechanisms drive motor neuron dysfunction.

2.) Proprioceptive synapses in SMA have significantly reduced numbers compared to age-matched WT mice at late stages of disease. Results of this study demonstrate that this is not due to synaptic arrest occurring during development and that synapses in SMA are formed normally, but subsequently eliminated, starting at the onset of diseases phenotype in SMA mice.

3.) Results of this study demonstrate a transient expression of C1q during early normal postnatal development in WT spinal cords as well as an aberrant upregulation of C1q at the onset of SMA in both mouse model and human tissue.

4.) In a mouse model of SMA, C1q aberrantly tags vulnerable proprioceptive synapses at the onset of the disease, which correlates with the time synaptic loss occurs, suggesting involvement in synaptic elimination. Furthermore, similar percentage of proprioceptive synapses on proximal dendrites were tagged by a downstream complement component C3, suggesting that early in the disease process the classical complement pathway is triggered and activated.

5.) While C1q aberrantly tags vulnerable excitatory synapses in SMA, there was no significant difference in C1q tagged inhibitory synapses between WT and SMA mice. Additionally, C1q was not found in the periphery, on NMJs, suggesting that complement proteins are not involved in the denervation of NMJs.

6.) Proprioceptive synapses are eliminated by resident macrophages within the central nervous system – microglia, upon the activation of the classical complement cascade, in a mouse model of SMA.

7.) Microglia are the major and likely the sole source of C1q in the spinal cord during normal early development as well as in SMA.

8.) Pharmacological depletion of microglia by PLX5622 *in vivo* treatment of SMA mice, revealed that depletion of microglia, rescued synapses that are eliminated in SMA. This pharmacological approach conferred significant behavioral benefit in SMA mice.

9.) Experiments in which SMN was selectively restored in proprioceptive neurons revealed that SMN deficiency in proprioceptive neurons drives C1q-tagging of proprioceptive synapses.

10.) The number and the function of proprioceptive synapses in SMA mice can be rescued with *in vivo* postnatal neutralization of C1q by a-C1q antibody treatment, demonstrating that C1q also plays a role early in synaptic dysfunction. Treatment with a-C1q antibody provided remarkable behavioral benefit, underling its significance as a potential combinatorial therapeutic approach in SMA patients.

11.) Genetic removal of C1q in SMA mice rescues number and the function of proprioceptive synapses which indicates that C1q mediated synaptic elimination is an active aberrant pathogenic process.

12.) This study uncovers previously unknown role for the C1q in the refinement of spinal sensory-motor circuit during normal development. In this process C1q mediates elimination of inappropriate proprioceptive synapses.

7. REFERENCES

Abraira, V.E., and Ginty, D.D. (2013). The sensory neurons of touch. Neuron *79*, 618-639.

Ackermann, B., Krober, S., Torres-Benito, L., Borgmann, A., Peters, M., Hosseini Barkooie, S.M., Tejero, R., Jakubik, M., Schreml, J., Milbradt, J.*, et al.* (2013). Plastin 3 ameliorates spinal muscular atrophy via delayed axon pruning and improves neuromuscular junction functionality. Human molecular genetics *22*, 1328-1347.

Akay, T., Tourtellotte, W.G., Arber, S., and Jessell, T.M. (2014). Degradation of mouse locomotor pattern in the absence of proprioceptive sensory feedback. Proceedings of the National Academy of Sciences of the United States of America *111*, 16877-16882.

Allan, D.W., and Greer, J.J. (1997). Development of phrenic motoneuron morphology in the fetal rat. The Journal of comparative neurology *382*, 469-479.

Altman, J., Bayer, SA. (1997). Development of the cerebellar system (New York: CRC Press;).

Arber, S., Ladle, D.R., Lin, J.H., Frank, E., and Jessell, T.M. (2000). ETS gene Er81 controls the formation of functional connections between group Ia sensory afferents and motor neurons. Cell *101*, 485-498.

Arkblad, E., Tulinius, M., Kroksmark, A.K., Henricsson, M., and Darin, N. (2009). A population-based study of genotypic and phenotypic variability in children with spinal muscular atrophy. Acta paediatrica (Oslo, Norway : 1992) *98*, 865-872.

Arnold, W.D., and Burghes, A.H. (2013). Spinal muscular atrophy: development and implementation of potential treatments. Annals of neurology *74*, 348-362.

Arnold, W.D., Kassar, D., and Kissel, J.T. (2015). Spinal muscular atrophy: diagnosis and management in a new therapeutic era. Muscle & nerve *51*, 157-167.

Bennett, M.L., Bennett, F.C., Liddelow, S.A., Ajami, B., Zamanian, J.L., Fernhoff, N.B., Mulinyawe, S.B., Bohlen, C.J., Adil, A., Tucker, A.*, et al.* (2016). New tools for studying microglia in the mouse and human CNS. *113*, E1738-E1746.

Betley, J.N., Wright, C.V., Kawaguchi, Y., Erdelyi, F., Szabo, G., Jessell, T.M., and Kaltschmidt, J.A. (2009). Stringent specificity in the construction of a GABAergic presynaptic inhibitory circuit. Cell *139*, 161-174.

Bignall, K.E. (1974). Ontogeny of levels of neural organization: The righting reflex as a model. Experimental Neurology *42*, 566-573.

Botto, M. (1998). C1q knock-out mice for the study of complement deficiency in autoimmune disease. Exp Clin Immunogenet *15*, 231-234.

Botto, M., Dell'Agnola, C., Bygrave, A.E., Thompson, E.M., Cook, H.T., Petry, F., Loos, M., Pandolfi, P.P., and Walport, M.J. (1998). Homozygous C1q deficiency causes glomerulonephritis associated with multiple apoptotic bodies. Nature genetics *19*, 56-59.

Brennan, F.H., Lee, J.D., Ruitenberg, M.J., and Woodruff, T.M. (2016). Therapeutic targeting of complement to modify disease course and improve outcomes in neurological conditions. Semin Immunol *28*, 292-308.

Brodsky-Doyle, B., Leonard, K.R., and Reid, K.B. (1976). Circular-dichroism and electron-microscopy studies of human subcomponent C1q before and after limited proteolysis by pepsin. The Biochemical journal *159*, 279-286.

Brown, A.G. (1981). Organization in the Spinal Cord. New York: Springer.

Brown, A.G., and Fyffe, R.E. (1979). The morphology of group Ib afferent fibre collaterals in the spinal cord of the cat. The Journal of physiology *296*, 215-226.

Burghes, A.H., and Beattie, C.E. (2009). Spinal muscular atrophy: why do low levels of survival motor neuron protein make motor neurons sick? Nature reviews Neuroscience *10*, 597-609.

Burke, R.E., Strick, P.L., Kanda, K., Kim, C.C., and Walmsley, B. (1977). Anatomy of medial gastrocnemius and soleus motor nuclei in cat spinal cord. Journal of neurophysiology *40*, 667-680.

Butchbach, M.E. (2016). Copy Number Variations in the Survival Motor Neuron Genes: Implications for Spinal Muscular Atrophy and Other Neurodegenerative Diseases. Frontiers in molecular biosciences *3*, 7.

Carroll, M.C., and Isenman, D.E. (2012). Regulation of humoral immunity by complement. Immunity *37*, 199-207.

Castro, D., and Iannaccone, S.T. (2014). Spinal muscular atrophy: therapeutic strategies. Current treatment options in neurology *16*, 316.

Catela, C., Shin, M.M., and Dasen, J.S. (2015). Assembly and function of spinal circuits for motor control. Annual review of cell and developmental biology *31*, 669-698.

Cecchini, M.G., Dominguez, M.G., Mocci, S., Wetterwald, A., Felix, R., Fleisch, H., Chisholm, O., Hofstetter, W., Pollard, J.W., and Stanley, E.R. (1994). Role of colony stimulating factor-1 in the establishment and regulation of tissue macrophages during postnatal development of the mouse. Development *120*, 1357-1372.

Chen, H.H., Hippenmeyer, S., Arber, S., and Frank, E. (2003). Development of the monosynaptic stretch reflex circuit. Current opinion in neurobiology *13*, 96-102.

Chiriboga, C.A. (2017). Nusinersen for the treatment of spinal muscular atrophy. Expert review of neurotherapeutics *17*, 955-962.

Cho, K. (2019). Emerging Roles of Complement Protein C1q in Neurodegeneration. Aging and disease *10*, 652-663.

Chu, Y., Jin, X., Parada, I., Pesic, A., Stevens, B., Barres, B., and Prince, D.A. (2010). Enhanced synaptic connectivity and epilepsy in C1q knockout mice. Proceedings of the National Academy of Sciences of the United States of America *107*, 7975-7980.

Clarke, L.E., and Barres, B.A. (2013). Emerging roles of astrocytes in neural circuit development. Nature reviews Neuroscience *14*, 311-321.

Coovert, D.D., Le, T.T., McAndrew, P.E., Strasswimmer, J., Crawford, T.O., Mendell, J.R., Coulson, S.E., Androphy, E.J., Prior, T.W., and Burghes, A.H. (1997). The survival motor neuron protein in spinal muscular atrophy. Human molecular genetics *6*, 1205-1214.

Corey, D.R. (2017). Nusinersen, an antisense oligonucleotide drug for spinal muscular atrophy. Nature neuroscience *20*, 497-499.

Coulthard, L.G., Hawksworth, O.A., and Woodruff, T.M. (2018). Complement: The Emerging Architect of the Developing Brain. Trends Neurosci *41*, 373-384.

Dachs, E., Hereu, M., Piedrafita, L., Casanovas, A., Caldero, J., and Esquerda, J.E. (2011). Defective neuromuscular junction organization and postnatal myogenesis in mice with severe spinal muscular atrophy. Journal of neuropathology and experimental neurology *70*, 444-461.

Darras, B.T. (2015). Spinal Muscular Atrophies. Pediatric Clinics of North America *62*, 743-766.

Dasen, J.S. (2009). Transcriptional networks in the early development of sensory-motor circuits. Curr Top Dev Biol *87*, 119-148.

Dasen, J.S., and Jessell, T.M. (2009). Hox networks and the origins of motor neuron diversity. Curr Top Dev Biol *88*, 169-200.

Davis, E.J., Foster, T.D., and Thomas, W.E. (1994). Cellular forms and functions of brain microglia. Brain research bulletin *34*, 73-78.

Degn, S.E., Thiel, S., and Jensenius, J.C. (2007). New perspectives on mannan-binding lectin-mediated complement activation. Immunobiology *212*, 301-311.

Deguise, M.-O., De Repentigny, Y., McFall, E., Auclair, N., Sad, S., and Kothary, R. (2017). Immune dysregulation may contribute to disease pathogenesis in spinal muscular atrophy mice. Human molecular genetics *26*, 801-819.

Dejanovic, B., Huntley, M.A., De Maziere, A., Meilandt, W.J., Wu, T., Srinivasan, K., Jiang, Z., Gandham, V., Friedman, B.A., Ngu, H.*, et al.* (2018). Changes in the Synaptic Proteome in Tauopathy and Rescue of Tau-Induced Synapse Loss by C1q Antibodies. Neuron *100*, 1322-1336.e1327.

DiDonato, C.J., Chen, X.N., Noya, D., Korenberg, J.R., Nadeau, J.H., and Simard, L.R. (1997). Cloning, characterization, and copy number of the murine survival motor neuron gene: homolog of the spinal muscular atrophy-determining gene. Genome research *7*, 339-352.

Dunkelberger, J.R., and Song, W.C. (2010). Complement and its role in innate and adaptive immune responses. Cell Res *20*, 34-50.

Eccles, J.C., Eccles, R.M., Iggo, A., and Lundberg, A. (1960). Electrophysiological studies on gamma motoneurones. Acta physiologica Scandinavica *50*, 32-40.

Eccles, J.C., Eccles, R.M., and Lundberg, A. (1957). The convergence of monosynaptic excitatory afferents on to many different species of alpha motoneurones. The Journal of physiology *137*, 22-50.

Edens, B.M., Ajroud-Driss, S., Ma, L., and Ma, Y.-C. (2015). Molecular mechanisms and animal models of spinal muscular atrophy. Biochimica et Biophysica Acta (BBA) - Molecular Basis of Disease *1852*, 685-692.

Ehlers, M.R. (2000). CR3: a general purpose adhesion-recognition receptor essential for innate immunity. Microbes Infect *2*, 289-294.

Elmore, M.R., Najafi, A.R., Koike, M.A., Dagher, N.N., Spangenberg, E.E., Rice, R.A., Kitazawa, M., Matusow, B., Nguyen, H., West, B.L., *et al.* (2014). Colony-stimulating factor 1 receptor signaling is necessary for microglia viability, unmasking a microglia progenitor cell in the adult brain. Neuron *82*, 380-397.

Elmore, M.R.P., Hohsfield, L.A., Kramar, E.A., Soreq, L., Lee, R.J., Pham, S.T., Najafi, A.R., Spangenberg, E.E., Wood, M.A., West, B.L., *et al.* (2018). Replacement of microglia in the aged brain reverses cognitive, synaptic, and neuronal deficits in mice. Aging cell *17*, e12832.

Erblich, B., Zhu, L., Etgen, A.M., Dobrenis, K., and Pollard, J.W. (2011). Absence of colony stimulation factor-1 receptor results in loss of microglia, disrupted brain development and olfactory deficits. PloS one *6*, e26317.

Fagan, K., Crider, A., Ahmed, A.O., and Pillai, A. (2017). Complement C3 Expression Is Decreased in Autism Spectrum Disorder Subjects and Contributes to Behavioral Deficits in Rodents. Molecular neuropsychiatry *3*, 19-27.

Feldkotter, M., Schwarzer, V., Wirth, R., Wienker, T.F., and Wirth, B. (2002). Quantitative analyses of SMN1 and SMN2 based on real-time lightCycler PCR: fast and highly reliable carrier testing and prediction of severity of spinal muscular atrophy. American journal of human genetics *70*, 358-368.

Fetcho, J.R. (1987). A review of the organization and evolution of motoneurons innervating the axial musculature of vertebrates. Brain research *434*, 243-280.

Fletcher, E.V., and Mentis, G.Z. (2017). Motor Circuit Dysfunction in Spinal Muscular Atrophy. In Spinal Muscular Atrophy, pp. 153-165.

Fletcher, E.V., Simon, C.M., Pagiazitis, J.G., Chalif, J.I., Vukojicic, A., Drobac, E., Wang, X., and Mentis, G.Z. (2017). Reduced sensory synaptic excitation impairs motor neuron function via Kv2.1 in spinal muscular atrophy. Nat Neurosci *20*, 905-916.

Fonseca, M.I., Chu, S.H., Hernandez, M.X., Fang, M.J., Modarresi, L., Selvan, P., MacGregor, G.R., and Tenner, A.J. (2017). Cell-specific deletion of C1qa identifies microglia as the dominant source of C1q in mouse brain. Journal of neuroinflammation *14*, 48.

Friese, A., Kaltschmidt, J.A., Ladle, D.R., Sigrist, M., Jessell, T.M., and Arber, S. (2009). Gamma and alpha motor neurons distinguished by expression of transcription factor Err3. *106*, 13588-13593.

Füger, P., Hefendehl, J.K., Veeraraghavalu, K., Wendeln, A.-C., Schlosser, C., Obermüller, U., Wegenast-Braun, B.M., Neher, J.J., Martus, P., Kohsaka, S.*, et al.* (2017). Microglia turnover with aging and in an Alzheimer's model via long-term in vivo single-cell imaging. Nature neuroscience *20*, 1371-1376.

Fujita, T. (2002). Evolution of the lectin-complement pathway and its role in innate immunity. Nat Rev Immunol *2*, 346-353.

Fukuhara, K., Imai, F., Ladle, D.R., Katayama, K., Leslie, J.R., Arber, S., Jessell, T.M., and Yoshida, Y. (2013). Specificity of monosynaptic sensory-motor connections imposed by repellent Sema3E-PlexinD1 signaling. Cell reports *5*, 748-758.

Gaboriaud, C., Frachet, P., Thielens, N.M., and Arlaud, G.J. (2011). The human c1q globular domain: structure and recognition of non-immune self ligands. Front Immunol *2*, 92.

Gaboriaud, C., Juanhuix, J., Gruez, A., Lacroix, M., Darnault, C., Pignol, D., Verger, D., Fontecilla-Camps, J.C., and Arlaud, G.J. (2003). The crystal structure of the globular head of complement protein C1q provides a basis for its versatile recognition properties. The Journal of biological chemistry *278*, 46974-46982.

Garber, K. (2016). Big win possible for Ionis/Biogen antisense drug in muscular atrophy. Nature biotechnology *34*, 1002-1003.

Gavrilina, T.O., McGovern, V.L., Workman, E., Crawford, T.O., Gogliotti, R.G., DiDonato, C.J., Monani, U.R., Morris, G.E., and Burghes, A.H. (2008). Neuronal SMN expression corrects spinal muscular atrophy in severe SMA mice while muscle-specific SMN expression has no phenotypic effect. Human molecular genetics *17*, 1063-1075.

Ghebrehiwet, B. (2018). Chapter 3 - C1q. In The Complement FactsBook (Second Edition), S. Barnum, and T. Schein, eds. (Academic Press), pp. 23-32.

Gilliam, T.C., Brzustowicz, L.M., Castilla, L.H., Lehner, T., Penchaszadeh, G.K., Daniels, R.J., Byth, B.C., Knowles, J., Hislop, J.E., Shapira, Y.*, et al.* (1990). Genetic homogeneity between acute and chronic forms of spinal muscular atrophy. Nature *345*, 823-825.

Ginhoux, F., Greter, M., Leboeuf, M., Nandi, S., See, P., Gokhan, S., Mehler, M.F., Conway, S.J., Ng, L.G., Stanley, E.R.*, et al.* (2010). Fate mapping analysis reveals that adult microglia derive from primitive macrophages. Science (New York, NY) *330*, 841-845.

Gogliotti, R.G., Quinlan, K.A., Barlow, C.B., Heier, C.R., Heckman, C.J., and Didonato, C.J. (2012). Motor neuron rescue in spinal muscular atrophy mice demonstrates that sensory-motor defects are a consequence, not a cause, of motor neuron dysfunction. The Journal of neuroscience : the official journal of the Society for Neuroscience *32*, 3818-3829.

Goulding, M., and Pfaff, S.L. (2005). Development of circuits that generate simple rhythmic behaviors in vertebrates. Current opinion in neurobiology *15*, 14-20.

Goulet, B.B., Kothary, R., and Parks, R.J. (2013). At the "junction" of spinal muscular atrophy pathogenesis: the role of neuromuscular junction dysfunction in SMA disease progression. Current molecular medicine *13*, 1160-1174.

Grillner, S., and Jessell, T.M. (2009). Measured motion: searching for simplicity in spinal locomotor networks. Current opinion in neurobiology *19*, 572-586.

Gutman, C.R., Ajmera, M.K., and Hollyday, M. (1993). Organization of motor pools supplying axial muscles in the chicken. Brain research *609*, 129-136.

Hancock, M.B., and Peveto, C.A. (1979). Preganglionic neurons in the sacral spinal cord of the rat: an HRP study. Neuroscience letters *11*, 1-5.

Heier, C.R., Satta, R., Lutz, C., and DiDonato, C.J. (2010). Arrhythmia and cardiac defects are a feature of spinal muscular atrophy model mice. Human molecular genetics *19*, 3906-3918.

Hoheisel U, L.-W.E., Mense S. (1989). Termination patterns of identified group II and III

afferent fibres from deep tissues in the spinal cord of the cat. Neuroscience *28:495–507*.

Holness, C., and Simmons, D. (1993). Molecular cloning of CD68, a human macrophage marker related to lysosomal glycoproteins. Blood *81*, 1607-1613.

Hong, S., Beja-Glasser, V.F., Nfonoyim, B.M., Frouin, A., Li, S., Ramakrishnan, S., Merry, K.M., Shi, Q., Rosenthal, A., Barres, B.A.*, et al.* (2016). Complement and microglia mediate early synapse loss in Alzheimer mouse models. Science (New York, NY) *352*, 712-716.

Howell, G.R., Macalinao, D.G., Sousa, G.L., Walden, M., Soto, I., Kneeland, S.C., Barbay, J.M., King, B.L., Marchant, J.K., Hibbs, M.*, et al.* (2011). Molecular clustering identifies complement and endothelin induction as early events in a mouse model of glaucoma. The Journal of clinical investigation *121*, 1429-1444.

Hsieh-Li, H.M., Chang, J.G., Jong, Y.J., Wu, M.H., Wang, N.M., Tsai, C.H., and Li, H. (2000). A mouse model for spinal muscular atrophy. Nature genetics *24*, 66-70.

Hua, J.Y., and Smith, S.J. (2004). Neural activity and the dynamics of central nervous system development. Nature neuroscience *7*, 327-332.

Imai, F., and Yoshida, Y. (2018). Molecular mechanisms underlying monosynaptic sensory-motor circuit development in the spinal cord. Developmental dynamics : an official publication of the American Association of Anatomists *247*, 581-587.

Imlach, W.L., Beck, E.S., Choi, B.J., Lotti, F., Pellizzoni, L., and McCabe, B.D. (2012). SMN is required for sensory-motor circuit function in Drosophila. Cell *151*, 427-439.

Janeway, T.P., Walport M, et al. (2001). The complement system and innate immunity. Immunobiology: The Immune System in Health and Disease. , Vol 5th edition. (New York: Garland Science).

Jessell, T.M. (2000). Neuronal specification in the spinal cord: inductive signals and transcriptional codes. Nature reviews Genetics *1*, 20-29.

Jung, H., and Dasen, J.S. (2015). Evolution of patterning systems and circuit elements for locomotion. Developmental cell *32*, 408-422.

Kang, Y.S., Do, Y., Lee, H.K., Park, S.H., Cheong, C., Lynch, R.M., Loeffler, J.M., Steinman, R.M., and Park, C.G. (2006). A dominant complement fixation pathway for pneumococcal polysaccharides initiated by SIGN-R1 interacting with C1q. Cell *125*, 47-58.

Kanning, K.C., Kaplan, A., and Henderson, C.E. (2010). Motor neuron diversity in development and disease. Annual review of neuroscience *33*, 409-440.

Kariya, S., Park, G.H., Maeno-Hikichi, Y., Leykekhman, O., Lutz, C., Arkovitz, M.S., Landmesser, L.T., and Monani, U.R. (2008). Reduced SMN protein impairs maturation of the neuromuscular junctions in mouse models of spinal muscular atrophy. Human molecular genetics *17*, 2552-2569.

Kashima, T., Rao, N., David, C.J., and Manley, J.L. (2007). hnRNP A1 functions with specificity in repression of SMN2 exon 7 splicing. Human molecular genetics *16*, 3149-3159.

Katz, L.C., and Shatz, C.J. (1996). Synaptic Activity and the Construction of Cortical Circuits. Science (New York, NY) *274*, 1133-1138.

Kierdorf, K., Erny, D., Goldmann, T., Sander, V., Schulz, C., Perdiguero, E.G., Wieghofer, P., Heinrich, A., Riemke, P., Holscher, C.*, et al.* (2013). Microglia emerge from erythromyeloid precursors via Pu.1- and Irf8-dependent pathways. Nature neuroscience *16*, 273-280.

Kilchherr, E., Hofmann, H., Steigemann, W., and Engel, J. (1985). Structural model of the collagen-like region of C1q comprising the kink region and the fibre-like packing of the six triple helices. Journal of molecular biology *186*, 403-415.

Kim, D.D., and Song, W.C. (2006). Membrane complement regulatory proteins. Clin Immunol *118*, 127-136.

Kishore, U., Gupta, S.K., Perdikoulis, M.V., Kojouharova, M.S., Urban, B.C., and Reid, K.B.M. (2003). Modular Organization of the Carboxyl-Terminal, Globular Head Region of Human C1q A, B, and C Chains. *171*, 812-820.

Kishore, U., and Reid, K.B. (2000). C1q: structure, function, and receptors. Immunopharmacology *49*, 159-170.

Kjaeldgaard, A.L., Pilely, K., Olsen, K.S., Pedersen, S.W., Lauritsen, A.O., Moller, K., and Garred, P. (2018). Amyotrophic lateral sclerosis: The complement and inflammatory hypothesis. Mol Immunol *102*, 14-25.

Knobel, H.R., Villiger, W., and Isliker, H. (1975). Chemical analysis and electron microscopy studies of human C1q prepared by different methods. European journal of immunology *5*, 78-82.

Kong, L., Wang, X., Choe, D.W., Polley, M., Burnett, B.G., Bosch-Marce, M., Griffin, J.W., Rich, M.M., and Sumner, C.J. (2009). Impaired synaptic vesicle release and immaturity of neuromuscular junctions in spinal muscular atrophy mice. The Journal of neuroscience : the official journal of the Society for Neuroscience *29*, 842-851.

Korinthenberg, R., Sauer, M., Ketelsen, U.P., Hanemann, C.O., Stoll, G., Graf, M., Baborie, A., Volk, B., Wirth, B., Rudnik-Schoneborn, S.*, et al.* (1997). Congenital axonal neuropathy caused by deletions in the spinal muscular atrophy region. Annals of neurology *42*, 364-368.

Kudo, N., and Yamada, T. (1987). Morphological and physiological studies of development of the monosynaptic reflex pathway in the rat lumbar spinal cord. The Journal of physiology *389*, 441-459.

Kuffler, S.W., Hunt, C.C., and Quilliam, J.P. (1951). Function of medullated small-nerve fibers in mammalian ventral roots; efferent muscle spindle innervation. Journal of neurophysiology *14*, 29-54.

Kuo, J.J., Schonewille, M., Siddique, T., Schults, A.N., Fu, R., Bar, P.R., Anelli, R., Heckman, C.J., and Kroese, A.B. (2004). Hyperexcitability of cultured spinal motoneurons from presymptomatic ALS mice. Journal of neurophysiology *91*, 571-575.

Kuru, S., Sakai, M., Konagaya, M., Yoshida, M., Hashizume, Y., and Saito, K. (2009). An autopsy case of spinal muscular atrophy type III (Kugelberg-Welander disease). Neuropathology : official journal of the Japanese Society of Neuropathology *29*, 63-67.

Landmesser, L. (1978). The distribution of motoneurones supplying chick hind limb muscles. The Journal of physiology *284*, 371-389.

Lansita, J.A., Mease, K.M., Qiu, H., Yednock, T., Sankaranarayanan, S., and Kramer, S. (2017). Nonclinical Development of ANX005: A Humanized Anti-C1q Antibody for Treatment of Autoimmune and Neurodegenerative Diseases. International journal of toxicology *36*, 449-462.

Le, T.T., Pham, L.T., Butchbach, M.E., Zhang, H.L., Monani, U.R., Coovert, D.D., Gavrilina, T.O., Xing, L., Bassell, G.J., and Burghes, A.H. (2005). SMNDelta7, the major product of the centromeric survival motor neuron (SMN2) gene, extends survival in mice with spinal muscular atrophy and associates with full-length SMN. Human molecular genetics *14*, 845-857.

Lee, Y.I., Mikesh, M., Smith, I., Rimer, M., and Thompson, W. (2011). Muscles in a mouse model of spinal muscular atrophy show profound defects in neuromuscular development even in the absence of failure in neuromuscular transmission or loss of motor neurons. Developmental biology *356*, 432-444.

Lefebvre, S., Burglen, L., Reboullet, S., Clermont, O., Burlet, P., Viollet, L., Benichou, B., Cruaud, C., Millasseau, P., Zeviani, M.*, et al.* (1995). Identification and characterization of a spinal muscular atrophy-determining gene. Cell *80*, 155-165.

Lefebvre, S., Burlet, P., Liu, Q., Bertrandy, S., Clermont, O., Munnich, A., Dreyfuss, G., and Melki, J. (1997). Correlation between severity and SMN protein level in spinal muscular atrophy. Nature genetics *16*, 265-269.

Lehrman, E.K., Wilton, D.K., Litvina, E.Y., Welsh, C.A., Chang, S.T., Frouin, A., Walker, A.J., Heller, M.D., Umemori, H., Chen, C.*, et al.* (2018). CD47 Protects Synapses from Excess Microglia-Mediated Pruning during Development. Neuron *100*, 120-134.e126.

Li, Y., and Burke, R.E. (2002). Developmental changes in short-term synaptic depression in the neonatal mouse spinal cord. Journal of neurophysiology *88*, 3218-3231.

Ling, K.K., Lin, M.Y., Zingg, B., Feng, Z., and Ko, C.P. (2010a). Synaptic defects in the spinal and neuromuscular circuitry in a mouse model of spinal muscular atrophy. PloS one *5*, e15457.

Ling, K.K.Y., Lin, M.-Y., Zingg, B., Feng, Z., and Ko, C.-P. (2010b). Synaptic Defects in the Spinal and Neuromuscular Circuitry in a Mouse Model of Spinal Muscular Atrophy. PloS one *5*, e15457.

Lipton, A.M., Cullum, C.M., Satumtira, S., Sontag, E., Hynan, L.S., White, C.L., 3rd, and Bigio, E.H. (2001). Contribution of asymmetric synapse loss to lateralizing clinical deficits in frontotemporal dementias. Archives of neurology *58*, 1233-1239.

Liu, Q., and Dreyfuss, G. (1996). A novel nuclear structure containing the survival of motor neurons protein. Embo j *15*, 3555-3565.

Loeffler, D.A., Camp, D.M., and Conant, S.B. (2006). Complement activation in the Parkinson's disease substantia nigra: an immunocytochemical study. Journal of neuroinflammation *3*, 29.

Lorson, C.L., and Androphy, E.J. (2000). An exonic enhancer is required for inclusion of an essential exon in the SMA-determining gene SMN. Human molecular genetics *9*, 259-265.

Louveau, A., Harris, T.H., and Kipnis, J. (2015). Revisiting the Mechanisms of CNS Immune Privilege. Trends in immunology *36*, 569-577.

Louveau, A., Herz, J., Alme, M.N., Salvador, A.F., Dong, M.Q., Viar, K.E., Herod, S.G., Knopp, J., Setliff, J.C., Lupi, A.L.*, et al.* (2018). CNS lymphatic drainage and neuroinflammation are regulated by meningeal lymphatic vasculature. Nature neuroscience *21*, 1380-1391.

Lui, H., Zhang, J., Makinson, S.R., Cahill, M.K., Kelley, K.W., Huang, H.Y., Shang, Y., Oldham, M.C., Martens, L.H., Gao, F.*, et al.* (2016). Progranulin Deficiency Promotes Circuit-Specific Synaptic Pruning by Microglia via Complement Activation. Cell *165*, 921-935.

Lutz, C.M., Kariya, S., Patruni, S., Osborne, M.A., Liu, D., Henderson, C.E., Li, D.K., Pellizzoni, L., Rojas, J., Valenzuela, D.M.*, et al.* (2011). Postsymptomatic restoration of SMN rescues the disease phenotype in a mouse model of severe spinal muscular atrophy. The Journal of clinical investigation *121*, 3029-3041.

Mailman, M.D., Heinz, J.W., Papp, A.C., Snyder, P.J., Sedra, M.S., Wirth, B., Burghes, A.H., and Prior, T.W. (2002). Molecular analysis of spinal muscular atrophy and modification of the phenotype by SMN2. Genetics in medicine : official journal of the American College of Medical Genetics *4*, 20-26.

Mallucci, G.R. (2009). Prion neurodegeneration: starts and stops at the synapse. Prion *3*, 195-201.

Malone, D.C., Dean, R., Arjunji, R., Jensen, I., Cyr, P., Miller, B., Maru, B., Sproule, D.M., Feltner, D.E., and Dabbous, O. (2019). Cost-effectiveness analysis of using onasemnogene abeparvocec (AVXS-101) in spinal muscular atrophy type 1 patients. Journal of market access & health policy *7*, 1601484.

Maretina, M.A., Zheleznyakova, G.Y., Lanko, K.M., Egorova, A.A., Baranov, V.S., and Kiselev, A.V. (2018). Molecular Factors Involved in Spinal Muscular Atrophy Pathways as Possible Disease-modifying Candidates. Current genomics *19*, 339-355.

Martinez, T.L., Kong, L., Wang, X., Osborne, M.A., Crowder, M.E., Van Meerbeke, J.P., Xu, X., Davis, C., Wooley, J., Goldhamer, D.J.*, et al.* (2012). Survival motor neuron protein in motor neurons determines synaptic integrity in spinal muscular atrophy. The Journal of neuroscience : the official journal of the Society for Neuroscience *32*, 8703-8715.

McGonigal, R., Cunningham, M.E., Yao, D., Barrie, J.A., Sankaranarayanan, S., Fewou, S.N., Furukawa, K., Yednock, T.A., and Willison, H.J. (2016). C1q-targeted inhibition of the classical complement pathway prevents injury in a novel mouse model of acute motor axonal neuropathy. Acta Neuropathol Commun *4*, 23.

Mears, S.C., and Frank, E. (1997). Formation of specific monosynaptic connections between muscle spindle afferents and motoneurons in the mouse. The Journal of neuroscience : the official journal of the Society for Neuroscience *17*, 3128-3135.

Medzhitov, R., and Janeway, C., Jr. (2000). Innate immunity. The New England journal of medicine *343*, 338-344.

Medzhitov, R., and Janeway, C.A., Jr. (2002). Decoding the patterns of self and nonself by the innate immune system. Science (New York, NY) *296*, 298-300.

Melki, J., Abdelhak, S., Sheth, P., Bachelot, M.F., Burlet, P., Marcadet, A., Aicardi, J., Barois, A., Carriere, J.P., Fardeau, M.*, et al.* (1990). Gene for chronic proximal spinal muscular atrophies maps to chromosome 5q. Nature *344*, 767-768.

Mende, M., Fletcher, E.V., Belluardo, J.L., Pierce, J.P., Bommareddy, P.K., Weinrich, J.A., Kabir, Z.D., Schierberl, K.C., Pagiazitis, J.G., Mendelsohn, A.I.*, et al.* (2016). Sensory-Derived Glutamate Regulates Presynaptic Inhibitory Terminals in Mouse Spinal Cord. Neuron *90*, 1189-1202.

Mendell, J.R., Al-Zaidy, S., Shell, R., Arnold, W.D., Rodino-Klapac, L.R., Prior, T.W., Lowes, L., Alfano, L., Berry, K., Church, K.*, et al.* (2017). Single-Dose Gene-Replacement Therapy for Spinal Muscular Atrophy. The New England journal of medicine *377*, 1713-1722.

Mendelsohn, A.I., Simon, C.M., Abbott, L.F., Mentis, G.Z., and Jessell, T.M. (2015). Activity Regulates the Incidence of Heteronymous Sensory-Motor Connections. Neuron *87*, 111-123.

Mentis, G.Z., Blivis, D., Liu, W., Drobac, E., Crowder, M.E., Kong, L., Alvarez, F.J., Sumner, C.J., and O'Donovan, M.J. (2011). Early functional impairment of sensory-motor connectivity in a mouse model of spinal muscular atrophy. Neuron *69*, 453-467.

Mentis, G.Z., Diaz, E., Moran, L.B., and Navarrete, R. (2007). Early alterations in the electrophysiological properties of rat spinal motoneurones following neonatal axotomy. The Journal of physiology *582*, 1141-1161.

Mi, Z.P., Jiang, P., Weng, W.L., Lindberg, F.P., Narayanan, V., and Lagenaur, C.F. (2000). Expression of a synapse-associated membrane protein, P84/SHPS-1, and its ligand, IAP/CD47, in mouse retina. The Journal of comparative neurology *416*, 335-344.

Michell-Robinson, M.A., Touil, H., Healy, L.M., Owen, D.R., Durafourt, B.A., Bar-Or, A., Antel, J.P., and Moore, C.S. (2015). Roles of microglia in brain development, tissue maintenance and repair. Brain : a journal of neurology *138*, 1138-1159.

Monani, U.R., Sendtner, M., Coovert, D.D., Parsons, D.W., Andreassi, C., Le, T.T., Jablonka, S., Schrank, B., Rossoll, W., Prior, T.W.*, et al.* (2000). The human centromeric survival motor neuron gene (SMN2) rescues embryonic lethality in Smn(-/-) mice and results in a mouse with spinal muscular atrophy. Human molecular genetics *9*, 333-339.

Montes, J., Gordon, A.M., Pandya, S., De Vivo, D.C., and Kaufmann, P. (2009). Clinical outcome measures in spinal muscular atrophy. Journal of child neurology *24*, 968-978.

Mortensen, S.A., Sander, B., Jensen, R.K., Pedersen, J.S., Golas, M.M., Jensenius, J.C., Hansen, A.G., Thiel, S., and Andersen, G.R. (2017). Structure and activation of C1, the complex initiating the classical pathway of the complement cascade. Proceedings of the National Academy of Sciences *114*, 986-991.

Mostacciuolo, M.L., Danieli, G.A., Trevisan, C., Muller, E., and Angelini, C. (1992). Epidemiology of spinal muscular atrophies in a sample of the Italian population. Neuroepidemiology *11*, 34-38.

Murray, L.M., Comley, L.H., Thomson, D., Parkinson, N., Talbot, K., and Gillingwater, T.H. (2008). Selective vulnerability of motor neurons and dissociation of pre- and post-synaptic pathology at the neuromuscular junction in mouse models of spinal muscular atrophy. Human molecular genetics *17*, 949-962.

Najafi, A.R., Crapser, J., Jiang, S., Ng, W., Mortazavi, A., West, B.L., and Green, K.N. (2018). A limited capacity for microglial repopulation in the adult brain. Glia *66*, 2385-2396.

Nayak, D., Roth, T.L., and McGavern, D.B. (2014). Microglia Development and Function. Annual Review of Immunology *32*, 367-402.

Neniskyte, U., and Gross, C.T. (2017). Errant gardeners: glial-cell-dependent synaptic pruning and neurodevelopmental disorders. Nature reviews Neuroscience *18*, 658-670.

Nimmerjahn, A., Kirchhoff, F., and Helmchen, F. (2005). Resting microglial cells are highly dynamic surveillants of brain parenchyma in vivo. Science (New York, NY) *308*, 1314-1318.

Noris, M., and Remuzzi, G. (2013). Overview of complement activation and regulation. Semin Nephrol *33*, 479-492.

Ohsawa, K., Imai, Y., Sasaki, Y., and Kohsaka, S. (2004). Microglia/macrophage-specific protein Iba1 binds to fimbrin and enhances its actin-bundling activity. J Neurochem *88*, 844-856.

Oosterhof, N., Kuil, L.E., van der Linde, H.C., Burm, S.M., Berdowski, W., van Ijcken, W.F.J., van Swieten, J.C., Hol, E.M., Verheijen, M.H.G., and van Ham, T.J. (2018). Colony-Stimulating Factor 1 Receptor (CSF1R) Regulates Microglia Density and Distribution, but Not Microglia Differentiation In Vivo. Cell reports *24*, 1203-1217.e1206.

Oskoui, M., Darras, B.T., and De Vivo, D.C. (2017). Chapter 1 - Spinal Muscular Atrophy: 125 Years Later and on the Verge of a Cure. In Spinal Muscular Atrophy, C.J. Sumner, S. Paushkin, and C.-P. Ko, eds. (Academic Press), pp. 3-19.

Oskoui, M., Levy, G., Garland, C.J., Gray, J.M., O'Hagen, J., De Vivo, D.C., and Kaufmann, P. (2007). The changing natural history of spinal muscular atrophy type 1. Neurology *69*, 1931-1936.

Ottesen, E.W. (2017). ISS-N1 makes the First FDA-approved Drug for Spinal Muscular Atrophy. Translational neuroscience *8*, 1-6.

Ozaki, S., and Snider, W.D. (1997). Initial trajectories of sensory axons toward laminar targets in the developing mouse spinal cord. The Journal of comparative neurology *380*, 215-229.

Palop, J.J., and Mucke, L. (2010). Amyloid-beta-induced neuronal dysfunction in Alzheimer's disease: from synapses toward neural networks. Nature neuroscience *13*, 812-818.

Paolicelli, R.C., Bolasco, G., Pagani, F., Maggi, L., Scianni, M., Panzanelli, P., Giustetto, M., Ferreira, T.A., Guiducci, E., Dumas, L.*, et al.* (2011). Synaptic pruning by microglia is necessary for normal brain development. Science (New York, NY) *333*, 1456-1458.

Papadimitriou, D., Le Verche, V., Jacquier, A., Ikiz, B., Przedborski, S., and Re, D.B. (2010). Inflammation in ALS and SMA: Sorting out the good from the evil. Neurobiology of Disease *37*, 493-502.

Park, G.H., Maeno-Hikichi, Y., Awano, T., Landmesser, L.T., and Monani, U.R. (2010). Reduced survival of motor neuron (SMN) protein in motor neuronal progenitors functions cell autonomously to cause spinal muscular atrophy in model mice expressing the human centromeric (SMN2) gene. The Journal of neuroscience : the official journal of the Society for Neuroscience *30*, 12005-12019.

Pecho-Vrieseling, E., Sigrist, M., Yoshida, Y., Jessell, T.M., and Arber, S. (2009). Specificity of sensory-motor connections encoded by Sema3e-Plxnd1 recognition. Nature *459*, 842-846.

Pellis, S.M., and Pellis, V.C. (1994). Development of righting when falling from a bipedal standing posture: Evidence for the dissociation of dynamic and static righting reflexes in rats. Physiology & Behavior *56*, 659-663.

Pellizzoni, L., Baccon, J., Rappsilber, J., Mann, M., and Dreyfuss, G. (2002). Purification of native survival of motor neurons complexes and identification of Gemin6 as a novel component. The Journal of biological chemistry *277*, 7540-7545.

Plant, G.W., Weinrich, J.A., and Kaltschmidt, J.A. (2018). Sensory and descending motor circuitry during development and injury. Current opinion in neurobiology *53*, 156-161.

Poliak, S., Norovich, A.L., Yamagata, M., Sanes, J.R., and Jessell, T.M. (2016). Muscle-type Identity of Proprioceptors Specified by Spatially Restricted Signals from Limb Mesenchyme. Cell *164*, 512-525.

Powis, R.A., and Gillingwater, T.H. (2016). Selective loss of alpha motor neurons with sparing of gamma motor neurons and spinal cord cholinergic neurons in a mouse model of spinal muscular atrophy. Journal of anatomy *228*, 443-451.

Prasad, A., and Hollyday, M. (1991). Development and migration of avian sympathetic preganglionic neurons. The Journal of comparative neurology *307*, 237-258.

Presumey, J., Bialas, A.R., and Carroll, M.C. (2017). Complement System in Neural Synapse Elimination in Development and Disease. Adv Immunol *135*, 53-79.

Price, S.R., and Briscoe, J. (2004). The generation and diversification of spinal motor neurons: signals and responses. Mechanisms of development *121*, 1103-1115.

Qin, X., Krumrei, N., Grubissich, L., Dobarro, M., Aktas, H., Perez, G., and Halperin, J.A. (2003). Deficiency of the mouse complement regulatory protein mCd59b results in spontaneous hemolytic anemia with platelet activation and progressive male infertility. Immunity *18*, 217-227.

Rademakers, R., Neumann, M., and Mackenzie, I.R. (2012). Advances in understanding the molecular basis of frontotemporal dementia. Nature reviews Neurology *8*, 423-434.

Ransohoff, R.M., and Perry, V.H. (2009). Microglial physiology: unique stimuli, specialized responses. Annu Rev Immunol *27*, 119-145.

Redman, S. (1979). Junctional mechanisms at group Ia synapses. Prog Neurobiol *12*, 33-83.

Ricklin, D., Hajishengallis, G., Yang, K., and Lambris, J.D. (2010). Complement: a key system for immune surveillance and homeostasis. Nat Immunol *11*, 785-797.

Rindt, H., Feng, Z., Mazzasette, C., Glascock, J.J., Valdivia, D., Pyles, N., Crawford, T.O., Swoboda, K.J., Patitucci, T.N., Ebert, A.D.*, et al.* (2015). Astrocytes influence the severity of spinal muscular atrophy. Human molecular genetics *24*, 4094-4102.

Rochette, C.F., Gilbert, N., and Simard, L.R. (2001). SMN gene duplication and the emergence of the SMN2 gene occurred in distinct hominids: SMN2 is unique to Homo sapiens. Hum Genet *108*, 255-266.

Romanes, G.J. (1951). The motor cell columns of the lumbo-sacral spinal cord of the cat. The Journal of comparative neurology *94*, 313-363.

Rotterman, T.M., Nardelli, P., Cope, T.C., and Alvarez, F.J. (2014). Normal distribution of VGLUT1 synapses on spinal motoneuron dendrites and their reorganization after nerve injury. The Journal of neuroscience : the official journal of the Society for Neuroscience *34*, 3475-3492.

SA., S. (1992). Sensory Neurons: Diversity, Development, and Plasticity. New York: Oxford Univ Press.

Schafer, D.P., Lehrman, E.K., Kautzman, A.G., Koyama, R., Mardinly, A.R., Yamasaki, R., Ransohoff, R.M., Greenberg, M.E., Barres, B.A., and Stevens, B. (2012). Microglia sculpt postnatal neural circuits in an activity and complement-dependent manner. Neuron *74*, 691-705.

Schrank, B., Gotz, R., Gunnersen, J.M., Ure, J.M., Toyka, K.V., Smith, A.G., and Sendtner, M. (1997a). Inactivation of the survival motor neuron gene, a candidate gene for human spinal muscular atrophy, leads to massive cell death in early mouse embryos. Proceedings of the National Academy of Sciences of the United States of America *94*, 9920-9925.

Schrank, B., Götz, R., Gunnersen, J.M., Ure, J.M., Toyka, K.V., Smith, A.G., and Sendtner, M. (1997b). Inactivation of the survival motor neuron gene, a candidate gene for human spinal muscular atrophy, leads to massive cell death in early mouse embryos. *94*, 9920-9925.

Seebach, B.S., and Ziskind-Conhaim, L. (1994). Formation of transient inappropriate sensorimotor synapses in developing rat spinal cords. The Journal of neuroscience : the official journal of the Society for Neuroscience *14*, 4520-4528.

Sekar, A., Bialas, A.R., de Rivera, H., Davis, A., Hammond, T.R., Kamitaki, N., Tooley, K., Presumey, J., Baum, M., Van Doren, V.*, et al.* (2016). Schizophrenia risk from complex variation of complement component 4. Nature *530*, 177-183.

Selkoe, D.J. (2002). Alzheimer's disease is a synaptic failure. Science (New York, NY) *298*, 789-791.

Shahryari, A., Saghaeian Jazi, M., Mohammadi, S., Razavi Nikoo, H., Nazari, Z., Hosseini, E.S., Burtscher, I., Mowla, S.J., and Lickert, H. (2019). Development and Clinical Translation of Approved Gene Therapy Products for Genetic Disorders. Front Genet *10*, 868-868.

Shneider, N.A., Brown, M.N., Smith, C.A., Pickel, J., and Alvarez, F.J. (2009). Gamma motor neurons express distinct genetic markers at birth and require muscle spindle-derived GDNF for postnatal survival. Neural development *4*, 42.

Shorrock, H.K., Gillingwater, T.H., and Groen, E.J.N. (2019). Molecular Mechanisms Underlying Sensory-Motor Circuit Dysfunction in SMA. Frontiers in Molecular Neuroscience *12*.

Shorrock, H.K., van der Hoorn, D., Boyd, P.J., Llavero Hurtado, M., Lamont, D.J., Wirth, B., Sleigh, J.N., Schiavo, G., Wishart, T.M., Groen, E.J.N.*, et al.* (2018). UBA1/GARS-dependent pathways drive sensory-motor connectivity defects in spinal muscular atrophy. Brain : a journal of neurology *141*, 2878-2894.

Simic, G., Seso-Simic, D., Lucassen, P.J., Islam, A., Krsnik, Z., Cviko, A., Jelasic, D., Barisic, N., Winblad, B., Kostovic, I.*, et al.* (2000). Ultrastructural analysis and TUNEL demonstrate motor neuron apoptosis in Werdnig-Hoffmann disease. Journal of neuropathology and experimental neurology *59*, 398-407.

Simon, C.M., Dai, Y., Van Alstyne, M., Koutsioumpa, C., Pagiazitis, J.G., Chalif, J.I., Wang, X., Rabinowitz, J.E., Henderson, C.E., Pellizzoni, L.*, et al.* (2017). Converging Mechanisms of p53 Activation Drive Motor Neuron Degeneration in Spinal Muscular Atrophy. Cell reports *21*, 3767-3780.

Simon, C.M., Janas, A.M., Lotti, F., Tapia, J.C., Pellizzoni, L., and Mentis, G.Z. (2016). A Stem Cell Model of the Motor Circuit Uncouples Motor Neuron Death from Hyperexcitability Induced by SMN Deficiency. Cell reports *16*, 1416-1430.

Smith, R., Brundin, P., and Li, J.Y. (2005). Synaptic dysfunction in Huntington's disease: a new perspective. Cellular and molecular life sciences : CMLS *62*, 1901-1912.

Somers, E., Lees, R.D., Hoban, K., Sleigh, J.N., Zhou, H., Muntoni, F., Talbot, K., Gillingwater, T.H., and Parson, S.H. (2016). Vascular Defects and Spinal Cord Hypoxia in Spinal Muscular Atrophy. Annals of neurology *79*, 217-230.

Sontheimer, R.D., Racila, E., and Racila, D.M. (2005). C1q: Its Functions within the Innate and Adaptive Immune Responses and its Role in Lupus Autoimmunity. Journal of Investigative Dermatology *125*, 14-23.

Spangenberg, E., Severson, P.L., Hohsfield, L.A., Crapser, J., Zhang, J., Burton, E.A., Zhang, Y., Spevak, W., Lin, J., Phan, N.Y.*, et al.* (2019). Sustained microglial depletion with CSF1R inhibitor impairs parenchymal plaque development in an Alzheimer's disease model. Nat Commun *10*, 3758.

Stephan, A.H., Barres, B.A., and Stevens, B. (2012). The complement system: an unexpected role in synaptic pruning during development and disease. Annual review of neuroscience *35*, 369-389.

Stevens, B., Allen, N.J., Vazquez, L.E., Howell, G.R., Christopherson, K.S., Nouri, N., Micheva, K.D., Mehalow, A.K., Huberman, A.D., Stafford, B.*, et al.* (2007). The classical complement cascade mediates CNS synapse elimination. Cell *131*, 1164-1178.

Sumner, C.J., and Fischbeck, K.H. (2007). 44 - Spinal Muscular Atrophy. In Neurobiology of Disease, S. Gilman, ed. (Burlington: Academic Press), pp. 501-511.

Surmeli, G., Akay, T., Ippolito, G.C., Tucker, P.W., and Jessell, T.M. (2011). Patterns of spinal sensory-motor connectivity prescribed by a dorsoventral positional template. Cell *147*, 653-665.

Takeoka, A., Vollenweider, I., Courtine, G., and Arber, S. (2014). Muscle spindle feedback directs locomotor recovery and circuit reorganization after spinal cord injury. Cell *159*, 1626-1639.

Tarabal, O., Caraballo-Miralles, V., Cardona-Rossinyol, A., Correa, F.J., Olmos, G., Llado, J., Esquerda, J.E., and Caldero, J. (2014). Mechanisms involved in spinal cord central synapse loss in a mouse model of spinal muscular atrophy. Journal of neuropathology and experimental neurology *73*, 519-535.

ten Donkelaar, H.J. (2000). Descending Pathways to the Spinal Cord in Tetrapods: A Brief Outline. In Development and Regenerative Capacity of Descending Supraspinal Pathways in Tetrapods: A Comparative Approach, H.J. ten Donkelaar, ed. (Berlin, Heidelberg: Springer Berlin Heidelberg), pp. 9-13.

Tenner, A.J., Stevens, B., and Woodruff, T.M. (2018). New tricks for an ancient system: Physiological and pathological roles of complement in the CNS. Mol Immunol *102*, 3-13.

Tisdale, S., and Pellizzoni, L. (2015). Disease mechanisms and therapeutic approaches in spinal muscular atrophy. J Neurosci *35*, 8691-8700.

Toth, A.B., Terauchi, A., Zhang, L.Y., Johnson-Venkatesh, E.M., Larsen, D.J., Sutton, M.A., and Umemori, H. (2013). Synapse maturation by activity-dependent ectodomain shedding of SIRPalpha. Nature neuroscience *16*, 1417-1425.

Tremblay, M.-È., Stevens, B., Sierra, A., Wake, H., Bessis, A., and Nimmerjahn, A. (2011). The Role of Microglia in the Healthy Brain. The Journal of Neuroscience *31*, 16064-16069.

Tremblay, M.E., Lowery, R.L., and Majewska, A.K. (2010). Microglial interactions with synapses are modulated by visual experience. PLoS Biol *8*, e1000527.

Umemiya, M., Araki, I., and Kuno, M. (1993). Electrophysiological properties of axotomized facial motoneurones that are destined to die in neonatal rats. The Journal of physiology *462*, 661-678.

Van Alstyne, M., Simon, C.M., Sardi, S.P., Shihabuddin, L.S., Mentis, G.Z., and Pellizzoni, L. (2018). Dysregulation of Mdm2 and Mdm4 alternative splicing underlies motor neuron death in spinal muscular atrophy. Genes Dev *32*, 1045-1059.

Vanderhorst, V.G., and Holstege, G. (1997). Organization of lumbosacral motoneuronal cell groups innervating hindlimb, pelvic floor, and axial muscles in the cat. The Journal of comparative neurology *382*, 46-76.

Verret, L., Mann, E.O., Hang, G.B., Barth, A.M., Cobos, I., Ho, K., Devidze, N., Masliah, E., Kreitzer, A.C., Mody, I.*, et al.* (2012). Inhibitory interneuron deficit links altered network activity and cognitive dysfunction in Alzheimer model. Cell *149*, 708-721.

Viollet, L., Bertrandy, S., Bueno Brunialti, A.L., Lefebvre, S., Burlet, P., Clermont, O., Cruaud, C., Guenet, J.L., Munnich, A., and Melki, J. (1997). cDNA isolation, expression, and chromosomal localization of the mouse survival motor neuron gene (Smn). Genomics *40*, 185-188.

von Gontard, A., Zerres, K., Backes, M., Laufersweiler-Plass, C., Wendland, C., Melchers, P., Lehmkuhl, G., and Rudnik-Schoneborn, S. (2002). Intelligence and cognitive function in children and adolescents with spinal muscular atrophy. Neuromuscular disorders : NMD *12*, 130-136.

Vukojicic, A., Delestree, N., Fletcher, E.V., Pagiazitis, J.G., Sankaranarayanan, S., Yednock, T.A., Barres, B.A., and Mentis, G.Z. (2019). The Classical Complement Pathway Mediates Microglia-Dependent Remodeling of Spinal Motor Circuits during Development and in SMA. Cell reports *29*, 3087-3100.e3087.

Wadman, R.I., Vrancken, A.F., van den Berg, L.H., and van der Pol, W.L. (2012). Dysfunction of the neuromuscular junction in spinal muscular atrophy types 2 and 3. Neurology *79*, 2050-2055.

Wake, H., Moorhouse, A.J., Jinno, S., Kohsaka, S., and Nabekura, J. (2009). Resting microglia directly monitor the functional state of synapses in vivo and determine the fate of ischemic terminals. The Journal of neuroscience : the official journal of the Society for Neuroscience *29*, 3974-3980.

Waldrop, M.A., and Kolb, S.J. (2019). Current Treatment Options in Neurology-SMA Therapeutics. Current treatment options in neurology *21*, 25.

Werneburg, S., Buettner, F.F., Erben, L., Mathews, M., Neumann, H., Muhlenhoff, M., and Hildebrandt, H. (2016). Polysialylation and lipopolysaccharide-induced shedding of E-selectin ligand-1 and neuropilin-2 by microglia and THP-1 macrophages. Glia *64*, 1314-1330.

Westbury, D.R. (1982). A comparison of the structures of alpha and gamma-spinal motoneurones of the cat. The Journal of physiology *325*, 79-91.

Williams, P.A., Tribble, J.R., Pepper, K.W., Cross, S.D., Morgan, B.P., Morgan, J.E., John, S.W.M., and Howell, G.R. (2016). Inhibition of the classical pathway of the complement cascade prevents early dendritic and synaptic degeneration in glaucoma. Molecular Neurodegeneration *11*, 26.

Windhorst, U. (2007). Muscle proprioceptive feedback and spinal networks. Brain research bulletin *73*, 155-202.

Wirth, B., Schmidt, T., Hahnen, E., Rudnik-Schoneborn, S., Krawczak, M., Muller-Myhsok, B., Schonling, J., and Zerres, K. (1997). De novo rearrangements found in 2% of index patients with spinal muscular atrophy: mutational mechanisms, parental origin, mutation rate, and implications for genetic counseling. American journal of human genetics *61*, 1102-1111.

Woodruff, T.M., Crane, J.W., Proctor, L.M., Buller, K.M., Shek, A.B., de Vos, K., Pollitt, S., Williams, H.M., Shiels, I.A., Monk, P.N.*, et al.* (2006). Therapeutic activity of C5a receptor antagonists in a rat model of neurodegeneration. Faseb j *20*, 1407-1417.

Wu, Y., Dissing-Olesen, L., MacVicar, B.A., and Stevens, B. (2015). Microglia: Dynamic Mediators of Synapse Development and Plasticity. Trends Immunol *36*, 605-613.

Yamada, T., McGeer, P.L., and McGeer, E.G. (1992). Lewy bodies in Parkinson's disease are recognized by antibodies to complement proteins. Acta Neuropathol *84*, 100-104.

Yona, S., Kim, K.W., Wolf, Y., Mildner, A., Varol, D., Breker, M., Strauss-Ayali, D., Viukov, S., Guilliams, M., Misharin, A.*, et al.* (2013). Fate mapping reveals origins and dynamics of monocytes and tissue macrophages under homeostasis. Immunity *38*, 79-91.

Zanetta, C., Riboldi, G., Nizzardo, M., Simone, C., Faravelli, I., Bresolin, N., Comi, G.P., and Corti, S. (2014). Molecular, genetic and stem cell-mediated therapeutic strategies for spinal muscular atrophy (SMA). Journal of cellular and molecular medicine *18*, 187-196.

Zerres, K., and Davies, K.E. (1999). 59th ENMC International Workshop: Spinal Muscular Atrophies: recent progress and revised diagnostic criteria 17-19 April 1998, Soestduinen, The Netherlands. Neuromuscular disorders : NMD *9*, 272-278.

Zerres, K., and Rudnik-Schoneborn, S. (1995). Natural history in proximal spinal muscular atrophy. Clinical analysis of 445 patients and suggestions for a modification of existing classifications. Archives of neurology *52*, 518-523.

Zerres, K., Rudnik-Schoneborn, S., Forrest, E., Lusakowska, A., Borkowska, J., and Hausmanowa-Petrusewicz, I. (1997). A collaborative study on the natural history of childhood and juvenile onset proximal spinal muscular atrophy (type II and III SMA): 569 patients. Journal of the neurological sciences *146*, 67-72.

Zhang, Z., Pinto, A.M., Wan, L., Wang, W., Berg, M.G., Oliva, I., Singh, L.N., Dengler, C., Wei, Z., and Dreyfuss, G. (2013). Dysregulation of synaptogenesis genes antecedes motor neuron pathology in spinal muscular atrophy. Proceedings of the National Academy of Sciences of the United States of America *110*, 19348-19353.

Zheng, Y., Liu, P., Bai, L., Trimmer, J.S., Bean, B.P., and Ginty, D.D. (2019). Deep Sequencing of Somatosensory Neurons Reveals Molecular Determinants of Intrinsic Physiological Properties. Neuron *103*, 598-616.e597.

Zipfel, P.F., and Skerka, C. (2009). Complement regulators and inhibitory proteins. Nat Rev Immunol *9*, 729-740.

BIOGRAPHY

Aleksandra Vukojičić was born on December 23rd, 1986 in Belgrade, Serbia. She received a bachelor's degree in Biology (module: Molecular Biology and Physiology) from Faculty of Biology, University of Belgrade in 2012. Same year she started master studies in Molecular Biology and Physiology (module: Immunobiology) at the Faculty of Biology, University of Belgrade. She carried out experimental part of her master studies in the lab of dr Monika Bradl, in the Center for Brain Research, dept. of Neuroimmunology, at the Medical University of Vienna, where she studied autoreactive antibodies involved in the pathogenesis of autoimmune disease neuromyelitis optica. She received a master's degree in 2013 and same year started Ph.D studies in Biology (module: Immunobiology) at the Faculty of Biology, University of Belgrade.

In November 2013, Aleksandra joined dr George Z. Mentis lab, at the Center for Motor Neuron Biology and Disease at Columbia University. Aleksandra carried out entire experimental part of her doctoral studies in dr Mentis lab, where she studied the molecular, cellular and neuronal circuit mechanisms involved in the dysfunction and elimination of synapses on motor neurons at the onset of the neurodegenerative disease spinal muscular atrophy (SMA). She has uncovered the role of the classical complement pathway in synaptic dysfunction and elimination of proprioceptive synapses in a mouse model of SMA, as well as the role of complement proteins in sensory-motor circuitry refinement during normal development.

Aleksandra Vukojičić has authored one and co-authored two more peer-reviewed papers in top international journals (category M21). She has given talks at six international meetings and one at a national meeting. Additionally, she had four poster presentations at international meetings and one at a national meeting. In 2017, Aleksandra was awarded F1000 prize for an outstanding presentation from the New York Academy of Sciences at the conference "Complement Pathways in Disease".

Прилог 1.

Изјава о ауторству

Потписани-а **Александра Вукојичић**

Број индекса   **Б3004/2013**

Изјављујем

да је докторска дисертација под насловом

Комплемент и микроглија као посредници губитка сензорно-моторних синапси током нормалног развића и у спиналној мишићној атрофији

- резултат сопственог истраживачког рада,
- да предложена дисертација у целини ни у деловима није била предложена за добијање било које дипломе према студијским програмима других високошколских установа,
- да су резултати коректно наведени и
- да нисам кршио/ла ауторска права и користио интелектуалну својину других лица.

Потпис аутора

У Београду, 03.12.2020.

Изјава о истоветности штампане и електронске верзије докторског рада

Име и презиме аутора **Александра Вукојичић**

Број индекса   **Б3004/2013**

Студијски програм   **Биологија**

    Наслов рада   **Комплемент и микроглија као посредници губитка сензорно-моторних синапси током нормалног развића и у спиналној мишићној атрофији**

Ментор **dr. George Z. Mentis** и др **Биљана Божић Недељковић**

Потписани/а Александра Вукојичић

Изјављујем да је штампана верзија мог докторског рада истоветна електронској верзији коју сам предао/ла за објављивање на порталу **Дигиталног репозиторијума Универзитета у Београду.**

Дозвољавам да се објаве моји лични подаци везани за добијање академског звања доктора наука, као што су име и презиме, година и место рођења и датум одбране рада.

Ови лични подаци могу се објавити на мрежним страницама дигиталне библиотеке, у електронском каталогу и у публикацијама Универзитета у Београду.

Потпис аутора

У Београду, 03.12.2020

Прилог 3.

Изјава о коришћењу

Овлашћујем Универзитетску библиотеку „Светозар Марковић“ да у Дигитални репозиторијум Универзитета у Београду унесе моју докторску дисертацију под насловом:

Комплемент и микроглија као посредници губитка сензорно-моторних синапси током нормалног развића и у спиналној мишићној атрофији

која је моје ауторско дело.

Дисертацију са свим прилозима предао/ла сам у електронском формату погодном за трајно архивирање.

Моју докторску дисертацију похрањену у Дигитални репозиторијум Универзитета у Београду могу да користе сви који поштују одредбе садржане у одабраном типу лиценце Креативне заједнице (Creative Commons) за коју сам се одлучио/ла.

1. Ауторство

2. Ауторство – некомерцијално

3. Ауторство – некомерцијално – без прераде

4. Ауторство – некомерцијално – делити под истим условима

5. Ауторство – без прераде

6. Ауторство – делити под истим условима

(Молимо да заокружите само једну од шест понуђених лиценци, кратак опис лиценци дат је на полеђини листа).

Потпис аутора

Београду, 03.12.2020

_____

1. Ауторство - Дозвољавате умножавање, дистрибуцију и јавно саопштавање дела, и прераде, ако се наведе име аутора на начин одређен од стране аутора или даваоца лиценце, чак и у комерцијалне сврхе. Ово је најслободнија од свих лиценци.

2. Ауторство – некомерцијално. Дозвољавате умножавање, дистрибуцију и јавно саопштавање дела, и прераде, ако се наведе име аутора на начин одређен од стране аутора или даваоца лиценце. Ова лиценца не дозвољава комерцијалну употребу дела.

3. Ауторство - некомерцијално – без прераде. Дозвољавате умножавање, дистрибуцију и јавно саопштавање дела, без промена, преобликовања или употребе дела у свом делу, ако се наведе име аутора на начин одређен од стране аутора или даваоца лиценце. Ова лиценца не дозвољава комерцијалну употребу дела. У односу на све остале лиценце, овом лиценцом се ограничава највећи обим права коришћења дела.

4. Ауторство - некомерцијално – делити под истим условима. Дозвољавате умножавање, дистрибуцију и јавно саопштавање дела, и прераде, ако се наведе име аутора на начин одређен од стране аутора или даваоца лиценце и ако се прерада дистрибуира под истом или сличном лиценцом. Ова лиценца не дозвољава комерцијалну употребу дела и прерада.

5. Ауторство – без прераде. Дозвољавате умножавање, дистрибуцију и јавно саопштавање дела, без промена, преобликовања или употребе дела у свом делу, ако се наведе име аутора на начин одређен од стране аутора или даваоца лиценце. Ова лиценца дозвољава комерцијалну употребу дела.

6. Ауторство - делити под истим условима. Дозвољавате умножавање, дистрибуцију и јавно саопштавање дела, и прераде, ако се наведе име аутора на начин одређен од стране аутора или даваоца лиценце и ако се прерада дистрибуира под истом или сличном лиценцом. Ова лиценца дозвољава комерцијалну употребу дела и прерада. Слична је софтверским лиценцама, односно лиценцама отвореног кода.